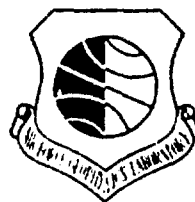


AD A138846

AFGL-TR-83-0155
ENVIRONMENTAL RESEARCH PAPERS, NO. 840

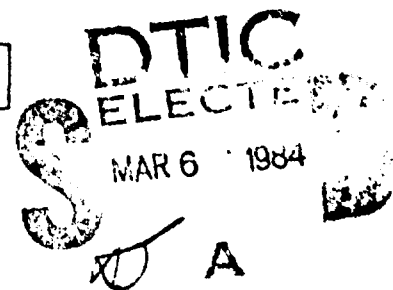


Atmospheric Temperature, Density and Pressure:
Chapter 15, 1983 Revision,
Handbook of Geophysics and Space Environments

ALLEN E. COLE
IRVING I. GRINGORTEN
YUTAKA IZUMI
ARTHUR J. KANTOR
PAUL TATELMAN

13 June 1983

Approved for public release; distribution unlimited.



METEOROLOGY DIVISION PROJECT 6670
AIR FORCE GEOPHYSICS LABORATORY
HANSOM AFB, MASSACHUSETTS 01731

AIR FORCE SYSTEMS COMMAND, USAF



DTIC FILE COPY

84 03 06 085

Unclassified

SECURITY CLASSIFICATION OF THIS PAGE (When Data Entered)

REPORT DOCUMENTATION PAGE		READ INSTRUCTIONS BEFORE COMPLETING FORM
1. REPORT NUMBER AFGL-TR-83-0155	2. GOVT ACCESSION NO. AD-A138846	3. RECIPIENT'S CATALOG NUMBER
4. TITLE (and Subtitle) ATMOSPHERIC TEMPERATURE, DENSITY AND PRESSURE: CHAPTER 15, 1983 REVISION, HANDBOOK OF GEOPHYSICS AND SPACE ENVIRONMENTS		5. TYPE OF REPORT & PERIOD COVERED Scientific. Interim.
7. AUTHOR(s) Allen E. Cole Irving I. Gringorten Yutaka Izumi		6. PERFORMING ORG. REPORT NUMBER ERP No. 840
9. PERFORMING ORGANIZATION NAME AND ADDRESS Air Force Geophysics Laboratory (LY) Hanscom AFB Massachusetts 01731		10. PROGRAM ELEMENT, PROJECT, TASK AREA & WORK UNIT NUMBERS 62101F 66700911
11. CONTROLLING OFFICE NAME AND ADDRESS Air Force Geophysics Laboratory (LY) Hanscom AFB Massachusetts 01731		12. REPORT DATE 13 June 1983
14. MONITORING AGENCY NAME & ADDRESS (if different from Controlling Office)		13. NUMBER OF PAGES 98
		15. SECURITY CLASS. (of this report) Unclassified
		15a. DECLASSIFICATION/DOWNGRADING SCHEDULE
16. DISTRIBUTION STATEMENT (of this Report) Approved for public release; distribution unlimited.		
17. DISTRIBUTION STATEMENT (of the abstract entered in Block 20, if different from Report)		
18. SUPPLEMENTARY NOTES		
19. KEY WORDS (Continue on reverse side if necessary and identify by block number) Temperature Density Pressure Variations		
20. ABSTRACT (Continue on reverse side if necessary and identify by block number) Temperature, density, and pressure, from the surface to 90 km, are discussed in this report. Information on seasonal and latitudinal variations, interlevel correlations, and variability with time are included. The information in this report will also be Chapter 15 of the 1983 <u>Handbook of Geophysics and Space Environments</u> . ↑		

Preface

This report is a revision of Chapter 3 of the 1965 Handbook of Geophysics and Space Environments.* Both the 1965 edition and the planned 1983 edition are intended to present geophysical and astrophysical information needed for the design and operation of aircraft, missiles, satellites, and surface-based material and equipment.

The order of chapters, and therefore, all the numbering has been changed from the 1965 to the 1983 Handbook; as a result, the cross-referencing to other chapters is not valid. Chapters in the 1983 Handbook are referred to by their titles; numbers, where given, are those planned at the time of publication of this report.

We thank Mrs. Helen Connell for typing this report.

Approved for	
FIRING	
FOR TAB	
UNRESTRICTED	
Classification	
Distribution	
Availability Codes	
Dist	Avail and/or Special
A-1	



*Published by the Air Force Cambridge Research Laboratories and by the McGraw-Hill Book Co. in 1965.

Contents

15.1 THERMAL PROPERTIES, SURFACE TO 90 km	11
15.1.1 Energy Supply and Transformation	12
15.1.2 Surface Temperature	15
15.1.2.1 Official Station Temperature	15
15.1.2.2 Daily Temperature	16
15.1.2.3 Horizontal Extent of Surface Temperature	19
15.1.2.4 Runway Temperatures	22
15.1.2.5 Temperature Extremes	23
15.1.2.6 The Gumbel Model	27
15.1.2.7 Temperature Cycles and Durations	30
15.1.3 Upper Air Temperature	37
15.1.3.1 Seasonal and Latitudinal Variations	37
15.1.3.2 Distribution Around Monthly Means and Medians	39
15.1.3.3 Distributions at Pressure Levels	45
15.1.3.4 Interlevel Correlation of Temperature	46
15.1.4 Speed of Sound vs Temperature	55
15.1.5 Earth/Air Interface Temperatures	56
15.1.6 Subsoil Temperatures	59
15.1.7 Degree-Day and Temperature-Wind Combinations	64
15.2 ATMOSPHERIC DENSITY UP TO 90 km	66
15.2.1 Seasonal and Latitudinal Variations	66
15.2.2 Day-to-Day Variations	66
15.2.3 Spatial Variation	73
15.2.4 Statistical Applications to Reentry Problems	75
15.2.5 Variability With Time	84

Contents

15.3 ATMOSPHERIC PRESSURE UP TO 90 km	88
15.3.1 Sea-Level Pressure	88
15.3.2 Seasonal and Latitudinal Variations	91
15.3.3 Day-to-Day Variations	92
15.3.4 Diurnal and Semidiurnal Variations	94
REFERENCES	97

Illustrations

15.1. Global Mean Energy Cycles of the Atmosphere	14
15.2. Surface Temperature at Hanscom AFB, Mass., Throughout the Year	17
15.3. The Correlation Coefficient of the Daily Mean Temperature of Columbus, Ohio With That of Nine Other U.S. Stations at Indicated Distances From Columbus	21
15.4. Temperature Equalled or Exceeded 1 Percent of the Time During the Warmest Month	25
15.5. Temperature Equalled or Colder 1 Percent of the Time During the Coldest Month	26
15.6a. Annual Highest Temperature, Hanscom AFB, Mass., 21 Ordered Values (1944-1964)	29
15.6b. Lowest Temperatures Occurring at Hanscom AFB, Mass. During 22 Winter Seasons (1943-1965) Ordered From Warmest to Coldest, and Plotted as the Probability That the Coldest Temperature Will Not Be Below the Given Value	29
15.7. Yuma, Arizona Typical July Diurnal Cycles When Maximum Daily Temperature Equals or Exceeds 44 C (111 F), Based on 1961-1968 Data	31
15.8. Longest Duration (h) of Temperature ≤ -23 C (-10 F) in 10 Winters, From Tattelman ⁷	35
15.9. Expected Longest Duration (h) of Temperature ≤ -23 C (-10 F) During a Single Winter Season, From Tattelman ⁷	36
15.10. The Distribution of the Averages of Consecutive Hours of Temperature at Minneapolis, Minn.	37
15.11. The Cumulative Probability of the M-Hour Minimum Temperature (1 January to 1 February) at Minneapolis, Minn.	38
15.12. The Frequency of Duration (h) of the Temperature ($\leq T$) in the Mid-Winter Month (1 January to 1 February) at Minneapolis, Minn. (Based on 1943-1952 Data)	38

Illustrations

15.13. Seasonal Differences in the Temperature-Altitude Profiles at Ascension Island, Wallops Island, and Ft. Churchill	40
15.14. Vertical Profiles of Interlevel Coefficients of Correlation of Surface Temperature With Temperature at Other Altitudes up to 60 km for the Mid-Season Months at Ascension Island, Kwajalein, Wallops Island, and Ft. Churchill	48
15.15. Speed of Sound vs Temperature (K)	55
15.16. Variations of Soil Temperature at Indicated Depths, North Station, Brookhaven, Long Island, October 1954 Through September 1955, After Singer and Brown ¹⁴	63
15.17. Extremes of Temperature in Combination With Windspeed	65
15.18. Latitudinal Differences in the Density-Altitude Profiles for the Mid-Season Months at Ascension Island, Wallops Island, and Ft. Churchill	67
15.19. Seasonal Differences in the Density-Altitude Profiles at Ascension Island, Wallops Island, and Ft. Churchill	68
15.20. Decay of Density Correlations With Distance at Various Altitudes in Midlatitudes	74
15.21. Diurnal Density (50 km) Variation at Ascension (Dots Indicate Observed Values, x's Represent 3-h Averages, and the Solid Line Depicts the Computed Diurnal Cycle)	85
15.22. Root Mean Square (rms) Lag Variability of Density With Time at Ascension	85
15.23. The rms Variation in Density for Time Lags of 1 to 6 h at Kwajalein	86
15.24. The Differences Between Densities Observed 1 to 72 h Apart at 50 km	87
15.25. Pressure-Altitude Profiles for Midseason Months	91

Tables

15.1. Short-Wave Radiation on a Horizontal Plane, Net Radiation, and Estimated Constituents of Heat Budget at the Earth/Air Interface, Showing the Effect of Difference in Soil Moisture, Caused by Rains Before 9 Aug and a Dry Spell Before 7 Sep 1953 ²	15
15.2. Temperatures at Various Stations Around the World	18
15.3. Estimates of the Horizontal Scale of Certain Local Meteorological Conditions	20

Tables

<p>15.4. Diurnal Cycles of Temperature and Other Associated Elements for Days When the Maximum Temperature Equals or Exceeds the Operational 1 Percent Extreme Temperature (49°C) in the Hottest Month in the Hottest Area</p> <p>15.5. Probability of Daily Solar Insolation Equalling or Exceeding Given Amounts for Given Number of Consecutive Days in June, at Albuquerque, N.M.</p> <p>15.6. Probability of Daily Solar Insolation Equalling or Exceeding Given Amounts for Given Number of Consecutive Days in June, at Caribou, Maine</p> <p>15.7. Durations of Cold Temperatures Associated With the -51°C Extreme</p> <p>15.8a. Median, High, and Low Percentile Values of Temperatures for January and July at 30°N</p> <p>15.8b. Median, High, and Low Percentile Values of Temperatures for January and July at 45°N</p> <p>15.8c. Median, High, and Low Percentile Values of Temperatures for January and July at 60°N</p> <p>15.8d. Median, High, and Low Percentile Values of Temperatures for January and July at 75°N</p> <p>15.9. Standard Deviations of Observed Day-to-Day Variations in Temperatures (K) at Ascension (8°S) at Altitudes up to 50 km During the Midseason Months</p> <p>15.10. Standard Deviations of Observed Densities (Percent) and Temperatures (K) Around the Mean Annual Values at Ascension (8°S)/Natal (6°S)</p> <p>15.11. Mean Temperature and Standard Deviation at Standard Pressure Levels Over North America</p> <p>15.12a. Churchill - Correlation of January Temperatures (K) From Surface to 60 km</p> <p>15.12b. Churchill - Correlation of July Temperatures (K) From Surface to 60 km</p> <p>15.12c. Wallops Island - Correlation of January Temperatures (K) From Surface to 60 km</p> <p>15.12d. Wallops Island - Correlation of July Temperatures (K) From Surface to 60 km</p> <p>15.12e. Kwajalein - Correlation of January Temperatures (K) From Surface to 60 km</p> <p>15.12f. Kwajalein - Correlation of July Temperatures (K) From Surface to 60 km</p> <p>15.13. Bolometric Records of Area (Approximately 37 m²) Surface Temperature From an Airplane Cruising at Approximately 370 m Along a Constant Flight Path, April 1944 (Condensed From Albrecht⁹)</p>	<p style="margin-top: 10px;">32</p> <p>33</p> <p>34</p> <p>36</p> <p>41</p> <p>42</p> <p>43</p> <p>44</p> <p>45</p> <p>46</p> <p>47</p> <p>49</p> <p>50</p> <p>51</p> <p>52</p> <p>53</p> <p>54</p> <p>57</p>
--	---

Tables

15.14. Temperature of the Air 10 cm Above, and of the Soil 0.5 cm Below, the Earth/Air Interface, Measured by Thermocouples (Davidson and Lettau ²)	58
15.15. Comparison of Air and Soil Temperature With Surface Temperatures of Materials Exposed on a Tropical Island With Normal Trade Winds	59
15.16. Physical Thermal Parameters of Diverse Ground Types (Lettau ¹¹)	61
15.17. Annual and Daily Temperature Cycles	62
15.18a. Median, High, and Low Percentile Values of Densities Given as Percentage Departures From U.S. Standard Atmosphere 1976 for January and July at 30°N	69
15.18b. Median, High, and Low Percentile Values of Densities Given as Percentage Departures From U.S. Standard Atmosphere 1976 for January and July at 45°N	70
15.18c. Median, High, and Low Percentile Values of Densities Given as Percentage Departures From U.S. Standard Atmosphere 1976 for January and July at 60°N	71
15.18d. Median, High, and Low Percentile Values of Densities Given as Percentage Departures From U.S. Standard Atmosphere 1976 for January and July at 75°N	72
15.19. Standard Deviations (percent) of Observed Day-to-Day Variations in Density Around the Monthly Mean at Ascension (8°S)	73
15.20. Correlation Coefficients Between Densities at Points up to 370 km (200 nmi) Apart in the Tropics	75
15.21. Estimated rms Differences (percent of mean) Between Densities at Locations 90, 180, and 360 km Apart During the Midseason Months in the Tropics	76
15.22. Mean Monthly Latitudinal Density Gradients (percent change per 180 km) in the Tropics	77
15.23a. Kwajalein - Correlation of January Density (kg/m ³) From Surface to 60 km	78
15.23b. Kwajalein - Correlation of July Density (kg/m ³) From Surface to 60 km	79
15.23c. Wallops Island - Correlation of January Density (kg/m ³) From Surface to 60 km	80
15.23d. Wallops Island - Correlation of July Density (kg/m ³) From Surface to 60 km	81
15.23e. Ft. Churchill - Correlation of January Density (kg/m ³) From Surface to 60 km	82
15.23f. Ft. Churchill - Correlation of July Density (kg/m ³) From Surface to 60 km	83
15.24. Sea-Level Pressures Exceeded 99 and 1 Percent of the Time in January	88

Tables

15.25. Worldwide Pressure Extremes	89
15.26. Mean Monthly Sea-Level Pressures and Standard Deviations of Daily Values	90
15.27. Average Height and Standard Deviation at Standard Pressure Levels Over North America, 90° to 100°W	93
15.28. Departures From Mean Monthly Pressures (Percent) Exceeded Less Than 5 Percent of the Time in January and July	94
15.29. Amplitudes of Systematic Pressure Variations and Time of Maximum at Terceira, Azores (Harris et al ²⁸)	95

Atmospheric Temperature, Density and Pressure: Chapter 15, 1983 Revision, Handbook of Geophysics and Space Environments

The three physical properties of the earth's atmosphere, temperature T, density ρ , and pressure P, are related by the ideal gas law $P = \rho TR$ where R is the gas constant for air. Except for the 1/1,000th of one percent of the atmosphere by mass that is above 80 km (\approx 263,000 ft), various gases comprise the atmosphere in essentially constant proportions. The principal exception is water vapor, which is discussed in Chapter 16 of the 1983 Handbook of Geophysics.

15.1 THERMAL PROPERTIES, SURFACE TO 90 km

In the following sections the units of measurement are primarily metric. Abbreviations are used whenever quantitative measures are presented. The temperature is in degrees Kelvin (K) or degrees Centigrade (C), density in kilograms per cubic meter (kg/m^3), pressure in millibars (mb), time in seconds (sec) or hours (h), length in centimeters (cm), meters (m) or kilometers (km), and speed in meters per second (m/sec) or kilometers per hour (km/h). The main unit of energy is the calorie (cal):

(Received for publication 7 June 1983)

$$1 \text{ cal} = 4.1860 \text{ joules (J)}$$

$$= 1.163 \times 10^{-3} \text{ watt-hours (W h).}$$

For energy per unit area an additional unit, the Langley (L), is introduced:

$$\begin{aligned} 1 \text{ Langley} &= 1 \text{ cal/cm}^2 \\ &= 11.62 \text{ W h/m}^2 \\ &= 41.84 \text{ kJ/m}^2 . \end{aligned}$$

The main unit of power is the watt (W), but solar power per unit area is given in Langleys per hour (L/h). In terms of the British Thermal Unit (BTU)

$$1 \text{ L/h} = 3.686 \text{ BTU ft}^{-2} \text{ h}^{-1}.$$

15.1.1 Energy Supply and Transformation*

The prime source of energy that produces and maintains atmospheric motions and the spatial and temporal variations of meteorological elements is the solar radiation intercepted by the earth. In comparison with solar radiation, other energy sources, such as heat from the interior of the earth, radiation from other celestial bodies, or the tidal forces of the moon and sun, are practically negligible.

The rate at which solar energy is received on a plane surface, perpendicular to the incident radiation outside of the atmosphere at the earth's mean distance from the sun, is the solar constant; the value used here is $2.0 \text{ cal cm}^{-2} \text{ min}^{-1}$, or 2.0 L/min , or 1395 W/m^2 . The rate at which direct solar energy is received on a unit horizontal plane at the earth's surface, or in the atmosphere above the earth's surface, is called the insolation. The planetary albedo, which is the reflected radiation divided by the total incident solar radiation, varies primarily with angle of incidence of the radiation, the type of surface, and the amount of cloudiness. On the average, roughly 30 to 40 percent of the incident solar energy is reflected back to space by the cloud surfaces, the clear atmosphere, the earth/air interface, and particles such as dust and ice crystals suspended in the atmosphere. The balance is available as the energy source for maintaining and driving atmospheric processes.

When the earth and its surrounding atmosphere are considered together as a complete thermodynamic system, it appears that there has been no major net

*Based on the section by H.H. Lettau and D.A. Haugen in the Handbook of Geophysics for Air Force Designers, 1957.

change of energy in the system within recent climatic history. In particular, there has been no obvious systematic change in (1) the heating of the earth's surface or the atmosphere, (2) the intensity of the atmospheric circulation, or (3) the balance between evaporation and precipitation. Thus the processes affecting the internal and latent heat and the mechanical energy within the earth-atmospheric system appear virtually balanced.

The main features of the global energy transformations are summarized in Figure 15.1, a flow chart, from which the relative importance of the major energy cycles within the earth-atmosphere thermodynamic system can be determined. The numerical data presented in this figure are useful for various quantitative estimates. For example, if all energy inputs for the system ceased and rates of energy expenditure were maintained, the reservoir of mechanical energy (momentum) would be depleted in about 3 days; the reservoir of latent heat (precipitable water) in about 12 days; and the reservoir of internal energy (heat) in about 100 days.

Although an absolutely dry and motionless atmosphere is conceivable, it is difficult to imagine an atmosphere at zero degrees Kelvin. It is perhaps more appropriate to interpret the above time intervals as fictitious cycles of turnover of the atmospheric properties. The relative magnitudes of these life cycles show that, in comparison with rainfall and winds, temperature is the most conservative and will exhibit relatively the smallest, and thus the most regular, temporal and spatial large-scale variation.

The solar energy input into the atmosphere at any one point varies during the earth's rotation about its axis and revolution about the sun. A consistent feature of this variation on a global scale is the driving force produced by differential latitudinal solar heating of the earth's surface. The reaction of the atmosphere to the solar driving force on an hourly, a daily, or an annual basis is observed most easily in the temperature field at low levels.

The solar energy input varies according to season, latitude, orientation of terrain to the incident energy, soil structure, and the surface differential between the incoming solar and sky radiation (short wave) and the outgoing atmosphere-terrestrial radiation (long wave). The difference between short-wave and long-wave radiation is the net radiation. Locally, net radiation is decreased primarily by atmospheric moisture (vapor and clouds). The latent heat required to evaporate soil moisture diminishes the net radiation available for heating air and soil at the ground. The importance of moisture in establishing general climatic zones is shown by comparing desert climates with adjacent climates at roughly the same latitude. Table 15.1 gives the effect of soil moisture on the heat budget of the earth/air interface.

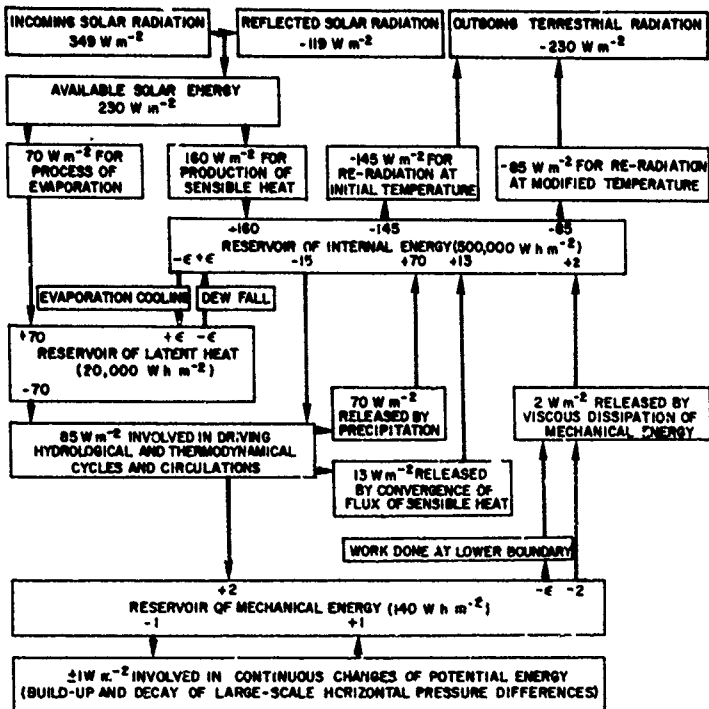


Figure 15.1. Global Mean Energy Cycles of the Atmosphere. A solar constant of 1395 W/m^2 and a global albedo value of 0.34 are assumed. The average total incoming radiation to the globe is $1/4$ of the solar constant. ϵ denotes an average rate of less than 0.5 W/m^2 . The estimated reliability of the solar constant is 3 percent; of the derived energy rates, this totals approximately 10 percent¹

Slopes facing south receive maximum solar energy. Slopes facing west are usually warmer and drier than those facing east, because the time of maximum insolation on a west slope is shifted to the afternoon when the general level of air temperature is higher than in the forenoon.

The energy balance of the earth/air interface requires that net radiation equals the sum of heat fluxes into the air and soil plus the heat equivalent of evaporation. In general, the maximum of heat flux into the soil precedes the maximum of heat flux into the air. The temperature maximum at standard instrument height (about 1.8 m) follows the maximum of heat flux into the air by roughly 1 to 2 h.

1. Lettau, H. (1954) A study of the mass, momentum and energy budget of the atmosphere, *Archiv fur Meteorologie, Geophysik und Bioklimatologie*, Serie A, 7:133.

Table 15.1. Short-Wave Radiation on a Horizontal Plane, Net Radiation, and Estimated Constituents of Heat Budget at the Earth/Air Interface, Showing the Effect of Difference in Soil Moisture, Caused by Rains Before 9 Aug and a Dry Spell Before 7 Sep 1953²

Mean Local Time	Radiation (W/m ²)								
	04h	06h	08h	10h	12h	14h	16h	18h	20h
9 Aug 1953*									
Short-wave	0	141	544	733	796	823	537	144	---
Net	-59	47	364	497	540	525	273	-13	---
Flux into soil	-40	29	186	63	74	73	28	-65	---
Flux into air	-11	---	81	158	176	190	64	-17	---
Heat of evap.	-8	---	97	276	290	262	181	69	---
7 Sept 1953**									
Short-wave	0	54	441	765	870	735	407	44	0
Net	-54	-32	181	403	488	398	154	-69	-77
Flux into soil	-44	-25	36	84	95	66	13	-29	-28
Flux into air	-6	-6	98	230	303	299	114	-30	-39
Heat of evap.	-4	-1	47	89	90	33	27	-10	-10

*Mean soil moisture in 0 to 10-cm layer, about 10 percent wet weight basis.

**Mean soil moisture in 0 to 10-cm layer, about 4 percent wet weight basis.

15.1.2 Surface Temperature

15.1.2.1 OFFICIAL STATION TEMPERATURE

The standard station temperature used in meteorology³ is measured by a thermometer enclosed within a white-painted, louvered, instrument shelter or

- 2. Davidson, B., and Lettau, H., Eds. (1957) Great Plains Turbulence Field Program, Pergamon Press, New York.
- 3. National Weather Service (1979) Surface Observations (Federal Meteorological Handbook 90.1) Superintendent of Documents, Government Printing Office, Washington, D. C. 20402.

Stevenson Screen. The shelter has a base about 1 m (1.7 to 2.0 m in Central Europe) above the ground and is mounted in an open field (close-cropped grass surface). The standardized height of the thermometer is about 1.8 m. The shelter permits air circulation past the thermometer and is designed to exclude direct solar and terrestrial radiation. However, the shelter unavoidably absorbs and radiates some heat energy which, although minimal, causes some deviation of the thermometer reading from the "true" air temperature. On calm, sunny days the recorded daytime shelter temperature will normally be 1/2 to 1 C higher than the free air temperature outside the shelter at the same level. On calm, clear nights it will most likely be cooler by 1/2 C. Therefore, the thermometer should be artificially ventilated. Spatial variations of the ambient air temperature, especially in the first meter above the ground, are dependent upon the type of soil and ground cover. Ground effects decrease with height, and for this reason the international standard heights of temperature measurement are a compromise between suppressing ground-cover effects and maintaining ease of access.

15.1.2.2 THE DAILY TEMPERATURE

The official station temperature, taken every hour on the hour, reveals a fairly regular diurnal cycle. This is true despite several superimposed phenomena such as frontal passages and thunderstorms. Usually there is a temperature maximum in midafternoon and a temperature minimum near sunrise. The amplitude of the diurnal cycle varies with location and season from as little as 1 C (2 F) to more than 17 C (31 F).

The annual cycle of daily mean temperature ranges from practically zero near the equator to as much as 40 C (72 F) in the temperate zone. As an example, Figure 15.2 shows temperatures at Hanscom AFB, Mass. The middle curve gives the annual cycle of the daily mean temperature (actually the monthly mean is plotted) and shows an annual range of 25 C (45 F). The diurnal range (given here by the difference between mean daily maximum and minimum in Figure 15.2, is fairly uniform throughout the year, averaging 12 C (22 F).

Superimposed on both the diurnal and the annual cycles of temperature are many influences including cloudiness, precipitation, wind speed and direction, type of soil, ground cover, and aerodynamic roughness of the terrain. In the example of Figure 15.2 there is a range from the uppermost 1 percent of the daily maximum to the lowermost 1 percent of the daily minimum that is 3 times the mean diurnal cycle. The standard deviation of hourly temperature averages 5 C (9 F). The range from the uppermost 1 percent of the maximum temperature of the hottest month to the lowermost 1 percent of the minimum temperature of the coldest month in Figure 15.2 is about 2-1/2 times the mean annual cycle.

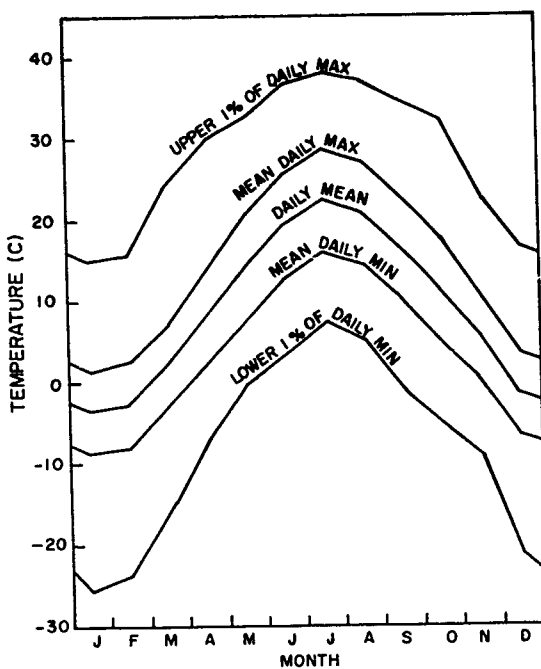


Figure 15.2. Surface Temperature at Hanscom AFB, Mass., Throughout the Year

The pattern of surface temperature varies with geographic location. This is illustrated by the statistics of some widely scattered stations and even by the statistics of neighboring stations (Table 15.2). The annual mean temperature is generally lowest in the polar regions and highest in the equatorial belt. In addition, the mean temperature generally decreases with increasing elevation. The diurnal range is greatest in desert climates and least in oceanic or maritime climates. The mean annual range tends to be greatest in temperate climates and least in equatorial climates.

In polar regions, where darkness (daylight) is continuous for several months of the year, the 24-h cycle is minimal and the small diurnal variations are controlled primarily by changing winds and cloudiness. In summer, nearly all of the solar energy is expended in melting ice; hence, the maximum temperature seldom exceeds 0 C. Extra-tropical regions characteristically have distinct diurnal and annual cycles. These cycles are superimposed over temperature variations caused by shifting air masses and frontal passages. In tropical regions, the diurnal range rarely exceeds 6 C.

Table 15.2. Temperatures at Various Stations Around the World

Station	Lat	Long	Elev. (m)	Annual Mean (°C)	Mean Diurnal Range (°C)	Mean Annual Range (°C)	Hottest Month 1% of Daily Max. (°C)	Coldest Month 1% of Daily Min. (°C)
Hanscom AFB, Mass.	42°28'N	71°17'W	43	9.3	11.7	25.6	38	-26
Boston, Mass.	42°22'N	71°02'W	5	10.8	8.6	24.3	--	--
Blue Hill Obs., Mass.	42°13'N	71°07'W	192	9.3	9.6	24.4	--	--
Nantucket, Mass.	41°15'N	70°04'W	13	9.7	7.2	20.4	--	--
Pittsfield, Mass.	42°26'N	73°18'W	357	7.2	11.4	25.6	--	--
Worcester, Mass.	42°16'N	71°52'W	301	8.2	9.5	25.4	--	--
Thule, Greenland	76°32'N	68°42'W	59	-11.2	6.4	31.9	16	-40
Ladd AFB, Alaska	64°41'N	147°05'W	270	-2.8	10.8	39.6	30	-49
Keflavik, Iceland	63°58'N	22°36'W	50	5.1	4.4	11.2	18	-15
Goose Bay, Newfoundland	53°19'N	60°25'W	44	0.2	9.5	33.7	34	-36
Berlin, Germany	52°28'N	13°26'E	50	9.8	7.2	20.6	34	-19
Limestone, Maine	46°57'N	67°53'W	230	3.9	9.4	29.4	35	-32
Bolling AFB, Wash. D. C.	38°49'N	76°51'W	20	14.0	10.2	23.0	38	-14
Scott AFB, Ill.	38°33'N	89°51'W	138	13.1	6.2	26.3	38	-23
Blytheville, Ark.	35°58'N	89°57'W	91	15.4	6.8	17.9	39	-18
Riverside, Calif.	33°54'N	117°15'W	461	19.7	16.8	14.4	41	-4
Tucson, Ariz.	32°10'N	110°53'W	809	16.4	11.7	19.0	43	-6
Ft. Huachuca, Ariz.	31°25'N	110°20'W	1439	17.0	14.8	17.0	39	-9
Dhahran, Saudi Arabia	26°17'N	50°09'E	22	26.8	11.8	19.8	48	3
Wheeler, Hawaii	21°29'N	158°02'W	256	22.8	7.5	4.0	32	10
Honolulu, Hawaii	21°20'N	153°55'W	39	24.7	6.7	4.2	35	18
Guam, Philippines	13°29'N	144°48'E	82	27.8	1.7	1.7	33	24
Diego Garcia Island	07°18'S	72°24'E	2	27.7	3.9	2.0	32	23
Canton Island	02°46'S	171°43'W	3	27.7	1.2	0.8	32	24

Depending on circumstances and ground characteristics, the surface air temperature could differ by several degrees over short distances ranging from a few meters to a few kilometers. Also, vertical temperature variations are observed from a few millimeters above the ground to the top of the instrument shelter. On windy, cloudy days or nights, the differences between thermometer readings, within short distances of one another in either the horizontal or the vertical, will be minimal. In high temperature regimes however, with a bright sun and light winds, the ground surface, especially if dry sand, can attain temperatures 17 to 33 C higher than the free air. The temperature of air layers within a few centimeters of the surface will differ only slightly from the ground, but the decrease with height is rapid. The temperature at 1/2 to 1 m above the ground will be only slightly warmer than that observed in the instrument shelter at 1 to 1-1/2 m above the ground. Conversely, on calm clear nights, the ground radiation can produce a temperature inversion, as much as 4 or 5 C, in the air within several meters of the ground.

The induced temperature in military equipment exposed to the sun's heat will vary greatly with physical properties such as heat conductivity, reflectivity, capacity, and type of exposure. Surface and internal temperatures, such as are induced in a boxcar, make the reading of the shelter thermometer only the beginning of the engineering problem.

Table 15.2 is only an initial guide to the effects of various influences on station temperature. Detailed temperature information should be obtained from the climatological record of each station or of stations close by. The latter should be modified for the influences of terrain, proximity to water, and elevation.

15.1.2.3 HORIZONTAL EXTENT OF SURFACE TEMPERATURE

Horizontal differences in surface temperature can arise both from large-scale weather disturbances and from local influences. Weather disturbances such as cold and warm fronts, thunderstorms, and squall lines account for unsystematic changes in the horizontal temperature gradient. Nonuniform radiational heating and cooling of the ground also contribute to turbulent mixing, cloudiness, and vertical motions in the lower troposphere, resulting in constantly changing temperatures at the surface.

Horizontal transport by air currents, referred to as advection, is a key factor in surface temperature differences. Large-scale advection will alternately bring both the relatively dry cold Arctic air masses and the relatively moist warm tropical air masses to the temperate zones. This can produce large changes in the day's mean and the diurnal range of temperature.

Table 15.3 gives estimates of surface temperature differences over varying horizontal distances associated with several kinds of weather phenomena.

Table 15.3. Estimates of the Horizontal Scale of Certain Local Meteorological Conditions

Local Conditions	Horizontal Scale (km)	Temperature Differences (C)
Changes in Air Mass	160 to 1600	3 to 22
Weather Fronts	16 to 160	3 to 22
Squall Lines	8 to 80	3 to 17
Thunderstorms	8 to 24	3 to 17
Sea Breezes	8 to 16	1 to 11
Land Breezes	3 to 8	1 to 6

Large-scale differences are greatest in winter, due to the more substantial differential heating by solar radiation from equator to pole and, consequently, the more intense large-scale motion of the atmosphere. In summer the north-south gradients in solar insolation are much less, but the general increase in the amount of insolation results in more thunderstorms and other air-mass activity.

Systematic differences in the surface temperature between neighboring stations are due to five prime factors: (1) aspect or orientation of the terrain with respect to incident solar radiation, (2) type of surface structure and of soil cover underlying the stations, (3) proximity to the moderating influences of large water bodies, (4) elevation, and (5) difference in solar time for stations that are several hundred miles apart. Sometimes the topography permits "pools" of cold air to drain locally at night into lower basins or valleys. Also, nonuniform distribution of water vapor and cloudiness will result in uneven distributions of short-wave and long-wave radiation and, consequently, uneven cooling and heating at the surface.

A striking example of local influences on surface temperature gradients is found in the temperature contrasts between cities and the surrounding countryside. The sheltering effect of buildings, their heat storage, products of fuel combustion, smog, rain water drainage, and snow removal all act to make the city a relative heat source. Thus, the city's nightly minimum temperature might be 5 to 14 C higher than that of the surrounding suburbs. As another example, in hilly or mountainous terrain the valley floor could have a diurnal temperature range 2 to 4 times as great as that over the peaks, and a temperature minimum from 5 to 17 C lower. Also, some pronounced horizontal temperature gradients

occur along coastlines in temperate latitudes due to the cooling effect of coastal sea breezes.

Generally, temperatures between two stations become more independent of one another with increasing distance (Figure 15.3). One model curve⁴ for fitting the correlation coefficient ρ as a function of distance s between stations is given by

$$\rho = \frac{2}{\pi} [(\cos^{-1} \alpha) - \alpha \sqrt{1 - \alpha^2}] , \quad (15.1)$$

where

$$\alpha = s/(128r) , \quad (15.2)$$

where r is the model parameter, and is in the same units as the distance s . The value of r is, in fact, the distance over which the correlation coefficient is 0.99. For the curve in Figure 15.3, $r = 17.7$ km. While this curve could be fitted by

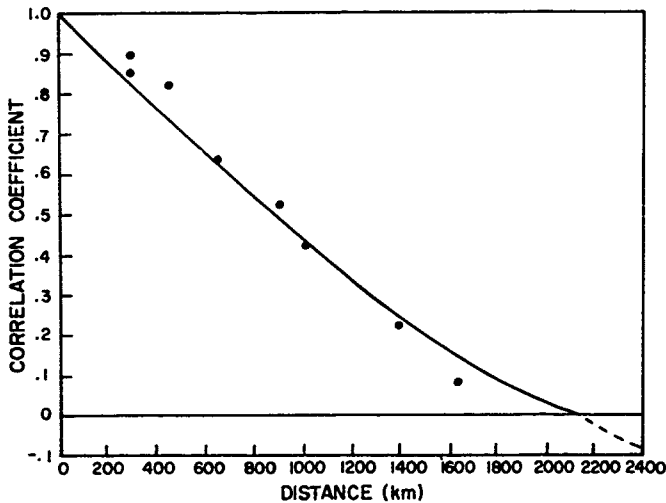


Figure 15.3. The Correlation Coefficient of the Daily Mean Temperature of Columbus, Ohio With That of Nine Other U.S. Stations at Indicated Distances From Columbus

4. Gringorten, I.I. (1979) Probability models of weather conditions occupying a line or an area, J. Appl. Met. 18(No. 8):957.

other models, the given model curve has the quality that the correlation coefficient decreases exponentially with distance between stations for the first few kilometers of separation. Eventually, the correlation coefficient drops to zero at distance 128 r.

In the United States the separation between weather stations averages about 160 km (100 miles), with the exception of the eastern states where it is 30 to 80 km. The root mean square difference of temperatures, as a function of the correlation coefficient ρ between two stations, is approximated by

$$\text{rmsd} = s_T \sqrt{2(1 - \rho)} , \quad (15.3)$$

where s_T is the standard deviation of the hourly temperature (estimated as 5 K for Hanscom AFB). For stations 150 km apart, with $\rho = 0.91$ [Eq. (15.1)], the rmsd should be approximately 2 C.

15 2.4 RUNWAY TEMPERATURES

At airports the desired length of the landing strip or runway is directly related to air temperature. Any discrepancy, therefore, between free air temperature over runways and shelter temperatures is important in establishing safe aircraft payloads and runway lengths. It had been thought, on days when insolation is strong, that the free air temperature over airfield landing strips is significantly higher than standard shelter temperature over the surrounding grassy areas. Results of observations, however, over four airstrips (Easterwood Airport, Hearne Air Force Satellite Field, and Bryan Air Force Base in Texas, and an auxiliary naval airstrip near Houma, Louisiana) have shown that the air between 0.3 and 6 m above a landing strip is about 1/2 C cooler than indicated by the shelter thermometer over adjacent grassy areas. The relative smoothness of the runway surface is the physical cause of daytime flow of air from grass to runway. During the transition from flow over the rough grassy surface the wind speeds up and entrains the cooler air immediately above the runway. When a daytime equilibrium state is established, there will be a large lapse rate close to the ground. This is the effect over both concrete and blacktop airstrips with surrounding grass having only a slightly modifying effect.

In exceptional cases the free air temperature over the runway exceeds the shelter temperature, but by no more than 1/2 C when averaged over 10 min, 1 C when averaged over 1 min with a dry soil environment, and 1/4 C (5-min mean) with a swamp environment. Thus, the standard method of temperature measurement in a properly exposed shelter over grass provides a representative temperature for the estimations of runway length and aircraft payloads.

15.1.2.5 TEMPERATURE EXTREMES

A knowledge of the occurrence of hot and cold temperature extremes is important for the design of equipment and the selection of material that will be exposed to the natural environment. The hourly temperature observations at most locations are not normally distributed around the mean monthly values. Departures from a normal distribution are largest in the temperate and northerly latitudes during the winter months when the temperature distributions tend to be bimodal. Thus, the straightforward method for determining the frequency distribution of hourly temperatures is to obtain a representative sample of observations for each location and compute the distributions. Estimates of the frequency distribution from such data can be made using the Blom formula, given by

$$\hat{P}(T) = (n_T - 3/8)/(N + 1/4) , \quad (15.4)$$

where $\hat{P}(T)$ is the estimated cumulative probability of the temperature T , n_T is the number of observations equal to or less than T , and N is the overall sample size. Since representative samples of data are not easily obtained for regions outside of North America, an objective method has been developed by Tattelman and Kantor⁵ so that the frequency distribution of surface temperature can be estimated at all locations from data in climatic summaries that are available for most locations throughout the world.

Because the warmest temperatures in the world are found at locations where the monthly means are high and the mean daily range is large, Tattelman et al,⁶ developed an index using these values. The index is expressed by

$$I_w = \bar{T} + (\bar{T}_{\max} - \bar{T}_{\min}) , \quad (15.5)$$

where I_w is the warm temperature index, \bar{T} is the monthly mean, \bar{T}_{\max} is the mean daily maximum, and \bar{T}_{\min} is the mean daily minimum temperature for ($K - 273$) for the warmest month. The index was related to temperature occurring 1, 5, and 10 percent of the time during the warmest months at a number of locations; it appears in the following regression equations for estimating monthly 1, 5, and 10 percent warm temperature extremes.⁵

-
5. Tattelman, P., and Kantor, A.J. (1977) A method for determining probabilities of surface temperature extremes, *J. Appl. Meteorol.* 16(No. 11):1175.
 6. Tattelman, P., Sissenwine, N., and Lenhard, R.W. (1969) World Frequency of High Temperature, AFCRL-69-0348.

$$\hat{T}_{1\%} = 0.676I_w + 10.657 \quad , \quad (15.6)$$

$$\hat{T}_{5\%} = 0.733I_w + 5.682 \quad , \quad (15.7)$$

$$\hat{T}_{10\%} = 0.762I_w + 2.902 \quad . \quad (15.8)$$

where \hat{T} is the estimated temperature in (K - 273) occurring 1, 5, and 10 percent of the time, respectively. The same principle can be used to estimate cold temperature extremes. The cold temperature index is

$$I_c = \bar{T} - (\bar{T}_{max} - \bar{T}_{min}) \quad , \quad (15.9)$$

where I_c is the cold temperature index, \bar{T} is the monthly mean, \bar{T}_{max} is the mean daily maximum, and \bar{T}_{min} is the mean daily minimum temperature (K - 273) for the coldest month. The corresponding regression equations (Tattelman and Kantor⁵) are

$$\hat{T}_{1\%} = 1.069I_c - 7.013 \quad , \quad (15.10)$$

$$\hat{T}_{5\%} = 1.084I_c - 3.050 \quad , \quad (15.11)$$

$$\hat{T}_{10\%} = 1.082I_c - 0.704 \quad . \quad (15.12)$$

This technique can be used to map global temperature extremes; percentiles of surface temperatures can be readily estimated for any geographic area or specific location for which monthly climatic temperature summaries are available. Estimates of the 1 percent warm and cold temperature extremes for the Northern Hemisphere are shown in Figures 15.4 and 15.5.

Most extreme high temperatures have been recorded near the fringes of the deserts of northern Africa and southwestern U.S. in shallow depressions where rocks and sand reflect the sun's heat from all sides. In the Sahara, the greatest extremes have been recorded toward the Mediterranean coast, leeward of the mountains after the air has passed over the heated desert. The highest temperature on record is 58 C (136 F) at Al Aziziyah, Libya (32°32'N, 13°1'E, elevation 112 m). Northern Africa and eastward throughout most of India is the hottest part of the world. Large areas attain temperatures greater than 43 C (110 F) more than 10 percent of the time during the hottest month. Sections of northwest

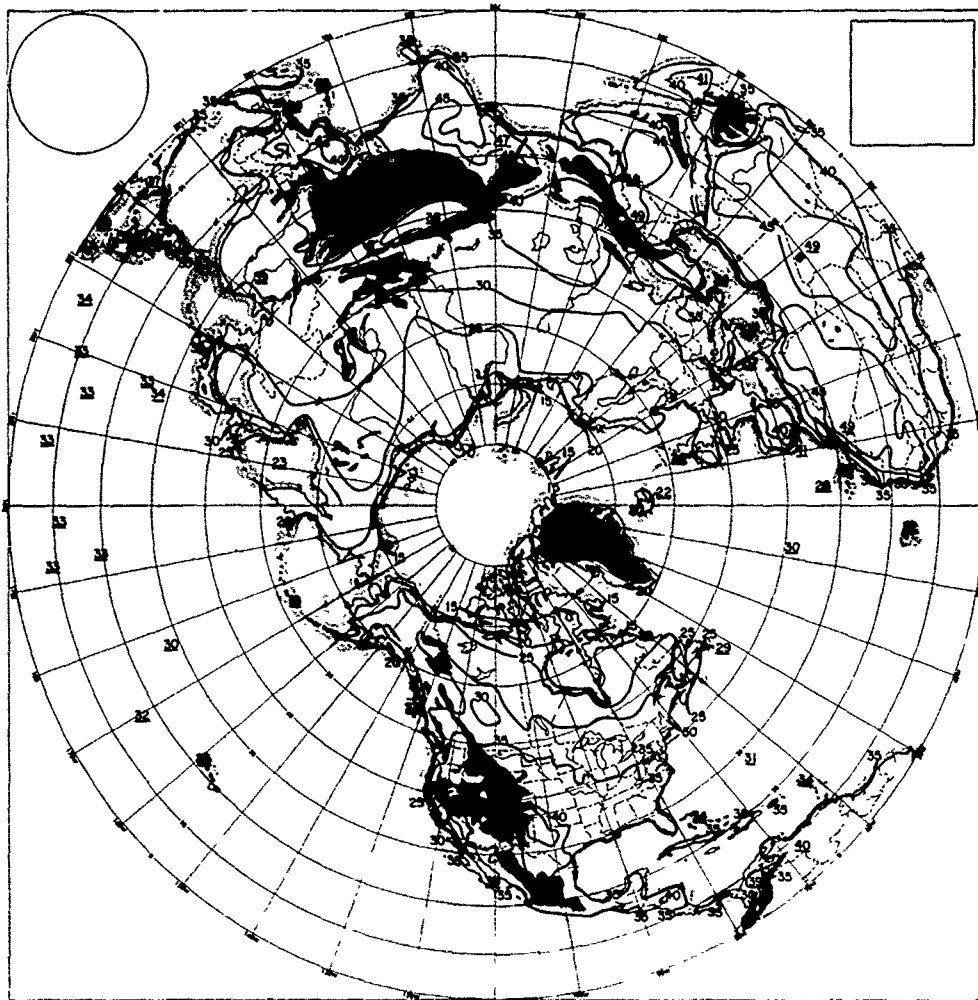


Figure 15.4. Temperature Equalled or Exceeded 1 Percent of the Time During the Warmest Month

Africa experienced temperatures greater than 49 C as much as 1 percent of the time during the hottest month of the year. Regions in Australia and South America have temperatures at and above 38 C (100 F) much of the time, but do not experience temperatures greater than 43 C (110 F) more than 1 percent of the time during the hottest month. The southwestern U.S. and a narrow strip of land in western Mexico are exceptionally hot. A substantial part of the area experiences temperatures equal to or greater than 43 C (110 F) for 1 percent of

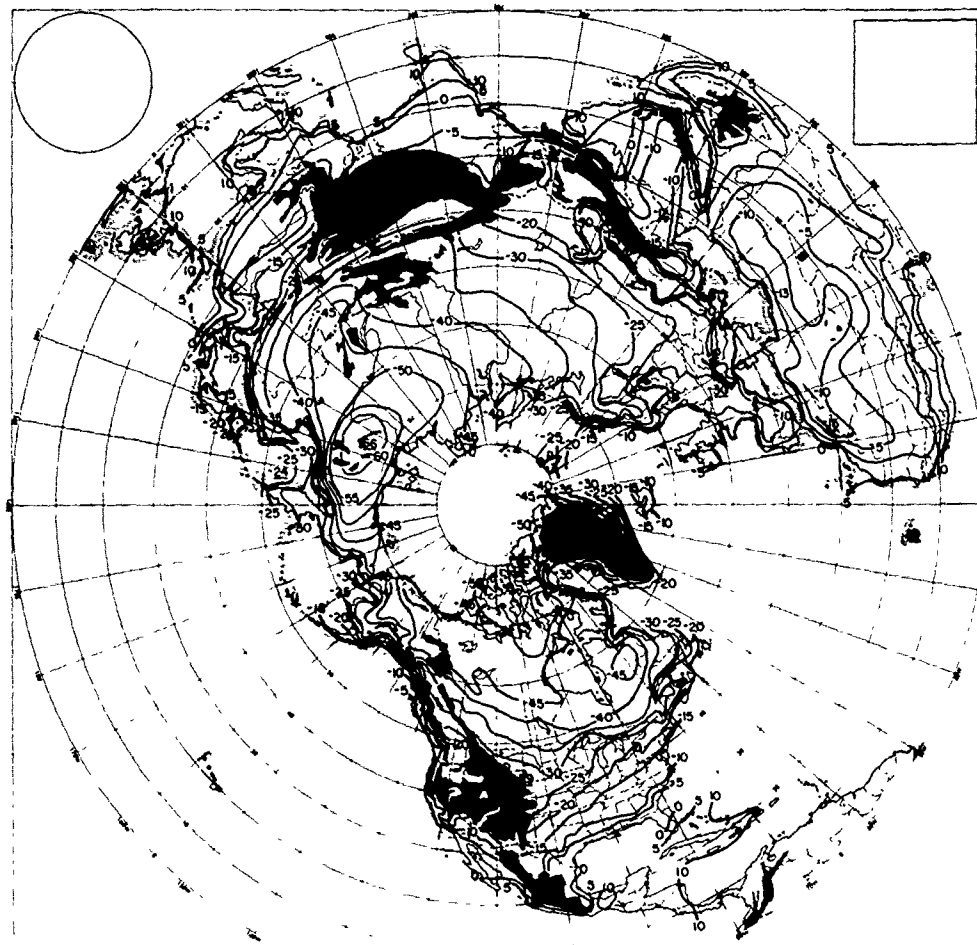


Figure 15.5. Temperature Equalled or Colder 1 Percent of the Time During the Coldest Month

the time in the hottest month. Death Valley, within this area, has temperatures equal to or greater than 49°C (120°F) for 1 percent of the time in the hottest month and it once had a record temperature of 57°C (134°F).

Geographic areas of extreme cold include the Antarctic Plateau (2700 to 3600 m elevation), the central part of the Greenland Icecap (2500 to 3000 m elevation), Siberia between 63°N and 68°N , 93°E and 160°E (less than 760 m elevation), and the Yukon Basin of Northwest Canada and Alaska (less than

760 m elevation). The generally accepted record low temperature (excluding readings in Antarctica) is -68 C (-90 F) in Siberia.

15.1.2.6 THE GUMBEL MODEL

For equipment that is either in continuous operation or is on standby status, thereby continuously exposed to all temperatures, the statistic of interest is the extreme temperature that is likely to occur during a full month, season, year, decade, or whatever period is considered to be the useful lifetime of the equipment.

Many extreme values have been estimated effectively by a model that has become known as the Gumbel distribution. Let us assume the annual highest temperature T_i has been recorded for each of N years ($i = 1, N$) with average \bar{T} and standard deviation s_T . Then the Gumbel estimate of the cumulative probability P_T of the annual extreme high temperature T is given by

$$P_T = \exp [-\exp(-y)] \quad . \quad (15.13)$$

where

$$y = \tilde{y} + \sigma_y (T - \bar{T}) / s_T \quad , \quad (15.14)$$

where, to five decimal places

$$\tilde{y} = 0.57722 \quad (15.15)$$

and

$$\sigma_y = 1.28255 \quad .$$

(There are other estimates to the Gumbel distribution. This one is preferred for its simplicity as well as degree of accuracy.) The quantity y is referred to as the reduced variate. If one is interested in the cold temperature, these formulas hold with T and \bar{T} reversed in Eq. (15.14).

If the lifetime of a piece of equipment is intended to be n years, then the cumulative probability $P_T(n)$ that the temperature T will not be exceeded in the n years, is

$$P_T(n) = \exp [-\exp(-y + \ln n)] \quad (15.16)$$

where y is given by Eq. (15.14). Assuming, for example, that we want to estimate the temperature T that has only a 10 percent probability or risk of being exceeded over n years, we set $P_T(n)$ equal to 0.9 in Eq. (15.16) and solve for y , obtaining

$$y = \ln n - \ln(-\ln P) \quad , \quad (15.17)$$

which we in turn use in Eq. (15.14) to obtain

$$\hat{T} = T + s_T(y - \bar{y})/\sigma_y \quad . \quad (15.18)$$

The return period is a term sometimes used in association with the extreme. In terms of the cumulative probability (P_T) of the annual extreme temperature it is equal to $1/(1 - P_T)$ years. The return period is not to be confused with the planned lifetime (n) of the equipment. Roughly speaking, the temperature with the 100-year return period, or the annual 1-percentile ($P_T = 0.99$) is approximately the 10-percentile temperature of a 10-year planned life.

The Gumbel distribution, with a set of periodic extremes, is the easiest model to use, but there are reservations in its application. Theoretically the basic distribution, such as the station temperature taken hourly, should be an exponential type, such as Pearson Type III or Gaussian. However, this condition may not be sufficient because the record may not be long enough to make the annual extreme fit into a Gumbel distribution. The Gumbel distribution is only the limiting form over long times and may not be adequately reached over short periods. It is advisable, therefore, to test the data to determine if the Gumbel distribution is applicable. Figure 15.6 illustrates the use of special-purpose "Extreme Probability Paper" in which the cumulative probability, P_{T_i} , is read on the vertical axis to correspond to T on the horizontal axis. Alongside the scale of P_T is the scale of the reduced variate y , which is uniform on this paper. A Gumbel distribution appears as a straight line.

Let us suppose a set of N extreme temperatures T_i for each of N years ($i = 1, N$) is ordered from lowest to highest value. The cumulative probability of the i th lowest temperature, since it is an extreme, is best estimated by

$$\hat{P}_T = (i - 0.44)/(N + 0.12) \quad (15.19)$$

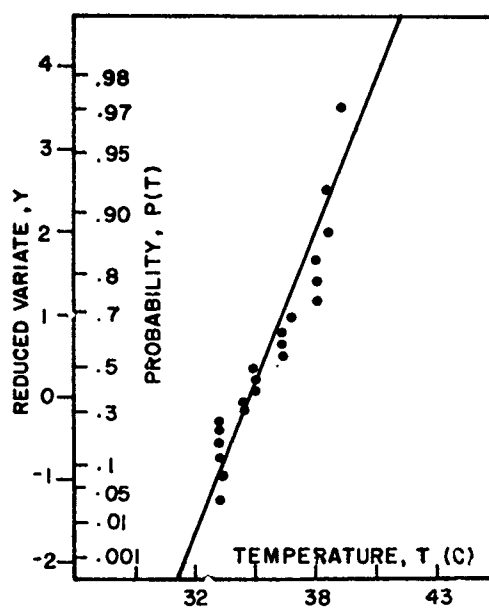


Figure 15.6a. Annual Highest Temperature, Hanscom AFB, Mass., 21 Ordered Values (1944-1964)

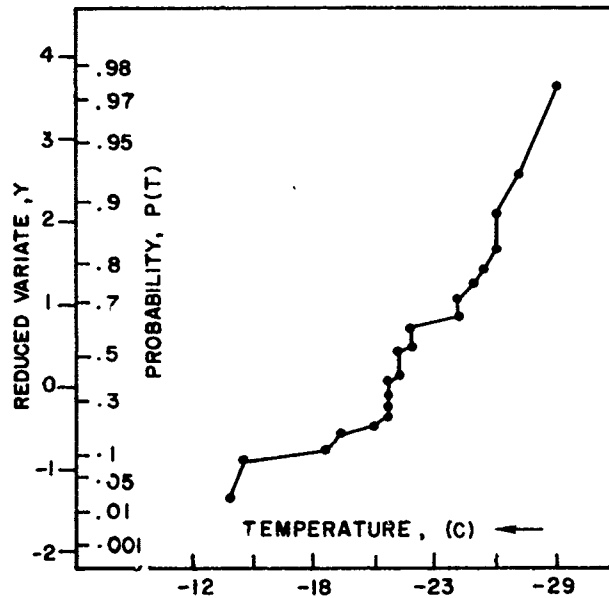


Figure 15.6b. Lowest Temperatures Occurring at Hanscom AFB, Mass. During 22 Winter Seasons (1943-1965) Ordered From Warmest to Coldest, and Plotted as the Probability That the Coldest Temperature Will Not Be Below the Given Value

rather than Eq. (15.4). Now, in the example of Figure 15.6a, we have the plot of the annual highest temperatures of 21 yr (1944-1964 at Hanscom AFB, Mass.) ordered from lowest to highest value and having cumulative probability estimates P_T given by Eq. (15.19). The mean is $T = \bar{T} = 309$ K and the standard deviation is $s_T = 1.9$ K. The solution of Eq. (15.14) gives the straight line plot between y and T as shown. Whether the straight line, and therefore the Gumbel distribution, adequately fits the distribution is a matter of judgment. If accepted, and it should be in this example, then the 99-percentile ($P_T = 0.99$), or the 1 percent extreme, is estimated, by Eqs. (15.17) and (15.18) with $n = 1$, as 315 K. For a lifetime of 25 yr ($n = 25$) the temperature of 10 percent risk ($P_T = 0.9$) is given, by Eqs. (15.17) and (15.18), as 316 K.

As another example, Figure 15.6b shows the plot of the extreme low temperatures of 22 winter seasons (1943-1965), at Hanscom AFB, Mass. The mean is $\bar{T} = 251$ K and the standard deviation is $s_T = 3.7$ K. A straight line fit of these data is not satisfactory. Possibly a concave curve would be more appropriate. The Gumbel model is not acceptable in this case, and consequently another model should be tried.

15.1.2.7 TEMPERATURE CYCLES AND DURATIONS

High temperature extremes inevitably occur in a well pronounced diurnal cycle, modified by wind and by moisture content. Typical of a hot climate, the record of Yuma, Arizona ($32^{\circ}51'N$, $114^{\circ}24'W$) (Figure 15.7) reveals a mean diurnal temperature range of 15.3 C for the middle 20 days in July. The dew-point has a median of 14 C with a small diurnal range. Relative humidity, consequently, has a large-amplitude diurnal cycle. Wind speed at anemometer levels of 6 to 8 m above ground averages approximately 4 m/sec, with little diurnal range. Solar insolation, on the other hand, has a large diurnal range, with a maximum clear-sky value of 88.2 L/h and a minimum value of zero from 2000 LST in the evening till 0500 LST in the morning. For the hottest areas on earth (for example, the Sahara Desert) Table 15.4 presents the associated cycles of temperature, relative humidity, windspeed, and solar insolation when the afternoon temperature in the middle of a 5-day period reaches 49 C, which occurs about 1 percent of the time in the hottest month.

Death Valley, California is also one of the hottest areas, but is close to 60 m below sea level, resulting in extreme absorption of solar radiation before it reaches the ground. Consequently its maximum clear-sky solar insolation of 82.5 L/h is less than that shown in Figure 15.7. Solar insolation increases with elevation roughly in accord with the exponential model given by

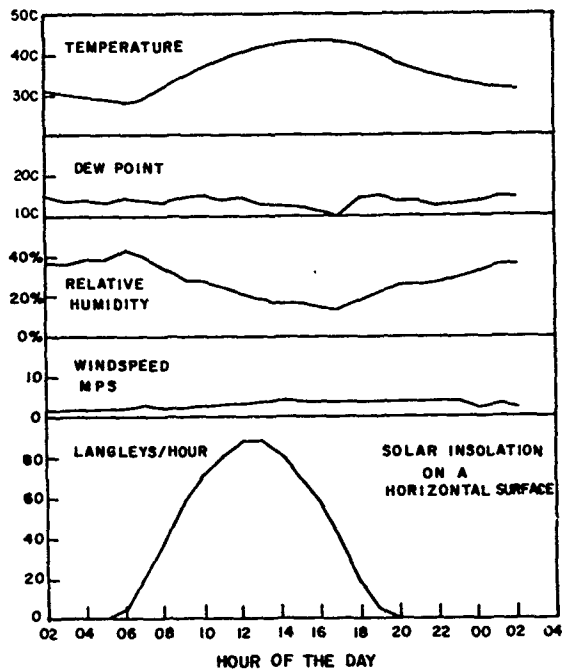


Figure 15.7. Yuma, Arizona Typical July Diurnal Cycles When Maximum Daily Temperature Equals or Exceeds 44 C (111 F), Based on 1961-1968 Data

$$I = I_1 e^{-a(p-p_1)} \quad , \quad (15.20)$$

where p and p_1 are, respectively, atmospheric surface pressures for a given station and another reference station, at roughly the same latitude, I_1 is the solar insolation at the reference station, and the value for a is dependent on the location. For Yuma and Death Valley, where the mean atmospheric surface pressures are about 1006 mb and 1020 mb respectively, $a = 0.00461 \text{ mb}^{-1}$.

The hottest locations in the Sahara Desert are relatively high, at about 300 m above sea level, with atmospheric pressure about 977 mb. Thus Eq. (15.20) yields an estimate for the peak solar insolation at these elevations of about 100 L/h. Most countries, however, including the U.S., Canada, and the United Kingdom, have adopted a peak figure for solar insolation, for operational and design purposes, of 96 L/h.

Heavy clouds and precipitation reduce the incident solar insolation. At a few stations, the National Weather Service has taken records of incoming solar

Table 15.4. Diurnal Cycles of Temperature and Other Associated Elements for Days When the Maximum Temperature Equals or Exceeds the Operational 1 Percent Extreme Temperature (322 K) in the Hottest Month in the Hottest Area

Item	Time of Day (hr)											
	1	2	3	4	5	6	7	8	9	10	11	12
Temperature (K)												
Hottest Day	308	307	307	306	306	305	306	308	311	314	316	317
1 day before or after	309	308	307	306	306	305	306	309	311	313	315	317
2 days before or after	307	307	306	306	305	305	306	308	310	312	314	315
Other Elements												
Relative Humidity (%) (dp = -7 C)	6	7	7	8	8	8	8	6	6	5	4	4
Windspeed (m/sec)	2.7	2.7	2.7	2.7	2.7	2.7	2.7	2.7	2.7	4.3	4.3	4.3
Solar Radiation (L/h)	0	0	0	0	0	5	23	43	63	79	90	96
Time of Day (hr)												
Item	13	14	15	16	17	18	19	20	21	22	23	24
Temperature (K)												
Hottest Day	320	321	321	322	321	321	319	315	314	312	311	310
1 day before or after	318	320	320	321	320	319	317	315	313	311	310	309
2 days before or after	316	317	319	320	319	318	317	314	312	311	310	309
Other Elements												
Relative Humidity (%) (dp = -7 C)	3	3	3	3	3	3	3	4	5	6	6	6
Windspeed (m/sec)	4.3	4.3	4.3	4.3	4.3	4.3	4.3	4.3	4.3	4.3	4.3	2.7
Solar Radiation (L/h)	96	90	79	63	43	23	5	0	0	0	0	0

insolation. Table 15.5 gives the results of processing such data from Albuquerque, N. M. It presents estimates of the probabilities with which daily incoming solar insolation equals or exceeds the given amount in June. In contrast,

Table 15.5. Probability of Daily Solar Insolation Equalling or Exceeding Given Amounts for Given Number of Consecutive Days in June, at Albuquerque, N.M. (Station elevation is 1620 m. Peak clear sky solar insolation was observed at 910 L/day)

Insolation L/Day	No. of Consecutive Days					
	1	2	4	8	15	30
850	0.03					
800	0.24	0.06				
750	0.49	0.28	0.09			
700	0.71	0.54	0.31	0.11		
650	0.81	0.70	0.52	0.29	0.09	
600	0.90	0.84	0.77	0.52	0.29	0.08
550	0.935	0.90	0.81	0.65	0.44	0.20
500	0.955	0.93	0.87	0.75	0.57	0.33
450	0.971	0.95	0.91	0.82	0.67	0.43
400	0.985	0.972	0.946	0.87	0.81	0.65
350	0.9933	--	0.973	0.945	0.902	0.82
300	0.9946	--	0.980	0.958	0.928	0.86
250	0.9975	--	--	0.980	0.963	0.932
200	0.999	--	--	--	--	0.970

Table 15.6 gives corresponding results for the insolation at Caribou, Maine, where there is much more frequent cloudiness and precipitation.

The operability of equipment in a cold climate is very much dependent on the duration of extreme cold. Unlike the hot extremes, cold extremes are usually accompanied by very small diurnal ranges. The direct approach for determining the duration of cold temperature is by an analysis of hourly data. Such data are available for many stations in North America, but are not generally available for other regions of the world. Data from 108 stations in the U.S. and Canada have been analyzed⁷ to obtain information on the longest period of time during which the temperature remained at or below eight "threshold" values (from 0 C to -53 C) during a 10-yr period. Figure 15.8, taken from that report, shows the results for a threshold-temperature of -23 C. The report also presents the expected (approximately 50 percent probability) duration of the temperature at or below six "threshold" temperatures (from 0 C to -40 C) during a

7. Tattelman, P. (1968) Duration of Cold Temperature Over North America, AFCRL-68-0232.

Table 15.6. Probability of Daily Solar Insolation Equalling or Exceeding Given Amounts for Given Number of Consecutive Days in June, at Caribou, Maine.
 (Station elevation is 190 m. Peak clear sky solar insolation was observed at 843 L/day)

Insolation L/Day	No. of Consecutive Days				
	1	2	4	8	15
850					
800	0.019				
750	0.085	< 0.02			
700	0.20	0.057			
650	0.31	0.13	0.02		
600	0.40	0.20	0.05		
550	0.47	0.26	0.086		
500	0.55	0.33	0.13	0.024	
450	0.59	0.40	0.18	0.037	
400	0.66	0.50	0.26	0.075	
350	0.72	0.56	0.33	0.12	0.02
300	0.78	0.67	0.47	0.22	0.062
250	0.82	0.72	0.54	0.30	0.10
200	0.88	0.80	0.66	0.42	0.22
150	0.921	0.87	0.77	0.59	0.37
100	0.965	0.943	0.90	0.79	0.63
90	0.975	0.96	0.92	0.84	0.72
80	0.980	0.962	0.93	0.86	0.75
70	0.987	0.978	0.956	0.912	0.83
60	0.9931	--	0.971	0.947	0.903
50	0.9961	--	--	0.977	0.95
40	0.99906	--	--	--	0.97

single winter season. Figure 15.9 shows the single winter results for a threshold value of -23 C.

Estimates of duration have been made using data that consisted mainly of daily, monthly and annual average maximum and minimum, and monthly and annual absolute maximum and minimum, for some 35 to 50 yr, at Siberian, Yukon, and Alaskan stations. The mean January temperature in eastern Siberia (Verkhoyansk and Oimyakon) is -48 C (-54 F). Table 15.7 presents estimates of the lower 20-percentile of (a) the average temperature (averaged for durations

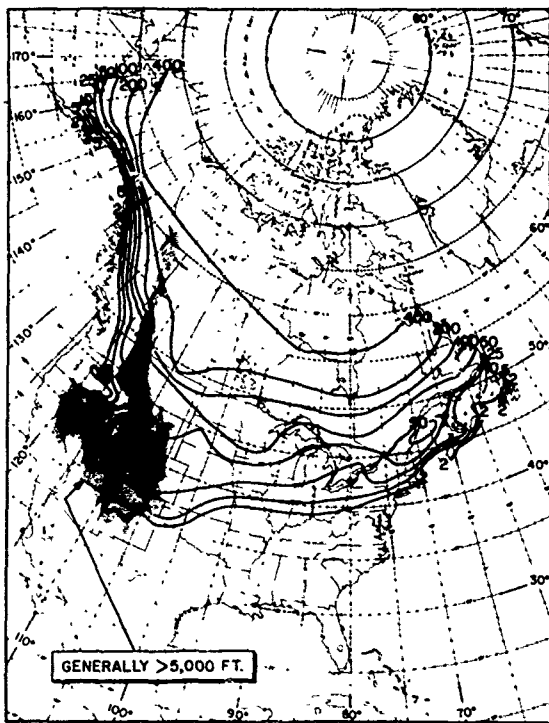


Figure 15.8. Longest Duration (h) of Temperature $\leq -23^{\circ}\text{C}$ (-10°F) in 10 Winters, From Tattelman⁷

ranging from 1 h to 32 days), (b) the maximum temperature for the durations shown, and (c) the minimum temperature for the same durations.

The duration of temperature, hot or cold, is of general interest anywhere. In the mid-latitude belt, the temperatures of Minneapolis, Minn., are typical (Figure 15.10). The January probability distribution of all hourly temperatures has a 1-percentile value of -28.3°C , and a 50-percentile or median value of -9.4°C . That is, the range from the lower 1-percentile to the median is 19°C . The 24-h averages, as expected, have a narrower range, from -26 to -9°C . The monthly average is much narrower, from -18°C for the 1-percentile to -10.6°C for the median. Similarly, the July temperatures, which range from the 50-percentile of 22°C to the 99-percentile of 34°C , have 24-h averages ranging from 23 to 31°C , and monthly averages in the narrower range from 23 to 25.5°C . These figures imply a relatively high hour-to-hour correlation, estimated at 0.982 in the midwinter month of January, and 0.919 in the midsummer month of July.

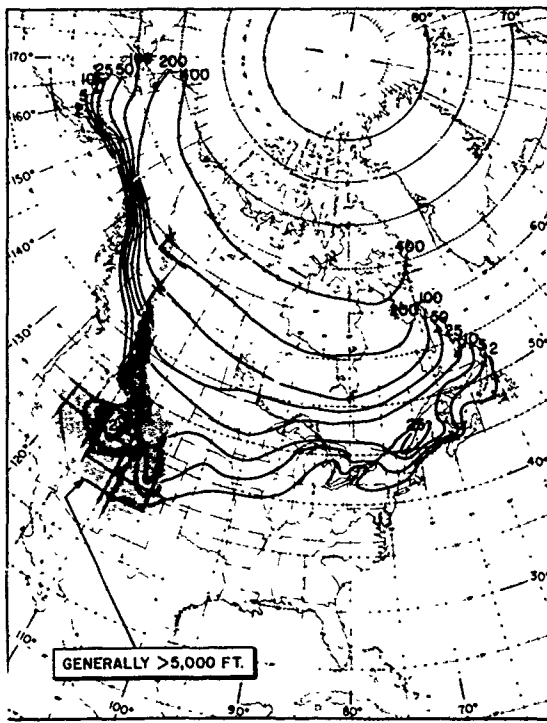


Figure 15.9. Expected Longest Duration (h) of Temperature $\leq -23^{\circ}\text{C}$ (-10°F) During a Single Winter Season, From Tattelman⁷

Table 15.7. Durations of Cold Temperatures Associated With the -51°C Extreme. (Each temperature in this table is the maximum, average, or the minimum in an operational time exposure of m hours, with 20 percent probability of occurrence, during January, in a Siberian cold center)

	Time m(hr)									
	1	3	6	12	24	48	96	192	384	768
Maximum Temperature	-51°C	-50	-49	-48	-47	-45	-43	-39	-35	-32
	-60°F	-58	-57	-55	-53	-49	-45	-38	-31	-25
Average Temperature	-51°C	-51	-51	-51	-51	-51	-51	-50	-50	-49
	-60°F	-60	-60	-60	-60	-60	-59	-58	-58	-57
Minimum Temperature	-52°C	-52	-53	-54	-56	-57	-58	-60	-62	-63
	-61°F	-62	-64	-65	-68	-70	-73	-76	-79	-82

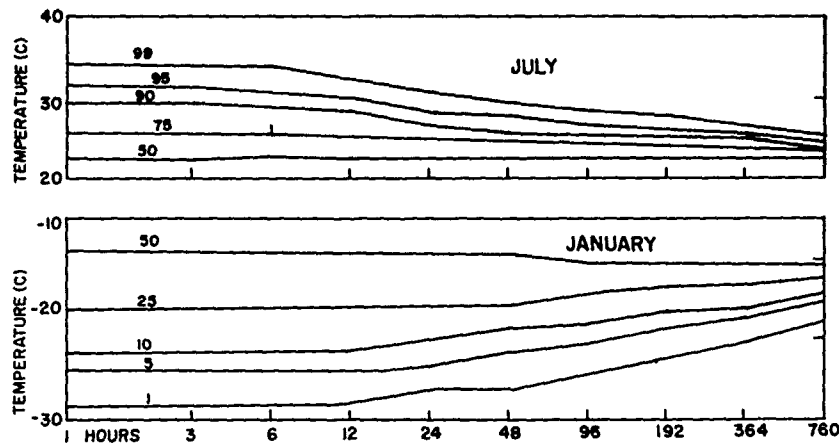


Figure 15.10. The Distribution of the Averages of Consecutive Hours of Temperature at Minneapolis, Minn. The upper half is for the mid-summer month from 1 July to 1 August; the lower half is for the mid-winter month from 1 January to 1 February. Each curve is labelled with percent probability of occurrence

Hourly observations have been taken at Minneapolis for many years, making many useful summaries possible. Figure 15.11 shows a sample distribution (1949-1958) of hourly January temperatures alongside the left axis and the distribution of m-hour minima over the body of the graph, m from 1 hour to 768 hours (1 Jan to 1 Feb inclusive). Figure 15.12 shows the sample distributions of hourly temperatures in January of m-hour maxima. As an example of the usefulness of such a chart, freezing conditions (≤ 0 C) are shown as 94 percent frequent for 1-h durations. For 24 consecutive hours this frequency reduces to 83 percent, for 8 days (192 h) to 42 percent, and for 16 days (384 h) to 10 percent.

15.1.3 Upper Air Temperature

The temperature data discussed in this section are from direct and indirect observations obtained from balloon-borne instruments, primarily radiosondes, for altitude up to 30 km, and from rockets and instruments released from rockets for altitudes between 30 and 90 km.

15.1.3.1 SEASONAL AND LATITUDINAL VARIATIONS

The Reference Atmospheres presented in Chapter 14 of the Handbook of Geophysics provide tables of mean monthly temperature-height profiles, surface to 90 km, for 15° intervals of latitude between the equator and North Pole. These profiles depict both the seasonal and latitudinal variations in mean monthly

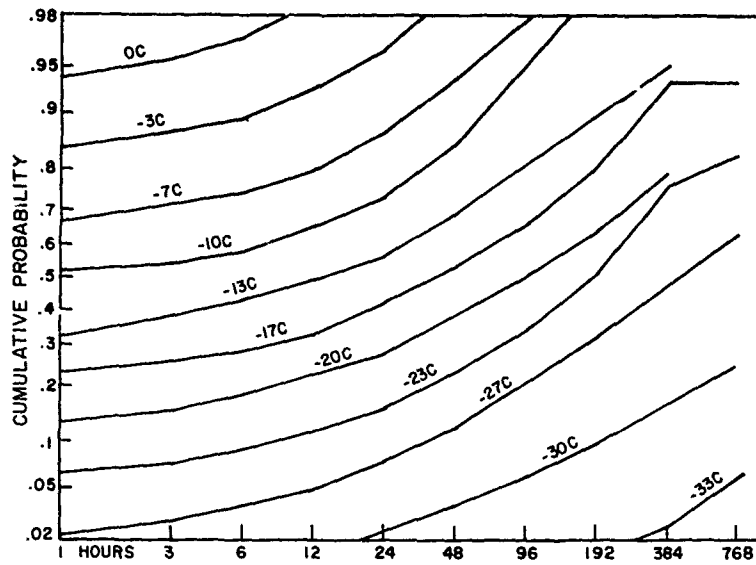


Figure 15.11. The Cumulative Probability of the M-Hour Minimum Temperature (1 January to 1 February) at Minneapolis, Minn.

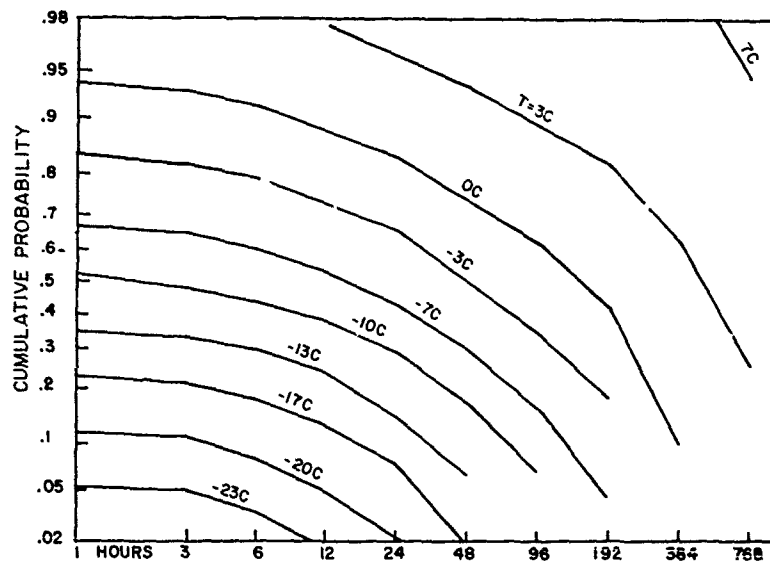


Figure 15.12. The Frequency of Duration (h) of the Temperature ($\leq T$) in the Mid-Winter Month (1 January to 1 February) at Minneapolis, Minn. (Based on 1943-1952 Data)

temperatures. The largest seasonal variations in temperature occur at altitudes between 70 and 80 km near 75°N latitude. In this region the mean monthly temperature fluctuates from 230 K in January to 160 K in July.

In the upper mesosphere, 60 to 85 km, mean monthly temperatures decrease toward the pole in summer and towards the equator in winter. In the upper stratosphere, 20 to 55 km, conditions are reversed; temperature decreases toward the pole in winter and toward the equator in summer. At altitudes between 15 and 20 km temperature decreases toward the equator in all seasons. Temperature-altitude profiles, surface to 60 km, for the midseason months at Ascension Island, 8°S, Wallops Island, 38°N, and Ft. Churchill, 59°N, are given in Figure 15.13 and illustrate the magnitude of the seasonal and latitudinal variations in mean monthly temperatures.

15.1.3.2 DISTRIBUTION AROUND MONTHLY MEANS AND MEDIANs

The distributions of observed temperatures around the median values for altitudes up to 90 km in January and July at 30°, 45°, 60°, and 75°N are shown in Tables 15.8a to 15.8d. Median and high and low values that are equalled or more severe 1, 10, and 20 percent of the time during these months are given for 5-km altitude increments between the surface and 90 km. Distributions below 30 km are based on radiosonde observations taken in the Northern Hemisphere, and those above 30 km are based on meteorological and experimental rocket observations taken primarily from launching sites in or near North America. The 1-percent values are considered to be rough estimates as they are based on the tails of the distributions of observed values plotted on probability paper. Estimates of values for altitudes above 50 km are less reliable than those below 50 km because of the paucity of data and larger observational errors at the higher altitudes. Only median temperatures are given above 55 km at 75°N for July due to the small number of observations available for the higher altitudes over the polar regions in summer.

In tropical regions, 0° to 15° latitude, the day-to-day variations of temperature are normally distributed about the mean at altitudes up to 50 km. Consequently, a reasonably accurate estimate of the distribution of temperature at a given altitude can be obtained from the standard deviations and the monthly means.

The standard deviations of observed temperatures around the mean monthly values for the midseason months at Ascension Island (Table 15.9) are typical of the day-to-day variations found in the tropics. Values are not given for altitudes above 50 km as there are too few daily observations on which to base the monthly temperature distributions. The observed standard deviations include the rms

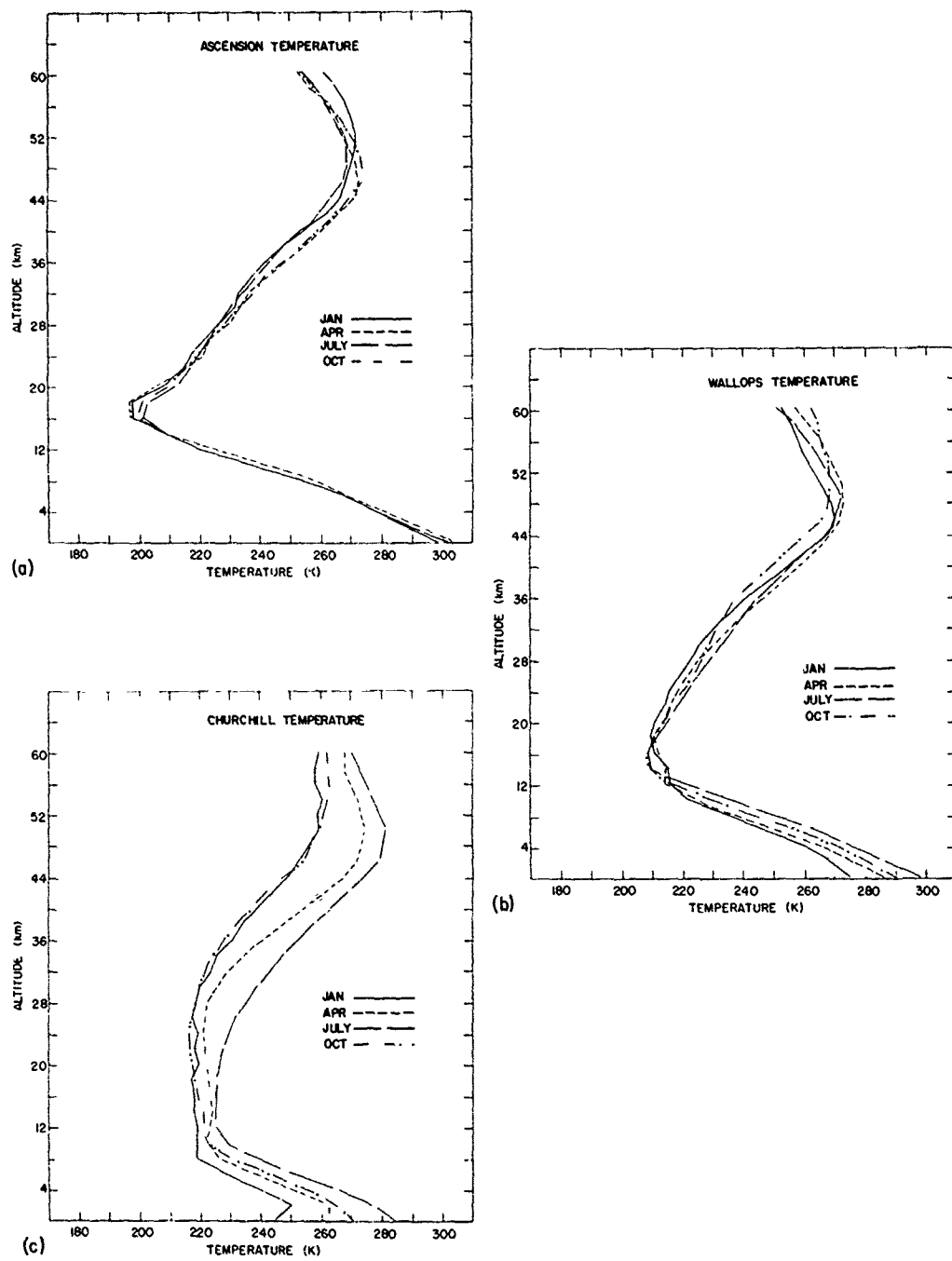


Figure 15.13. Seasonal Differences in the Temperature-Altitude Profiles at Ascension Island, Wallops Island, and Ft. Churchill

Table 15.8a. Median, $H_{1\%}$, and Low Percentile Values of Temperatures for January and July at 30°N

Altitude (km)	Median (K)	1%		10%		20%	
		High (K)	Low (K)	High (K)	Low (K)	High (K)	Low (K)
J A N U A R Y							
5	262	272	251	267	256	265	258
10	229	239	219	235	223	233	225
15	208	221	198	216	203	214	205
20	208	222	200	216	203	214	204
25	220	231	210	226	216	224	217
30	229	239	218	236	224	234	226
35	240	254	222	248	232	245	235
40	252	270	240	262	249	258	250
45	264	283	253	277	258	272	260
50	266	281	256	276	260	273	262
55	254	272	231	267	243	263	248
60	243	254	223	248	232	246	235
65	231	254	218	242	226	238	228
70	220	235	198	227	204	225	210
75	218	253	197	237	203	227	208
80	209	243	187	230	194	217	197
J U L Y							
5	272	278	262	274	266	275	268
10	238	249	227	246	232	242	234
15	204	216	196	211	200	210	200
20	212	223	203	218	206	216	206
25	223	230	216	227	218	226	219
30	234	241	226	238	229	236	231
35	244	254	237	250	240	247	242
40	256	267	247	263	251	261	253
45	266	275	259	272	264	269	265
50	269	282	258	278	262	275	264
55	264	273	247	269	253	267	256
60	247	262	231	255	240	252	243
65	228	240	215	236	219	234	222
70	209	222	186	219	194	214	200
75	200	218	178	214	192	209	196
80	193	207	182	200	189	198	191

Table 15.8b. Median, High, and Low Percentile Values of Temperatures for January and July at 45°N

Altitude (km)	Median (K)	1%		10%		20%	
		High (K)	Low (K)	High (K)	Low (K)	High (K)	Low (K)
J A N U A R Y							
5	250	263	233	257	239	254	242
10	220	233	206	227	212	225	214
15	217	231	202	225	208	222	211
20	215	227	203	222	208	220	210
25	215	233	197	226	205	224	209
30	221	240	209	230	214	226	219
35	233	258	215	251	223	243	226
40	247	272	226	264	236	257	240
45	262	288	240	283	250	271	254
50	265	282	249	274	256	270	258
55	253	275	229	267	239	263	245
60	244	266	220	263	230	257	241
65	235	255	214	246	223	243	228
70	226	246	206	238	211	234	217
75	225	261	197	245	205	235	210
80	216	248	185	237	197	228	202
J U L Y							
5	267	277	255	274	259	272	262
10	235	247	222	240	227	239	230
15	216	227	205	222	206	220	212
20	219	233	207	227	213	225	215
25	225	233	216	229	217	228	221
30	234	242	228	239	231	237	232
35	245	254	238	250	241	248	243
40	256	268	250	265	254	263	255
45	268	280	260	276	263	272	265
50	273	283	264	279	268	277	270
55	264	273	249	269	255	267	260
60	247	270	230	264	235	260	238
65	230	245	216	241	223	238	220
70	213	226	188	219	196	216	202
75	195	210	175	205	186	201	190
80	183	203	154	195	163	191	170

Table 15.8c. Median, High, and Low Percentile Values of Temperatures for January and July at 60°N

Altitude (km)	Median (K)	1%		10%		20%	
		High (K)	Low (K)	High (K)	Low (K)	High (K)	Low (K)
J A N U A R Y							
5	240	255	225	249	231	246	234
10	217	231	203	224	209	222	211
15	217	231	203	225	209	222	212
20	215	236	194	226	204	222	208
25	212	241	185	229	197	223	203
30	216	253	203	235	204	225	210
35	221	277	204	259	209	238	214
40	227	300	206	278	211	246	219
45	243	303	219	282	225	255	231
50	251	289	226	280	240	271	245
55	251	263	225	275	233	256	238
60	243	271	210	261	224	253	234
65	238	262	208	258	218	249	222
70	239	264	212	253	219	249	225
75	232	255	180	249	203	246	213
80	223	248	173	243	195	239	204
J U L Y							
5	260	271	250	266	254	264	256
10	225	238	214	233	219	231	221
15	225	235	217	231	221	229	223
20	225	233	219	230	222	229	223
25	229	236	222	233	225	232	226
30	239	245	232	243	234	241	235
35	252	258	243	256	247	253	248
40	265	272	259	269	263	268	262
45	277	287	271	283	274	280	275
50	279	290	273	286	277	284	279
55	271	278	257	275	264	273	266
60	259	273	212	265	250	263	253
65	238	259	225	253	230	248	233
70	214	239	202	226	208	222	211
75	190	202	178	196	182	194	186
80	166	180	142	176	153	174	155

Table 15.8d. Median, High, and Low Percentile Values of Temperatures for January and July at 75°N

Altitude (km)	Median (K)	1%		10%		20%	
		High (K)	Low (K)	High (K)	Low (K)	High (K)	Low (K)
J A N U A R Y							
5	235	246	222	241	229	238	230
10	214	224	202	219	207	217	209
15	209	219	195	213	201	211	203
20	204	225	179	215	189	210	194
25	205	233	181	221	193	216	198
30	209	255	194	231	198	224	202
35	219	256	199	249	210	236	213
40	229	284	207	256	219	248	224
45	239	281	203	264	224	260	233
50	249	282	201	265	225	259	229
55	255	291	208	262	221	253	226
60	247	303	206	263	213	255	219
65	238	310	186	277	202	263	209
70	242	297	166	277	201	261	207
75	234	289	183	259	201	261	207
80	224	277	165	254	194	240	201
J U L Y							
5	254	264	244	259	248	257	250
10	229	238	219	234	223	232	225
15	230	237	225	235	228	233	229
20	230	237	227	235	228	234	229
25	230	240	226	238	227	237	229
30	243	262	233	247	235	246	240
35	256	262	238	260	246	258	250
40	268	275	252	271	260	270	262
45	281	292	268	287	275	284	278
50	284	296	270	291	279	288	280
55	281	288	254	284	270	283	275
60	268						
65	246						
70	218						
75	189						
80	161						

Table 15.9. Standard Deviations of Observed Day-to-Day Variations in Temperatures (K) at Ascension (8°S) at Altitudes up to 50 km During the Midseason Months

Altitude (km)	S. D. of Temperature (K)			
	Jan	April	July	Oct
5	0.8	0.6	0.7	0.6
10	0.8	1.0	0.8	1.1
15	1.6	2.0	1.9	1.5
20	2.2	2.2	2.4	2.1
25	2.2	2.2	2.7	2.1
30	3.1	2.8	3.8	3.6
35	3.7	3.2	3.7	3.8
40	5.2	3.9	3.3	3.5
45	3.6	2.8	3.2	3.3
50	5.8	2.9	3.9	3.0

instrumentation errors as well as the actual rms climatic variations. Consequently, the observed variations are somewhat larger than the actual values.

Day-to-day variations of temperature around the annual mean at levels between 50 and 90 km in tropical areas (Table 15.10) were computed from data derived from grenade and pressure-gage experiments at Natal, 6°S , and Ascension Island, 8°S . These data were not uniformly distributed with respect to season or time of day. An analysis of the relatively sparse data that are available for individual months indicates that if the seasonal and diurnal variations are removed from the data, standard deviations around monthly means due to day-to-day changes in synoptic conditions would be roughly 50 percent of those given in Table 15.10.

15.1.3.3 DISTRIBUTIONS AT PRESSURE LEVELS

The mean January and July temperatures over North America for standard pressure levels up to 20 mb (≈ 31 km) are presented in Table 15.11. Standard deviations of the daily values around these means are also shown, thereby providing information on seasonal changes in monthly mean temperatures and interdiurnal (day-to-day) variability at various pressure levels and latitudes. Standard deviations are not shown above 100 mb north of 50° latitude because a bimodal temperature distribution exists in the winter stratosphere in arctic and subarctic regions over eastern North America. As a result, the standard deviations do not provide reliable information on the temperature distributions at these levels.

Table 15.10. Standard Deviations of Observed Densities (percent) and Temperatures (K) Around the Mean Annual Values at Ascension (8°S)/Natal (6°S)

Altitude (km)	Density S.D. (% of mean)	Temperature S.D. (K)	No. of Observations
50	4.1	6	33
55	4.3	3	33
60	4.8	6	33
65	4.7	7	33
70	6.4	9	32
75	8.6	10	31
80	7.8	10	30
85	10.2	13	29
90	12.3	21	28

15.1.3.4 INTERLEVEL CORRELATION OF TEMPERATURE

The manner in which the correlation between temperatures at two levels decreases (or decays) with increasing separation between the levels is an example of the general problem of correlation decay. Correlation decay is similar for most meteorological elements as the horizontal or vertical distance between the points of observations increases. As yet, no fully satisfactory description of the decay rate, based on fundamental properties or assumptions, is available. Consequently, many empirical models that are valid for specific elements over restricted ranges have been proposed.

Profiles of the correlation coefficient R of surface temperature with temperature at other altitudes are shown in Figure 15.14 for the midseason months at Kwajalein, Wallops Island, and Ft. Churchill. At most locations, the correlation between surface temperatures and temperatures at other altitudes decreases rapidly with increasing altitudes, reaching a minimum or becoming negative between 12 and 16 km and then remaining near zero, plus or minus 0.3, from 20 to 60 km. Individual arrays of the mean temperatures, standard deviations and interlevel correlation coefficients for altitudes to 60 km are given in Table 15.12a to 15.12f for the months of January and July at Kwajalein, Wallops Island, and Ft. Churchill. Additional information useful in design studies is given by Cole and Kantor.⁸

8. Cole, A.E., and Kantor, A.J. (1980) Interlevel Correlations of Temperature and Density, Surface to 60 km, AFGL-TR-80-0163, AD A090515.

Table 15.11. Mean Temperature and Standard Deviation at Standard Pressure Levels Over North America

Pressure (mb)	Mean Temperature and Standard Deviation (C)																				
	20°N		30°N		40°N		50°N		60°N		70°N		80°N								
Mean	S.D.	Mean	S.D.	Mean	S.D.	Mean	S.D.	Mean	S.D.	Mean	S.D.	Mean	S.D.								
JANUARY											JULY										
700	7	2	2	5	-6	6	-17	8	-22	8	-26	7	-28	6							
500	-9	3	-14	4	-21	6	-31	7	-35	7	-39	5	-41	5							
300	-37	3	-41	3	-46	4	-52	4	-53	4	-56	4	-59	5							
200	-56	3	-57	5	-57	6	-54	7	-54	7	-57	6	-60	6							
100	-75	3	-69	4	-61	4	-56	5	-54	6	-57	7	-63	6							
50	-65	3	-64	3	-60	3	-58	4	-57	*	-60	*	-67	*							
25	-55	2	-55	3	-57	4	-61	5	-61	*	-65	*	-70	*							
15	-48	2	-50	3	-52	4	-55	6	-58	*	-62	*	-66	*							
10	-43	2	-46	3	-49	4	-52	6	-56	*	-60	*	-64	*							

*Not normally distributed.

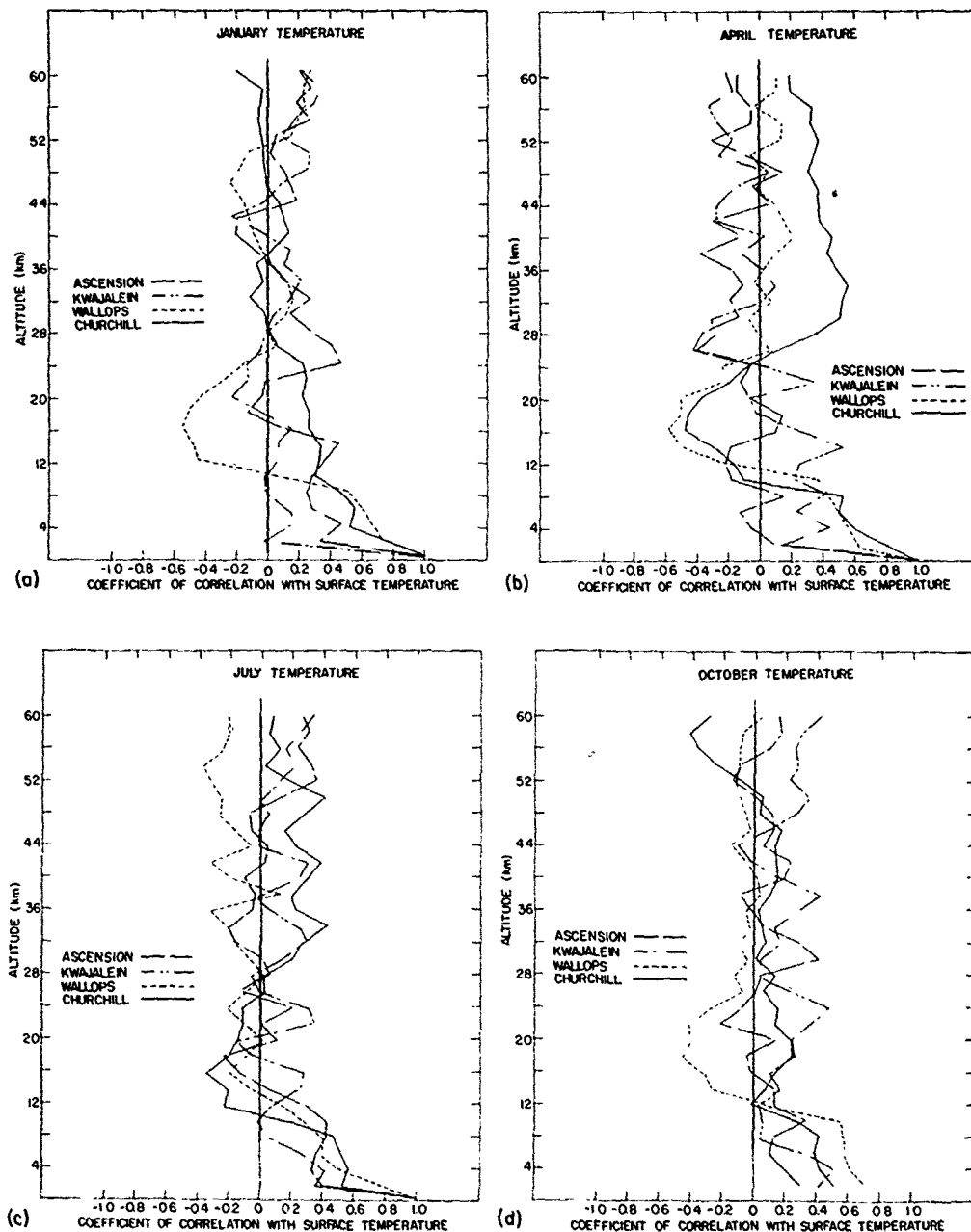


Figure 15.14. Vertical Profiles of Interlevel Coefficients of Correlation of Surface Temperature With Temperature at Other Altitudes up to 60 km for the Mid-Season Months at Ascension Island, Kwajalein, Wallops Island, and Ft. Churchill

Table 15.12a. Ft. Churchill - Correlation of January Temperatures (K) From Surface to 60 km

KM	KILOMETERS ABOVE SEA LEVEL											
	MEAN			AVERAGE OF OBSERVED VALUES			STDEV			STANDARD DEVIATION OF VALUES TIMES 10		
	N			NUMBER OF VALUES AT EACH ALTITUDE			VALUES			TIMES 10		
.035	2	4	6	8	10	12	14	16	18	20	22	24
MEAN	244	250	240	226	219	219	219	218	218	217	219	219
STDEV	75	58	49	43	45	52	61	70	75	63	69	70
N	50	50	50	50	50	50	50	46	40	30	29	23
2	72	66	75	82	77	47	30	34	36	32	34	36
4	46	32	36	42	49	96	98	96	98	95	96	98
10	12	32	19	12	12	68	69	68	69	67	68	69
14	14	35	44	12	12	56	56	57	56	55	56	57
16	16	22	26	13	13	45	45	45	45	45	45	45
20	22	34	46	4	34	61	73	78	83	54	60	65
22	22	24	34	17	4	30	51	59	65	60	63	64
24	24	24	26	17	4	39	51	59	65	60	63	64
26	26	24	24	17	4	39	51	59	65	60	63	64
30	-1	4	14	10	4	19	29	33	53	66	72	83
32	-1	3	14	14	4	14	29	33	53	66	72	87
34	-1	3	14	14	4	14	29	33	53	66	72	87
36	-1	3	14	14	4	14	29	33	53	66	72	87
38	-1	3	14	14	4	14	29	33	53	66	72	87
40	1	6	6	-2	-14	-27	-34	-37	-37	-29	-3	0
42	9	4	4	-2	-15	-32	-42	-46	-50	-46	-16	-16
44	4	-1	-1	-6	-22	-22	-22	-22	-22	-22	-22	-22
46	0	-1	-1	-6	-15	-32	-42	-46	-50	-46	-16	-16
48	-1	-1	-1	-6	-15	-32	-42	-46	-50	-46	-16	-16
50	-1	-11	-17	-29	-33	-44	-52	-53	-57	-52	-16	-36
52	-52	-33	-21	-34	-29	-37	-44	-44	-44	-44	-44	-44
54	-54	-32	-20	-34	-25	-32	-37	-37	-37	-37	-37	-37
56	-56	-34	-20	-32	-23	-23	-26	-26	-26	-26	-26	-26
60	-20	-23	-16	-16	-15	-15	-15	-15	-15	-15	-15	-15

** MULTIPLY TABULAR VALUES BY 0.01 TO OBTAIN CORRELATION COEFFICIENTS

Table 15.12b. Ft. Churchill - Correlation of July Temperatures (K) From Surface to 60 km

KM	KILOMETERS ABOVE SEA LEVEL											
	MEAN AVERAGE OF OBSERVED VALUES											
	STDEV STANDARD DEVIATION OF VALUES TIMES 10											
N	NUMBER OF VALUES AT EACH ALTITUDE											
0.035	2	4	6	8	10	12	14	16	18	20	22	24
MEAN	277	263	252	238	226	224	225	223	225	226	227	229
STDEV	53	37	48	47	49	25	49	22	23	22	20	18
N	26	26	28	28	28	28	28	28	28	28	28	28
0.06	2	4	6	8	10	12	14	16	18	20	22	24
MEAN	242	232	222	212	202	192	182	172	162	152	142	132
STDEV	44	35	42	42	55	42	35	24	16	10	7	5
N	20	19	35	42	42	55	42	35	24	16	10	7
0.09	2	4	6	8	10	12	14	16	18	20	22	24
MEAN	214	204	194	184	174	164	154	144	134	124	114	104
STDEV	44	35	42	42	55	42	35	24	16	10	7	5
N	20	19	35	42	42	55	42	35	24	16	10	7
0.12	2	4	6	8	10	12	14	16	18	20	22	24
MEAN	194	184	174	164	154	144	134	124	114	104	94	84
STDEV	44	35	42	42	55	42	35	24	16	10	7	5
N	20	19	35	42	42	55	42	35	24	16	10	7
0.15	2	4	6	8	10	12	14	16	18	20	22	24
MEAN	174	164	154	144	134	124	114	104	94	84	74	64
STDEV	44	35	42	42	55	42	35	24	16	10	7	5
N	20	19	35	42	42	55	42	35	24	16	10	7
0.18	2	4	6	8	10	12	14	16	18	20	22	24
MEAN	154	144	134	124	114	104	94	84	74	64	54	44
STDEV	44	35	42	42	55	42	35	24	16	10	7	5
N	20	19	35	42	42	55	42	35	24	16	10	7
0.21	2	4	6	8	10	12	14	16	18	20	22	24
MEAN	134	124	114	104	94	84	74	64	54	44	34	24
STDEV	44	35	42	42	55	42	35	24	16	10	7	5
N	20	19	35	42	42	55	42	35	24	16	10	7
0.24	2	4	6	8	10	12	14	16	18	20	22	24
MEAN	114	104	94	84	74	64	54	44	34	24	14	04
STDEV	44	35	42	42	55	42	35	24	16	10	7	5
N	20	19	35	42	42	55	42	35	24	16	10	7
0.27	2	4	6	8	10	12	14	16	18	20	22	24
MEAN	94	84	74	64	54	44	34	24	14	04	-04	-14
STDEV	44	35	42	42	55	42	35	24	16	10	7	5
N	20	19	35	42	42	55	42	35	24	16	10	7
0.30	2	4	6	8	10	12	14	16	18	20	22	24
MEAN	74	64	54	44	34	24	14	04	-04	-14	-24	-34
STDEV	44	35	42	42	55	42	35	24	16	10	7	5
N	20	19	35	42	42	55	42	35	24	16	10	7
0.33	2	4	6	8	10	12	14	16	18	20	22	24
MEAN	54	44	34	24	14	04	-04	-14	-24	-34	-44	-54
STDEV	44	35	42	42	55	42	35	24	16	10	7	5
N	20	19	35	42	42	55	42	35	24	16	10	7
0.36	2	4	6	8	10	12	14	16	18	20	22	24
MEAN	34	24	14	04	-04	-14	-24	-34	-44	-54	-64	-74
STDEV	44	35	42	42	55	42	35	24	16	10	7	5
N	20	19	35	42	42	55	42	35	24	16	10	7
0.39	2	4	6	8	10	12	14	16	18	20	22	24
MEAN	14	04	-04	-14	-24	-34	-44	-54	-64	-74	-84	-94
STDEV	44	35	42	42	55	42	35	24	16	10	7	5
N	20	19	35	42	42	55	42	35	24	16	10	7
0.42	2	4	6	8	10	12	14	16	18	20	22	24
MEAN	-14	-04	04	14	24	34	44	54	64	74	84	94
STDEV	44	35	42	42	55	42	35	24	16	10	7	5
N	20	19	35	42	42	55	42	35	24	16	10	7
0.45	2	4	6	8	10	12	14	16	18	20	22	24
MEAN	-34	-24	-14	-04	04	14	24	34	44	54	64	74
STDEV	44	35	42	42	55	42	35	24	16	10	7	5
N	20	19	35	42	42	55	42	35	24	16	10	7
0.48	2	4	6	8	10	12	14	16	18	20	22	24
MEAN	-54	-44	-34	-24	-14	-04	04	14	24	34	44	54
STDEV	44	35	42	42	55	42	35	24	16	10	7	5
N	20	19	35	42	42	55	42	35	24	16	10	7
0.51	2	4	6	8	10	12	14	16	18	20	22	24
MEAN	-74	-64	-54	-44	-34	-24	-14	-04	04	14	24	34
STDEV	44	35	42	42	55	42	35	24	16	10	7	5
N	20	19	35	42	42	55	42	35	24	16	10	7
0.54	2	4	6	8	10	12	14	16	18	20	22	24
MEAN	-94	-84	-74	-64	-54	-44	-34	-24	-14	-04	04	14
STDEV	44	35	42	42	55	42	35	24	16	10	7	5
N	20	19	35	42	42	55	42	35	24	16	10	7
0.57	2	4	6	8	10	12	14	16	18	20	22	24
MEAN	-114	-104	-94	-84	-74	-64	-54	-44	-34	-24	-14	-04
STDEV	44	35	42	42	55	42	35	24	16	10	7	5
N	20	19	35	42	42	55	42	35	24	16	10	7
0.60	2	4	6	8	10	12	14	16	18	20	22	24
MEAN	-134	-124	-114	-104	-94	-84	-74	-64	-54	-44	-34	-24
STDEV	44	35	42	42	55	42	35	24	16	10	7	5
N	20	19	35	42	42	55	42	35	24	16	10	7
0.63	2	4	6	8	10	12	14	16	18	20	22	24
MEAN	-154	-144	-134	-124	-114	-104	-94	-84	-74	-64	-54	-44
STDEV	44	35	42	42	55	42	35	24	16	10	7	5
N	20	19	35	42	42	55	42	35	24	16	10	7
0.66	2	4	6	8	10	12	14	16	18	20	22	24
MEAN	-174	-164	-154	-144	-134	-124	-114	-104	-94	-84	-74	-64
STDEV	44	35	42	42	55	42	35	24	16	10	7	5
N	20	19	35	42	42	55	42	35	24	16	10	7

** MULTIPLY TABULAR VALUES OF 0.01 TO OBTAIN CORRELATION COEFFICIENTS

Table 16.12c. Wallops Island - Correlation of January Temperatures (K) From Surface to 60 km

MULTIPLY TABLES VALUES BY 0.91 IN DATA ENVELOPMENT COEFFICIENTS

Table 15.12d. Wallops Island - Correlation of July Temperatures (K) From Surface to 60 km

KM	KM KILOMETERS ABOVE SEA LEVEL																																
	MEAN AVERAGE OF OBSERVED VALUES																																
	STDEV STANDARD DEVIATION OF VALUES TIMES 10																																
	N NUMBER OF VALUES AT EACH ALTITUDE																																
0.015	2	4	6	8	10	12	14	16	20	22	24	26	28	30	32	34	36	38	40	42	44	46	48	50	52	54	56	58	60				
MEAN	297	286	275	264	251	236	220	210	209	212	216	220	223	226	229	233	237	241	246	251	256	262	267	270	271	270	267	264	260	256	251		
STDEV	34	21	16	14	20	22	22	27	29	23	16	17	16	24	25	30	28	30	27	27	32	37	43	42	36	38	40	47	55	62	88		
N	37	37	37	37	37	37	37	37	37	37	37	37	37	37	37	37	37	37	37	37	37	37	37	37	37	37	37	37	34	33	16		
2	7.5	6.6	5.3	8.6	6.6	4.8	6.9	6.7	6.8	5.0	5.1	8.1	5.0	5.1	5.1	5.1	5.1	5.1	5.1	5.1	5.1	5.1	5.1	5.1	5.1	5.1	5.1	5.1	5.1	5.1	5.1		
6	10	2.5	3.7	4.6	5.1	8.1	12	1.2	2.9	2.7	4.8	8.0	-1.6	-1.1	-1.1	-1.1	-1.1	-1.1	-1.1	-1.1	-1.1	-1.1	-1.1	-1.1	-1.1	-1.1	-1.1	-1.1	-1.1	-1.1	-1.1		
10	14	-1.6	-1.6	-1.6	-1.6	-1.6	-1.6	-1.6	-1.6	-1.6	-1.6	-1.6	-1.6	-1.6	-1.6	-1.6	-1.6	-1.6	-1.6	-1.6	-1.6	-1.6	-1.6	-1.6	-1.6	-1.6	-1.6	-1.6	-1.6	-1.6	-1.6		
14	-1.6	-1.6	-1.6	-1.6	-1.6	-1.6	-1.6	-1.6	-1.6	-1.6	-1.6	-1.6	-1.6	-1.6	-1.6	-1.6	-1.6	-1.6	-1.6	-1.6	-1.6	-1.6	-1.6	-1.6	-1.6	-1.6	-1.6	-1.6	-1.6	-1.6	-1.6		
18	-1.6	-1.6	-1.6	-1.6	-1.6	-1.6	-1.6	-1.6	-1.6	-1.6	-1.6	-1.6	-1.6	-1.6	-1.6	-1.6	-1.6	-1.6	-1.6	-1.6	-1.6	-1.6	-1.6	-1.6	-1.6	-1.6	-1.6	-1.6	-1.6	-1.6	-1.6		
20	0	-5	-1.1	-2.0	-1.1	-3.3	-3.2	-1.7	4.8	5.7	1.6	1.6	1.6	1.6	1.6	1.6	1.6	1.6	1.6	1.6	1.6	1.6	1.6	1.6	1.6	1.6	1.6	1.6	1.6	1.6	1.6	1.6	
24	-1.3	-1.1	-1.1	-1.1	-1.1	-1.1	-1.1	-1.1	-1.1	-1.1	-1.1	-1.1	-1.1	-1.1	-1.1	-1.1	-1.1	-1.1	-1.1	-1.1	-1.1	-1.1	-1.1	-1.1	-1.1	-1.1	-1.1	-1.1	-1.1	-1.1	-1.1		
28	-1.2	-1.2	-1.2	-1.2	-1.2	-1.2	-1.2	-1.2	-1.2	-1.2	-1.2	-1.2	-1.2	-1.2	-1.2	-1.2	-1.2	-1.2	-1.2	-1.2	-1.2	-1.2	-1.2	-1.2	-1.2	-1.2	-1.2	-1.2	-1.2	-1.2	-1.2		
30	-6	-6	-1.7	6	1.6	3.2	2.5	-5	8	-18	-2	1.0	3.3	4.9	7.6	1.6	1.6	1.6	1.6	1.6	1.6	1.6	1.6	1.6	1.6	1.6	1.6	1.6	1.6	1.6	1.6	1.6	1.6
32	1.6	2.5	1.0	1.1	1.7	2.9	-1.1	1.6	1.6	1.6	1.6	1.6	1.6	1.6	1.6	1.6	1.6	1.6	1.6	1.6	1.6	1.6	1.6	1.6	1.6	1.6	1.6	1.6	1.6	1.6	1.6		
36	1.6	1.6	1.6	1.6	1.6	1.6	1.6	1.6	1.6	1.6	1.6	1.6	1.6	1.6	1.6	1.6	1.6	1.6	1.6	1.6	1.6	1.6	1.6	1.6	1.6	1.6	1.6	1.6	1.6	1.6	1.6		
40	-1.6	-1.6	-1.6	-1.6	-1.6	-1.6	-1.6	-1.6	-1.6	-1.6	-1.6	-1.6	-1.6	-1.6	-1.6	-1.6	-1.6	-1.6	-1.6	-1.6	-1.6	-1.6	-1.6	-1.6	-1.6	-1.6	-1.6	-1.6	-1.6	-1.6	-1.6		
44	-3.3	-2.6	1	-1	-1	-1	-1	-1	-1	-1	-1	-1	-1	-1	-1	-1	-1	-1	-1	-1	-1	-1	-1	-1	-1	-1	-1	-1	-1	-1	-1		
48	-1.6	-1.6	-1.6	-1.6	-1.6	-1.6	-1.6	-1.6	-1.6	-1.6	-1.6	-1.6	-1.6	-1.6	-1.6	-1.6	-1.6	-1.6	-1.6	-1.6	-1.6	-1.6	-1.6	-1.6	-1.6	-1.6	-1.6	-1.6	-1.6	-1.6	-1.6		
52	-3.1	-2.1	-1.6	-1.6	-1.6	-1.6	-1.6	-1.6	-1.6	-1.6	-1.6	-1.6	-1.6	-1.6	-1.6	-1.6	-1.6	-1.6	-1.6	-1.6	-1.6	-1.6	-1.6	-1.6	-1.6	-1.6	-1.6	-1.6	-1.6	-1.6	-1.6		
56	-3.1	-2.1	-1.6	-1.6	-1.6	-1.6	-1.6	-1.6	-1.6	-1.6	-1.6	-1.6	-1.6	-1.6	-1.6	-1.6	-1.6	-1.6	-1.6	-1.6	-1.6	-1.6	-1.6	-1.6	-1.6	-1.6	-1.6	-1.6	-1.6	-1.6	-1.6		
60	-7	6	1	5.8	4.8	3.5	-4.2	-2.2	-1.3	4.1	5.6	6.3	6.5	7.2	5.0	5.4	7.9	7.7	3.0	3.7	3.1	4.0	2.5	3.6	6.3	6.6	9.0	9.0	9.0	9.5	9.5		

** MULTIPLY TABULAR VALUES BY 0.01 TO OBTAIN CORRELATION COEFFICIENTS

Table 15.12e. Kwajalein - Correlation of January Temperatures (K) From Surface to 60 km

KMH		KILOMETERS ABOVE SEA LEVEL											
MEAN		AVERAGE OF OBSERVED VALUES											
STDV		STANDARD DEVIATION OF VALUES TIMES 10											
N		NUMBER OF VALUES AT EACH ALTITUDE											
KMH		2	4	6	8	10	12	14	16	18	20	22	24
MEAN	30.1	28.8	27.9	26.7	25.5	26.1	22.4	20.8	19.5	19.2	20.6	21.2	21.7
STDV	1.4	1.3	1.3	1.4	1.4	1.5	1.6	1.5	1.6	1.6	2.6	2.3	2.2
N	42	42	42	42	42	42	42	42	42	42	42	42	42
2	-3	-15	-11	-11	-20	-23	-28	-6	-6	-7	-7	-7	-7
4	6	39	35	48	46	46	46	46	46	46	46	46	46
6	8	39	35	48	46	46	46	46	46	46	46	46	46
8	18	-2	6	47	43	70	70	-1	-1	-1	-1	-1	-1
10	12	5	13	44	52	46	85	80	80	80	80	80	80
12	14	5	14	44	52	46	85	80	80	80	80	80	80
14	15	10	12	23	60	71	80	85	85	85	85	85	85
16	16	10	12	23	60	71	80	85	85	85	85	85	85
18	16	10	12	23	60	71	80	85	85	85	85	85	85
20	20	-23	-16	-12	0	4	1	-9	-6	-24	10	10	10
22	22	-13	-3	-12	-27	-21	-27	-34	-33	37	33	37	33
24	22	-13	-3	-12	-27	-21	-27	-34	-33	37	33	37	33
26	22	-14	-4	-15	-21	-16	-21	-15	-16	-17	-17	-17	-17
28	28	0	-14	-5	-16	-17	-16	-17	-18	-17	-17	-17	-17
30	30	3	-1	9	-26	1	-16	-29	-19	1	25	-6	-6
32	32	16	-3	-3	-13	-29	-31	-16	-19	-20	-16	-6	-6
34	34	16	-3	-3	-13	-29	-31	-16	-19	-20	-16	-6	-6
36	36	16	-3	-3	-13	-29	-31	-16	-19	-20	-16	-6	-6
38	38	16	-3	-3	-13	-29	-31	-16	-19	-20	-16	-6	-6
40	40	-1	-32	-46	-6	-12	-19	-26	19	24	-16	2	-2
42	42	-22	37	-3	-3	-2	-13	-16	-32	26	-4	-3	-5
44	44	-22	37	-3	-3	-2	-13	-16	-32	26	-4	-3	-5
46	46	-25	-25	-25	-25	-25	-25	-25	-25	-25	-25	-25	-25
50	50	27	8	6	-7	-7	-9	-12	-22	26	11	-26	-43
52	52	29	13	6	-6	-6	-11	-16	-22	16	5	-31	-22
54	54	29	13	6	-6	-6	-11	-16	-22	16	5	-31	-22
56	56	29	13	6	-6	-6	-11	-16	-22	16	5	-31	-22
58	58	29	13	6	-6	-6	-11	-16	-22	16	5	-31	-22
60	60	21	16	10	-2	-7	-7	-14	-24	13	18	-21	-42

* MULTIPLY TABLEAUX VALUES BY .01 TO OBTAIN CORRELATION COEFFICIENTS

Table 15. 12f. Kwajalein - Correlation of July Temperatures (K) From Surface to 60 km

MILITARY TACTICS AND WARFARE IN CERTAIN CONFESSIONS

15.1.4 Speed of Sound vs Temperature

The speed of sound is primarily a function of temperature. It is given by:

$$C_s = \frac{(\gamma \cdot R^* \cdot T_M)^{1/2}}{M_0} \quad (15.21)$$

where γ is the ratio of specific heat of air at constant pressure to that at constant volume, and is taken to be 1.40 exact (dimensionless). This equation is valid only when the sound wave is a small perturbation on the ambient condition. Figure 15.15 shows the relationship between temperature and the speed of sound. It can be used with the various temperature presentations given in this section to estimate the probable speed of sound for various altitudes and geographical areas.

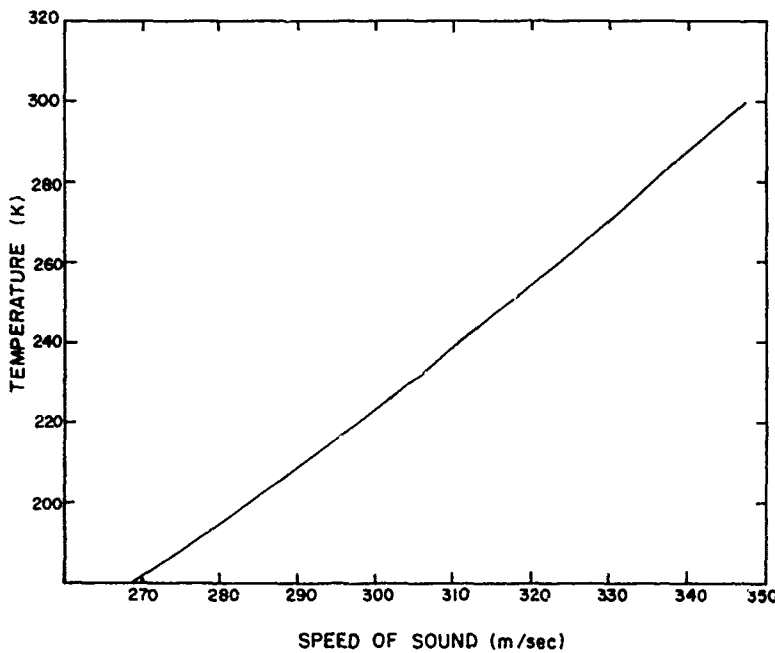


Figure 15.15. Speed of Sound vs Temperature (K)

15.1.5 Earth/Air Interface Temperatures

The earth/air interface is either a land, snow, or water surface. At many locations, the physical structure of the interface is overwhelmingly complex. The land surface can be covered with seasonally varying vegetation of great diversity, and even without plant cover there is normally a considerable variability produced by small-scale terrain features, differences in soil moisture, and cultivation. A snow surface is markedly affected by aging. The physical conditions of water in a shallow puddle are quite different from the open ocean. All these conditions reflect themselves in the micro-climatological aspects of natural or unnatural surfaces.

As discussed in Section 15.1.2, the use of ordinary thermometers to measure surface temperature will result in meaningful values only in the rare cases of a flat, uniform, and homogeneous surface. In general, area averages of temperature obtained by an integrating method over certain defined sections will be more representative than any one of a multitude of widely varying point values. Bolometric temperature measurements from an airplane cruising at low altitude provide a more reasonable approach to the problem of surface temperature determination than a series of thermometric point measurements. Table 15.13 lists some results of bolometric measurements from an airplane. The data illustrate the great horizontal variability of surface temperature even when effects on the scale of less than 6 m linear dimension are averaged out.

The processes that determine the temperature of the earth/air interface and the surface characteristics that influence these processes may be separated into the following four classes:

- (1) radiative energy transformation (or net radiation intensity), which depends upon the albedo and selective absorption and emission;
- (2) turbulent heat transfer into the air (by both convective and mechanical air turbulence);
- (3) conduction of heat into or out of the ground, which depends upon the thermal admittance of the soil; and
- (4) transformation of radiant energy into latent heat by evaporation, which depends upon the dampness of the surface or available soil moisture at the ground level.

The aerodynamic roughness of a natural surface strongly influences the momentum exchange between ground and air flowing past it. The momentum exchange establishes the low-level profile of mean wind speed. The mechanical turbulence produced by surface roughness also determines to a certain degree the relative amount of heat transported into or from the air at mean ground level. Other conditions being equal, an increase in roughness and hence mechanical

Table 15.13. Bolometric Records of Area (Approximately 37 m^2) Surface Temperature From an Airplane Cruising at Approximately 370 m Along a Constant Flight Path, April 1944 (Condensed From Albrecht⁹)

Day	Hour	Sun's Elevation (degree)	Sky Cover	Surface Temperature (C) - Bolometric Data						
				Standard Shelter Temp. at Airport (C)	Baltic Sea	Sand Beach	Down Land	City	Woods	Opening in Woods
9	13 to 14	40.4	10/10	9	2	12	14	8	7	8
11	19 to 20	-1.6	1/10	10	2	7	2	3	3	5
16	19 to 20	-1.8	9/10	14	4	8	7	7	4	2
20	05 to 06	0.5	1/10	2	5	-2	-7	-1	-3	-7
28	14 to 15	42.1	4/10	7	7	46	42	17	16	23
				Wind Speed (m/sec)	Woods	Clear Cutting in Woods	Dry Peat	Swamp	Pond	
7	19	--	4/10	0.5	2	-2	-6	0	1	
20	20	--	2/10	1.5	0	-1	-4	0	0	
26	20	--	3/10	2.5	2	-3	-1	-1	1	
Albedo values as determined by Albrecht:				5%	8%	8%	7%	7%	5%	

9. Albrecht, F. (1952) Mikrometeorologische Temperaturmessungen vom Flugzeug aus, Ber. Deutsch. Wetterd., Bad Kissingen 38:332.

turbulence will cause lowering of maximum surface temperature during daytime and raising of minimum surface temperature during nighttime. For ordinary sandy soil, under average conditions of overall airflow and net radiation on summer days in temperate zones, the diurnal range of surface temperature is about 17 C if the roughness coefficient is 0.06 mm or 14 C if it is 6.3 mm (roughness coefficient, also called roughness "length", is $\epsilon/30$ where ϵ is the average height of surface irregularities in millimeters).

A special and rather extreme case of the influence of surface characteristics is represented by forests. The trees intercept solar radiation, and the heat absorbed is given off into the air that is trapped between the stems. Although deep snow may lie on the ground, daytime temperatures in wooded areas in spring can reach 16 C.

The thermal admittance (Sec 15.1.6) of most soils depends on porosity and moisture content. Because both the thermal conductivity and heat capacity of soils increase with soil moisture, the thermal admittance may be significantly affected by humidity variations during rainy or wet weather periods, whereas the normal diffusivity may remain unaltered. These effects are difficult to assess, however, because the dampness of the surface is also a major factor in the utilization of solar energy for evaporation. If soil moisture is readily available at the earth's surface, part of the net radiation that would have been used for heating air and ground is used instead for latent heat of evaporation. Table 15.14 lists observed temperatures in the air and soil at levels close to the earth/air interface.

Table 15.14. Temperature of the Air 10 cm Above, and of the Soil 0.5 cm Below, the Earth/Air Interface, Measured by Thermocouples (Davidson and Lettau²)

Condition	Temperature (C) at Mean Local Time								
	0400	0600	0800	1000	1200	1400	1600	1800	2000
*Air	14.7	10.6	23.0	27.4	30.7	31.7	32	46.7	24.5
*Soil	17.6	17.9	23.0	31.1	35.6	36.2	33.8	29.3	25.5
**Air	8.1	9.5	18.8	24.9	28.7	30.0	28.1	23.1	19.3
**Soil	11.8	11.6	18.4	19.0	37.8	37.3	31.3	24.8	20.8

*Mean soil moisture in 0 to 10 cm layer about 10% wet weight basis.

**Mean soil moisture in 0 to 10 cm layer about 4% wet weight basis.

Engineers must consider the effect of albedo and color or net radiation in artificially changing surface or ground temperature. In India, a very thin layer of white powdered lime dusted over a test surface made ground temperatures up to 15 C cooler; the effect was felt at a depth of at least 200 mm.

Another effective method of controlling surface temperature is shading. Thin roofs (metal, canvas), however, may attain a temperature so high that the under surface acts as an intense radiator of long-wavelength radiation, thus warming the ground. In hot climates, multilayer shades with natural or forced ventilation in the intermediate space, or active cooling of the outer surface by water sprinkling, can be used to cool the ground with some success. Table 15.15 compares temperature measurements of various material surfaces with corresponding air and soil temperatures.

Table 15.15. Comparison of Air and Soil Temperature With Surface Temperatures of Materials Exposed on a Tropical Island With Normal Trade Winds. Air and material surface temperatures at 1.2 m above, soil temperature at 2.5 cm below, the earth/air interface. Exposed surface area about 0.1 m² (Draeger and Lee¹⁰)

Material	Temperature (C)		
	Highest Recorded	Average	
		Max.	Min.
Air (1.2 m)	29	28	26
Soil (2.5 cm)	34	34	26
Wood	41	37	25
Aluminum	40	36	25
Galvanized Iron	45	38	25
Black Iron	51	42	25
Concrete Slab	37	34	25

15.1.6 Subsoil Temperatures

The thermal reaction of the soil to the daily and seasonal variations (due to the earth's rotation and its revolution about the sun) of net radiation is governed by the molecular thermal conductivity of the soil k , and by the volumetric heat capacity of the soil, $C = \rho c$ (where ρ is the density, and c is the heat capacity

10. Draeger, R. H., and Lee, R. H. (1953) Meteorological Data Eniwetok Atoll, Naval Medical Res. Inst. Memo Rept. 53-8, Bethesda, Md.

per unit mass). For a cyclic forcing function of frequency n , the quotient $(nk/C)^{1/2}$ (which has the physical units of velocity) determines the downward propagation, or amplitude decrement with depth, of the soil-temperature response. The product $(nkC)^{-1/2}$, which has the physical units of degrees divided by Langleys per unit time (one Langley per second equals $4.186 \times 10^4 \text{ W/m}^2$), governs the amplitude of the temperature profile in time at the soil surface. The ratio k/C is the thermal diffusivity (physical units of length squared per unit time). The expression $(kC)^{1/2}$ defines thermal admittance of the soil.

The continuous flow of heat from the earth's hot, deep interior to the surface is the order of 10^{-5} L/min . This is very small compared with a solar constant of 2 L/min , average net-radiation rates of 0.2 L/min , and induced soil-heat fluxes in the uppermost several feet of the earth's crust of 0.1 L/min . Only for depth intervals in excess of about 30 m must the heat flow from the earth's interior be considered, inasmuch as it results in vertical temperature gradients of the order of $2 \frac{1}{2}$ to 25 C/km .

Table 15.16 gives experimental data on thermal admittance and theoretical values of the half-amplitude depth interval based on experimental thermal diffusivity data for diverse ground types. The smaller the thermal admittance, the larger the surface-temperature amplitude for a given forcing function. This latter inverse proportionality is valid only when turbulent heat transfer into the atmosphere is negligible.

In a simple theoretical model of thermal diffusion, an effective atmospheric thermal conductivity K is introduced. For air, K is many times larger than the molecular thermal conductivity of the air. For the same forcing function, the surface-temperature amplitudes at two different kinds of ground (1 and 2) follow the ratio

$$\left[(\text{TAR})_2 + (K/k)_{\text{air}}^{1/2} \right] / \left[(\text{TAR})_1 + (K/k)_{\text{air}}^{1/2} \right] . \quad (15.22)$$

where TAR represents the ratio of the thermal admittance of the ground to that of air. For diurnal cycles of net radiation, the ratio $(K/k)_{\text{air}}$ is the order of 10^4 .

The most extreme surface temperature oscillation occurs over feathery snow where the amplitude may reach approximately 4 times that over still water or sandy soil, and is at least 100 times as large as that over the turbulent ocean. An amplitude ratio of about 3.5 can be expected for surface temperature over dry vs moist sand surfaces. Theoretically, the penetration of thermal "oscillations" into the soil is inversely proportional to the frequency of the

Table 15.16. Physical Thermal Parameters of Diverse Ground Types (Lettau¹¹)

Ground Type	Thermal Admittance Ratio (TAR), Ground to Air	Half-Amplitude Depth Interval (theoretical)	
		Annual Cycle (m)	Diurnal Cycle (m)
SOILS			
Quartz sand, medium-fine dry	110	1.0	0.05
8% moisture	230	1.6	0.08
22% moisture	360	1.5	0.08
Sandy clay, 15% moisture	280	1.3	0.07
Swamp land, 90% moisture	340	1.0	0.05
ROCKS			
Basalt	350	1.8	0.09
Sandstone	380	2.2	0.12
Granite	440	2.5	0.13
Concrete	440	2.3	0.12
SNOW, ICE, AND WATER			
Feathery snow	10	0.7	0.04
Packed snow	100	1.4	0.07
Still water	280	0.8	0.04
Ice	320	1.4	0.07
Turbulent ocean	10^3 to 10^5	60 to 600	3 to 30

"oscillations".¹¹ The best insulator is still air or any porous material with air-filled pores, such as feathery snow; materials such as leaf litter have similar insulating properties.¹²

Much information is available on soil-temperature variations in various climatic zones. Table 15.17 gives annual and daily temperature cycles in different soil types. In addition to the type of ground, certain meteorological

11. Lettau, H. (1954) Improved models of thermal diffusion in the soil, *Trans. Am. Geophys. Union* 35:121.

12. Geiger, R. (1957) *The Climate Near the Ground*, Harvard University Press (translated by M.N. Stewart et al).

Table 15.17. Annual and Daily Temperature Cycles. Annual values are averages for the years 1939 through 1940 at Giessen, Germany.¹³ Daily values are averages of clear weather, 10 through 12 August 1893, Finland, after Homen (Geiger¹²)

Temperature (C)						
	Annual Means			Daily Means		
	Loam	Sand	Humus	Swamp Land	Sandy Heath	Granite Rock
Surface	9.1	9.3	10.1	51.6	25.0	24.6
1 m above	10.8	11.3	11.3	---	---	---
0.6 m above	---	---	---	11.5	14.0	20.4
Surface Amplitude	10.5	10.7	11.4	10.4	17.0	10.2
Half-Amplitude Depth Interval (m)						
Depth	1.8	1.6	1.4	0.05	0.08	0.15

factors such as rainfall and melting snow have marked effects on the soil temperature. Snow cover is a leading factor in protecting the soil from severe frost. On one extreme occasion with an air temperature of -18 C, the temperature was -1 C under a 130-mm snow cover, whereas on bare soil it was -22 C.

The soil-temperature variations illustrated in Figure 15.16 were obtained at a station cleared of pine trees but in generally wooded country. Topsoil and brown sandy loam (0 to 0.6 m) changed to brown sand and gravel that varied from medium (0.6 to 2 m), to coarse (2 to 4 m), and again to medium (4 to 18 m). The water level was at 15 m. The figure illustrates the amplitude decrease and phase retardation of the annual cycle with depth. Amplitudes of weather disturbances with periods of several days, as illustrated by the temperature curve of the 0.75-m level, decrease with depth more rapidly than the annual amplitudes. Qualitatively, this agrees with the theoretical prediction of an amplitude decrement proportional to the square root of the length of the period of oscillation. The actual half-amplitude depth interval of the annual cycle can be estimated from Figure 15.16 as being nearly 3 m, which is much larger than the depth inferred from experimental values of thermal diffusivity. The discrepancy may be caused by seepage or downward migration of rain water and the accompanying

13. Kreutz, W. (1943) Der Jahresgang der Temperatur in verschiedenen Boeden unter gleichen Witterungs Verhaeltnisser, Zeitschr. f. angewandte Meteorologie 60:65.

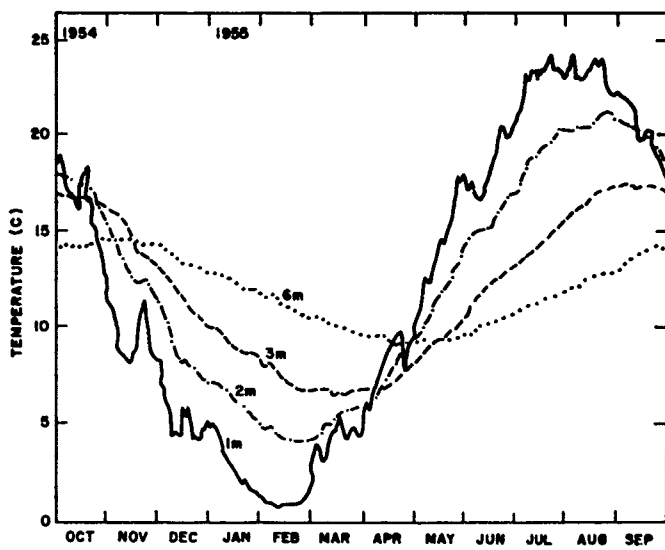


Figure 15.16. Variations of Soil Temperature at Indicated Depths, North Station, Brookhaven, Long Island, October 1954 Through September 1955, After Singer and Brown¹⁴

advection or transfer of heat. This process could increase the apparent or effective thermal diffusivity for annual soil-temperature variations by factors of 4 to 8 times the experimental values obtained in soil of constant moisture. The data in Table 15.17 are more in line with experimental findings than the curves in Figure 15.16. The limitation of Table 15.17 is that the data are for clearly defined and nearly ideal soil types that are seldom matched by actual ground conditions.

Factors that must be investigated and assessed for any one set of soil-temperature observations are: (1) type and state of compaction of the soil, (2) moisture content and seepage of the soil during the test, (3) position of the water table during the test, (4) type and color of surface cover, (5) amount and nature of traffic over the site, and (6) local climatic conditions.

Subsoil temperature information is useful in computing thermal stresses and loads. Some examples are the determination of the depth to which a structure should be buried when proximity to natural isothermal conditions is desired to conserve on the air conditioning load, or to dissipate heat generated by power cables. The determination of frost penetration depths is usually the principal concern.

14. Singer, I. A., and Brown, R. M. (1956) Annual variation of sub-soil temperatures about a 600-foot diameter circle, Trans. Am. Geophys. Union 37:743.

15.1.7 Degree-Day and Temperature-Wind Combinations

A degree-day is a unit adopted to measure the departure of the daily mean temperature from a given standard. In the United States the number of heating degree-days (18 C), on any one day, is the number of degrees of the 24-hour mean temperature below 65 F. Cumulated, day by day, over the heating season, the total number of degree days becomes an index of heating fuel requirements. In such cumulation, the days on which the mean temperature exceeds 65 F (18 C) are ignored. When the centigrade scale is used, the base is usually 19 C. The United States Army Corps of Engineers computes "freezing-degree days" as the departure of the daily mean temperature from 32 F, a negative departure when above 32 F (0 C). The National Weather Service supplies "normal degree-days", both monthly and annual totals. A few examples of the 30-year annual normals are: 9274 (F) for Fargo, N.D., 5634 (F) for Boston, Mass., and 108 (F) for Key West, Florida.

The wind-chill concept was introduced in 1939 by the famous antarctic explorer, Paul Siple, to measure the cooling effect of low temperature and strong wind combined. The wind-chill index is the equivalent temperature, in a normal walk (1.9 m/sec) in calm air, corresponding to the combination of actual air temperature and windspeed. It can be related to the heat loss H from a nude body in the shade. H is given by

$$H = (10\sqrt{V} + 10.45 - V)(33 - T_a) \quad , \quad (15.23)$$

where H is the heat loss in kilogram calories per square meter of body surface per hour, T_a is the air temperature (C), and V is the windspeed (m/sec). Neutral skin temperature is roughly 33 C. For windspeeds greater than 1.9 m/sec the wind-chill index (T_{wc}), in C, is given closely by

$$T_{wc} = (33 - H/22) \quad . \quad (15.24)$$

This formula gives only an approximation because of individual body variations, incoming radiation and other factors affecting heat loss from the body. The formula is not used, or needed, with wind speeds less than 6 km/hr (2 m/sec, 3 kt, or 4 mph).

Extreme temperature-wind combinations are frequently important in thermal equilibrium design problems, requiring estimates of the maximum steady wind speeds likely to be encountered at various temperatures. Figure 15.17 was prepared from 4 years of 6-hourly and 1 year of hourly data for 22 stations in

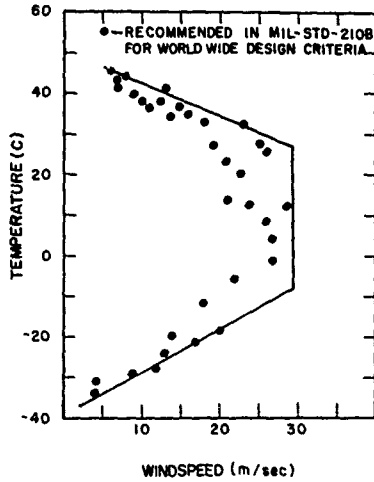


Figure 15.17. Extremes of Temperature in Combination With Windspeed. Windspeeds, in general, were observed 12 to 30 m above the surface. The 35 observations were taken over a 5-yr period at some 22 stations widely scattered in the United States. The envelope is for the recommended U.S. design criteria.

the United States.¹⁵ It shows maximum steady (5-min) wind speeds that occurred with temperatures in the range from -37 C to 46 C during this period. The stations used in this study were selected as representative of climatic areas in the United States. Mountainous stations were unrepresentative of generally operational areas and were not among those selected. Also, the high winds of hurricanes and tornadoes were omitted from the figure.

The wind speeds of Figure 15.17 occurred at anemometer heights, usually at 12 to 30 m above ground level during the years of observation. The wind speeds at the 3-m level are approximately 20 percent less and even 50 percent less for the extreme low temperature (less than -21 C).

The combination of values of temperature and windspeed, recommended for extreme U.S. thermal equilibrium design criteria, are shown by the envelope in Figure 15.17. This recommendation is not valid in mountainous areas or in Death Valley. For the latter the criteria are the same as for world-wide criteria, as plotted in Figure 15.17.

15. Sissenwine, N., and Court, A. (1951) Climatic Extremes for Military Equipment, Env. Protection Br., Rpt. No. 146, Dept. of Army, Washington, D.C.

15.2 ATMOSPHERIC DENSITY UP TO 90 km

The density data discussed in this section are from direct and indirect observations obtained from balloon-borne instrumentation for altitudes up to 30 km, and measurements from rockets and instruments released from rockets for altitudes between 30 and 90 km.

15.2.1 Seasonal and Latitudinal Variations

The Reference Atmospheres presented in Chapter 3 of the Handbook of Geophysics provide tables of mean monthly density-height profiles, surface to 90 km, for 15° intervals of latitude between the equator and the North Pole. Densities at altitudes between 10 and 90 km are highest during the months of June and July and lowest in December and January at locations north of 30° latitude. In tropical and subtropical areas seasonal variations are relatively small with highest densities at levels above 30 km occurring in the spring and fall.

Mean monthly density profiles, surface to 60 km, observed during the mid-season months at Ascension Island, 8°S, 14°W, Wallops Island, 38°N, 75°W, and Ft. Churchill, 59°N, 94°W, are plotted in Figure 15.18. Densities are shown as percent departure from the U.S. Standard Atmosphere 1976. The individual mean monthly profiles cross or converge near 8 km and between 22 and 26 km. Both are levels of minimum density variability. There is a level near 8 km that is considered an isopycnic level because mean monthly densities depart from standard by no more than 1 or 2 percent regardless of the geographical location or season. Between 22 to 26 km, however, there is a marked seasonal variability, even though there is very little longitudinal or latitudinal variability during individual months. Seasonal differences in the density profiles at the same three locations are shown in Figure 15.19. The minimum seasonal variability of the mean monthly values, 1 to 2 percent, occurs at 8 km and the maximum seasonal variability occurs above 60 km. The seasonal variations are largest at Ft. Churchill and are smallest at Ascension Island.

15.2.2 Day-to-Day Variations

The density at a specific altitude may differ from the seasonal or monthly mean at that altitude due to day-to-day changes in the weather pattern. The distribution of observed densities in January and July at the most climatically extreme locations for which data are available near 30°, 45°, 60°, and 75°N are shown in Tables 15.18a to 15.18d for altitudes up to 80 km. Median, and high and low values that are equalled or more severe 1, 10, and 20 percent of

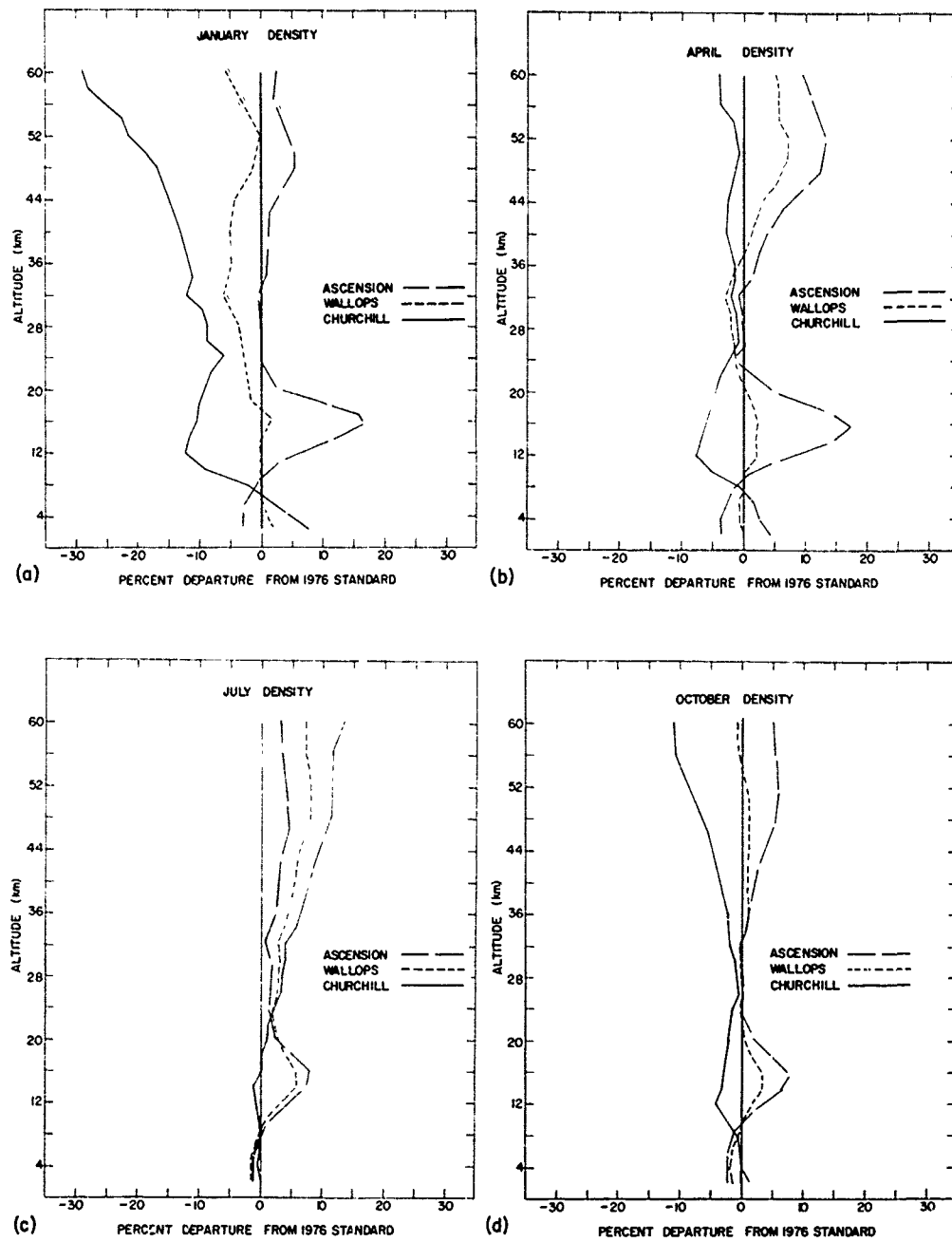


Figure 15.18. Latitudinal Differences in the Density-Altitude Profiles for the Mid-Season Months at Ascension Island, Wallops Island, and Ft. Churchill

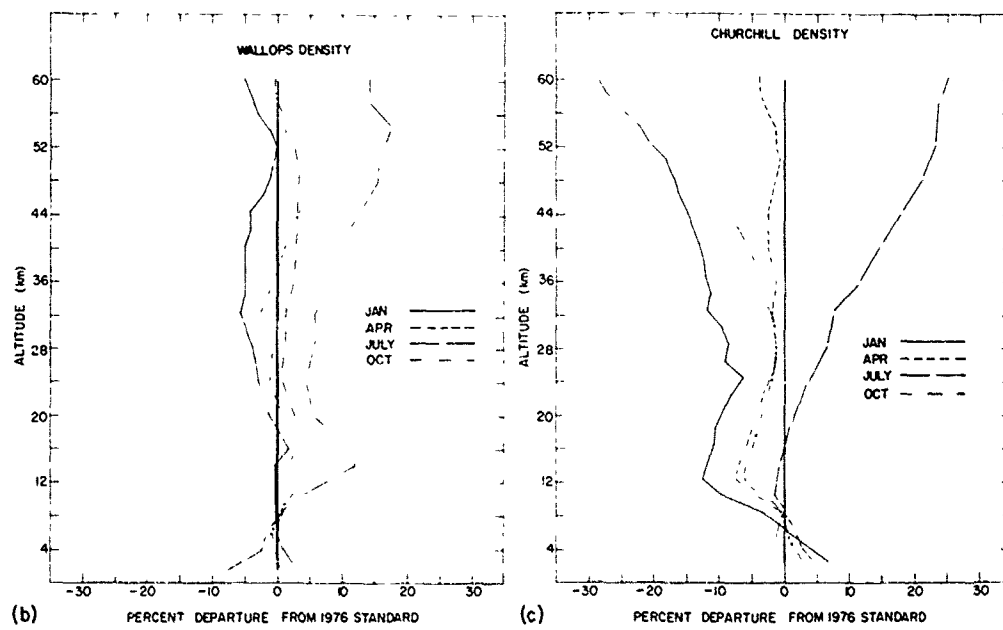
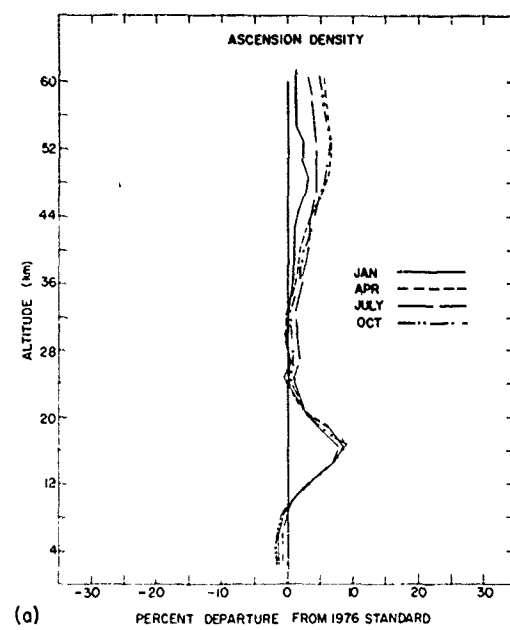


Figure 15.19. Seasonal Differences in the Density-Altitude Profiles at Ascension Island, Wallops Island, and Ft. Churchill

Table 15.18a. Median, High, and Low Percentile Values of Densities Given as Percentage Departures From U.S. Standard Atmosphere 1976 for January and July at 30°N

Altitude (km)	Median (% of Std)	1%		10%		20%		U.S. Std Density (kg m ⁻³)
		High	Low	High	Low	High	Low	
J A N U A R Y								
5	-1	+1	-3	0	-2	0	-2	7.3643-1
10	+1	+4	-3	+3	-1	+2	0	4.1351
15	+7	+15	-1	+12	+4	+10	+5	1.9476
20	+3	+7	-2	+5	+1	+4	+2	8.8910-2
25	-2	+4	-6	+3	-4	+1	-2	4.0084
30	-4	+2	-10	-2	-8	-3	-6	1.8410
35	-3	+3	-12	0	-8	-1	-6	8.4634-3
40	-1	+2	-10	+1	-7	0	-5	3.9957
45	0	+8	-10	+3	-7	+2	-5	1.9663
50	+1	+12	-8	+7	-4	+5	-2	1.0269
55	0	+9	-10	+5	-6	+3	-4	5.6810-4
60	-2	+12	-15	+5	-9	+2	-6	3.0968
65	-4	+21	-25	+13	-13	+7	-6	1.6321
70	-5	+16	-26	+9	-17	+6	-12	8.2828-5
75	-7	+21	-25	+13	-15	+8	-10	3.9921
80	-4	+21	-22	+15	-13	+8	-7	1.8458
J U L Y								
5	-3	0	-5	-1	-4	-2	-4	7.3643-1
10	+1	+3	-1	+2	0	+2	0	4.1351
15	+16	+20	+11	+17	+13	+17	+14	1.9476
20	+8	+11	+14	+10	+5	+9	+6	8.8910-2
25	+4	+9	0	+7	+2	+6	+3	4.0084
30	+3	+7	-1	+5	+1	+4	+2	1.8410
35	+6	+10	+2	+8	+3	+7	+4	8.4634-3
40	+9	+15	+2	+11	+5	+10	+7	3.9957
45	+12	+19	+4	+14	+7	+13	+9	1.9663
50	+13	+23	+6	+17	+8	+15	+10	1.0269
55	+11	+20	+2	+15	+5	+13	+7	5.6810-4
60	+13	+24	-1	+21	+3	+19	+7	3.0968
65	+15	+43	-6	+38	0	+30	+6	1.6321
70	+15	+32	-9	+23	+1	+20	+8	8.2828-5
75	+10	+24	-11	+20	-6	+15	+1	3.9921
80	+6	+22	-15	+17	-6	+14	+1	1.8458

Table 15.18b. Median, High, and Low Percentile Values of Densities Given as Percentage Departures From U.S. Standard Atmosphere 1976 for January and July at 45°N

Altitude (km)	Median (% of Std)	1%		10%		20%		U.S. Std Density (kg m ⁻³)
		High	Low	High	Low	High	Low	
J A N U A R Y								
5	0	+4	-3	+3	-2	+2	-1	7.3643-1
10	-2	+6	-10	+3	-6	+1	-4	4.1351
15	-3	+4	-12	+1	-8	-1	-6	1.9476
20	-2	+2	-8	0	-6	-1	-5	8.8910-2
25	-2	+2	-8	0	-6	-1	-5	4.0084
30	-5	+1	-17	-2	-13	-4	-9	1.8410
35	-6	+2	-20	-2	-16	-4	-12	8.4634-3
40	-8	+5	-23	0	-17	-4	-13	3.9957
45	-9	+8	-22	+2	-16	-3	-14	1.9663
50	-8	+11	-20	+4	-16	-3	-14	1.0269
55	-9	+9	-25	+2	-18	-4	-16	5.6810-4
60	-12	+7	-28	0	-23	-7	-20	3.0968
65	-14	0	-38	-5	-34	-10	-28	1.6321
70	-15	+2	-38	-9	-30	-12	-26	8.2828-5
75	-16	-3	-38	-9	-30	-12	-26	3.9921
80	-23	-2	-42	-8	-36	-10	-30	1.8458
J U L Y								
5	-2	+1	-5	-1	-4	-1	-3	7.3643-1
10	0	+3	-4	+2	-2	+1	-1	4.1351
15	+8	+17	+2	+15	+4	+13	+5	1.9476
20	+6	+11	0	+8	+2	+7	+3	8.8910-3
25	+7	+10	+4	+9	+5	+8	+6	4.0084
30	+7	+12	0	+9	+2	+8	+4	1.8410
35	+9	+16	0	+12	+3	+10	+6	8.4634-3
40	+13	+21	+4	+16	+8	+14	+10	3.9957
45	+15	+26	+6	+20	+10	+18	+12	1.9663
50	+17	+31	+9	+25	+12	+21	+14	1.0269
55	+17	+32	+8	+25	+11	+22	+14	5.6810-4
60	+19	+30	+4	+26	+10	+24	+13	3.0968
65	+20	+40	+4	+35	+10	+30	+13	1.6321
70	+20	+37	0	+32	+9	+27	+12	8.2828-5
75	+19	+40	-2	+30	+7	+26	+11	3.9921
80	+14	+32	-4	+30	+4	+25	+9	1.8458

Table 15.18c. Median, High, and Low Percentile Values of Densities Given as Percentage Departures From U.S. Standard Atmosphere 1976 for January and July at 60°N

Altitude (km)	Median (% of Std)	1%		10%		20%		U.S. Std Density (kg m ⁻³)
		High	Low	High	Low	High	Low	
J A N U A R Y								
5	+1	+6	-3	+4	-1	+2	0	7.3643-1
10	-6	+3	-15	+2	-15	-3	-10	4.1351
15	-9	-2	-15	-5	-12	-6	-11	1.9476
20	-8	-1	-15	-5	-11	-6	-10	8.8910-2
25	-7	+3	-16	-2	-12	-4	-10	4.0084
30	-10	+7	-32	+2	-18	-2	-15	1.8410
35	-12	+8	-35	+3	-27	-3	-19	8.4634-3
40	-15	+10	-36	+5	-30	-4	-20	3.9957
45	-21	+12	-39	+5	-34	-10	-24	1.9663
50	-26	+14	-43	+3	-36	-15	-29	1.0269
55	-32	+9	-48	-10	-39	-20	-35	5.6810-4
60	-36	+4	-54	-12	-40	-25	-39	3.0968
65	-36	-5	-50	-16	-46	-27	-42	1.6321
70	-37	-12	-54	-25	-49	-32	-43	8.2828-5
75	-35	-10	-53	-24	-47	-30	-42	3.9921
80	-28	-11	-53	-17	-47	-21	-40	1.8458
J U L Y								
5	-2	+2	-5	+1	-4	0	-3	7.3643-1
10	0	+7	-8	+4	-5	+2	-3	4.1351
15	0	+6	-7	+3	-4	+2	-2	1.9476
20	+3	+7	-2	+6	0	+5	+1	8.8910-2
25	+5	+8	+1	+7	+2	+6	+3	4.0084
30	+7	+12	-1	+9	+2	+8	+4	1.8410
35	+10	+18	0	+14	+3	+12	+7	8.4634-3
40	+15	+23	+5	+19	+10	+17	+12	3.9957
45	+20	+28	+7	+25	+13	+23	+16	1.9663
50	+25	+35	+10	+30	+16	+28	+22	1.0269
55	+27	+35	+11	+30	+16	+29	+22	5.6810-4
60	+28	+42	+11	+39	+16	+33	+22	3.0968
65	+35	+50	+11	+44	+18	+39	+28	1.6321
70	+42	+52	+12	+46	+20	+44	+30	8.2828-5
75	+44	+58	+12	+52	+20	+48	+35	3.9921
80	+40	+56	+10	+50	+18	+44	+30	1.8458

Table 15.18d. Median, High, and Low Percentile Values of Densities Given as Percentage Departures From U.S. Standard Atmosphere 1976 for January and July at 75°N

Altitude (km)	Median (% of Std)	1%		10%		20%		U.S. Std Density (kg m ⁻³)
		High	Low	High	Low	High	Low	
J A N U A R Y								
5	+2	+6	-1	+5	0	+4	+1	7.3643-1
10	-8	+2	-18	-3	-13	-5	-10	4.1351
15	-10	-1	-18	-6	-14	-8	-13	1.9476
20	-12	-1	-22	-6	-17	-8	-15	8.8910-2
25	-15	-2	-28	-8	-20	-10	-18	4.0084
30	-21	-4	-36	-9	-26	-16	-24	1.8410
35	-25	0	-43	-10	-32	-16	-30	8.4634-3
40	-29	+4	-48	-9	-38	-16	-38	3.9957
45	-33	+8	-52	-6	-45	-16	-39	1.9663
50	-38	+4	-56	-8	-48	-20	-42	1.0269
55	-44	+5	-65	-10	-56	-23	-50	5.6810-4
60	-46	0	-70	-16	-60	-32	-55	3.0968
65	-47	+1	-66	-27	-62	-35	-58	1.6321
70	-48	-1	-69	-21	-62	-35	-60	8.2828-5
75	-45	-10	-65	-25	-57	-35	-53	3.9921
80	-40	-8	-55	-24	-50	-34	-45	1.8458
J U L Y								
5	1	+4	-2	+3	-1	+2	0	7.3643-1
10	-4	+5	-12	+3	-10	0	-7	4.1351
15	-4	+2	-9	0	-7	-2	-6	1.9476
20	+1	+6	-4	+4	-2	+3	-1	8.8910-2
25	+1	+10	-8	+6	-3	+5	-2	4.0084
30	+7	+13	+2	+10	+5	+8	+6	1.8410
35	+12	+25	+3	+18	+8	+16	+10	8.4634-3
40	+19	+27	+6	+23	+13	+21	+16	3.9957
45	+25	+35	+10	+30	+18	+28	+21	1.9663
50	+27	+40	+10	+35	+20	+32	+24	1.0269
55	+32	+42	+10	+39	+20	+35	+25	5.6810-4
60	+37							3.0968
65	+48							1.6321
70	+60							8.2828-5
75	+67							3.9921
80	+64							1.8458

the time are given as percent departures from the U.S. Standard Atmosphere at 5-km altitude increments. The 1 percent values for altitudes above 30 km are considered rough estimates as they are based on the tails of the distributions of observed values plotted on probability paper. Estimates above 60 km are less reliable than those at lower levels because of the paucity of data and larger observational errors at the higher altitudes. In tropical regions the monthly density distributions are nearly normal for altitudes up to 50 km. Consequently, reasonable estimates of the distributions of density in the tropics can be obtained from monthly means and standard deviations. Standard deviations of the observed densities around the mean monthly values at Ascension, given in Table 15.19, are typical of the day-to-day variations found in the tropics.⁸

Table 15.19. Standard Deviations (Percent) of Observed Day-to-Day Variations in Density Around the Monthly Mean at Ascension (8°S)

Altitude (km)	S.D. of Density (% of Monthly Mean)			
	Jan	Apr	July	Oct
5	0.4	0.3	0.3	0.4
10	0.4	0.4	0.4	0.4
15	0.8	0.7	0.8	0.7
20	1.5	1.3	1.8	1.3
25	1.3	1.3	1.2	1.3
30	1.2	1.2	1.4	1.2
35	1.8	1.8	1.4	1.2
40	2.3	2.1	1.8	1.8
45	2.3	2.3	2.6	2.3
50	2.7	2.5	2.6	2.7

15.2.3 Spatial Variation

The rate of decay of the correlation coefficient between densities at two points with increasing horizontal separation is directly related to the scale of the major features of the weather patterns that are experienced at a specific latitude and altitude. Figure 15.20 shows how the density correlations decay with distance near 60°N for altitudes up to 60 km. The decay in density correlations below 20 km is based on an interpretation of data from studies of the spatial correlations of pressure, temperature, density, and wind at radiosonde levels at

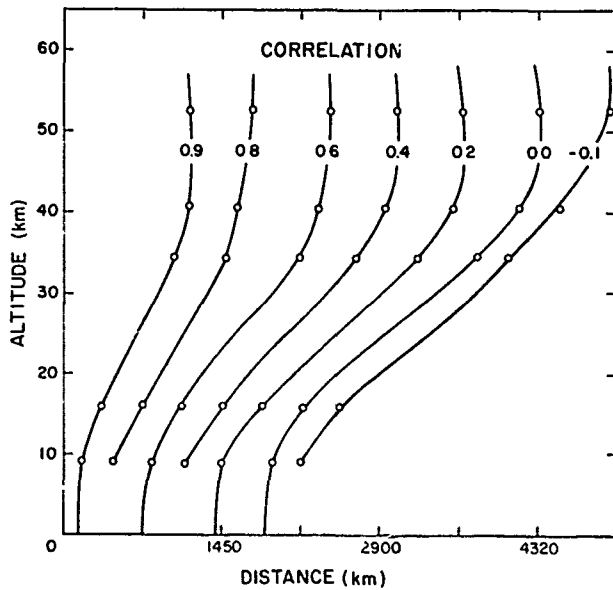


Figure 15.20. Decay of Density Correlations With Distance at Various Altitudes in Midlatitudes

locations between 30 and 70°N latitude.¹⁶ Information on the spatial correlations at altitudes above 20 km is from a study by Cole.¹⁷ In that paper, data from constant pressure maps for 5.0-, 2.0-, and 0.4-mb levels were used together with nearly simultaneous rocket observations at several pairs of stations near 60°N to determine the rates of decay of density correlation at levels between 30 and 55 km. As Figure 15.20 indicates, the rate of decay in density correlation with distance decreases substantially with altitude. At 10 km, for example, zero correlation is attained at about 2000 km; at 50 km, zero correlation is attained at more than twice that distance, or 4450 km. This analysis indicates the presence of disturbances with wavelengths of roughly 18500 km at 50 km, close to planetary wavelength number one at 60°N . Information from Kantor and Cole¹⁸ on the correlations between densities at points up to 370 km apart in tropical regions is provided in Table 15.20, for levels between 10 and 60 km.

-
- 16. Bertoni, E.A., and Lund, I.A. (1964) Winter Space Correlations of Pressure, Temperature and Density to 16 km, AFCRL-64-1020, AD A611002.
 - 17. Cole, A.E. (1979) Review of data and models of the middle atmosphere, Space Research 1979.
 - 18. Kantor, A.J., and Cole, A.E. (1979) Time and Space Variations of Density in the Tropics, AFGL-TR-79-0109, AD A074472.

Table 15.20. Correlation Coefficients Between Densities at Points up to 370 km (200 nmi) Apart in the Tropics

Altitude (km)	Correlation Coefficient		
	90 km	180 km	370 km
10	0.97	0.95	0.90
20	0.98	0.97	0.92
30	0.98	0.97	0.92
40	0.98	0.97	0.92
50	0.98	0.97	0.92
60	0.98	0.97	0.92

The rms difference between the densities at two points can be estimated by:

$$\hat{\sigma}_{xy} = \sqrt{\sigma_x^2 + \sigma_y^2 - 2r_{xy}\sigma_x\sigma_y} \quad (15.25)$$

where $\hat{\sigma}_{xy}$ is the estimated rms difference between densities at points x and y, σ_x^2 and σ_y^2 are the variances of density around the monthly mean values, and r_{xy} is the correlation coefficient between the densities at points x and y. For short distances (up to 550 km), σ_x^2 and σ_y^2 can usually be assumed to be equal.

The estimated rms difference between densities that are observed simultaneously at locations 90, 180, and 370 km apart in the tropics are presented in Table 15.21 for altitudes between 10 and 60 km. For a given month, the rms differences provided in Table 15.21 may be considered to represent variability around the mean monthly density gradients, which are given in Table 15.22 for the latitudinal differences.¹⁹ Longitudinal differences remain near zero in tropical areas. Information on the spatial variability of density is useful in determining how accurately a density observation taken 90 to 550 km from the point of vehicle reentry represents the conditions encountered in the reentry corridor.

15.2.4 Statistical Applications to Reentry Problems

The relatively large number of available radiosondes and meteorological rocket observations permit a detailed analysis of the characteristics of

19. Cole, A.E., and Kantor, A.J. (1975) Tropical Atmospheres, 0 to 90 km, AFCRL-TR-75-0527, AD A019940.

Table 15.21. Estimated rms Differences (Percent of Mean) Between Densities at Locations 90, 180, and 360 km Apart During the Midseason Months in the Tropics

Altitude (km)	January			April			July			October		
	90 km	180 km	360 km									
10	0.10	0.13	0.18	0.10	0.13	0.18	0.10	0.13	0.18	0.10	0.13	0.18
15	0.13	0.17	0.25	0.11	0.14	0.21	0.16	0.20	0.30	0.16	0.20	0.30
18	0.50	0.61	1.00	0.34	0.42	0.68	0.30	0.37	0.60	0.34	0.42	0.68
20	0.28	0.34	0.56	0.28	0.34	0.56	0.24	0.29	0.48	0.24	0.29	0.48
25	0.28	0.34	0.56	0.28	0.34	0.56	0.24	0.29	0.48	0.26	0.32	0.52
30	0.30	0.37	0.60	0.30	0.37	0.60	0.28	0.34	0.56	0.30	0.37	0.60
35	0.34	0.42	0.68	0.30	0.37	0.60	0.30	0.37	0.60	0.36	0.44	0.72
40	0.40	0.49	0.80	0.44	0.54	0.88	0.48	0.59	0.96	0.44	0.54	0.88
45	0.46	0.56	0.92	0.40	0.49	0.80	0.60	0.73	1.20	0.52	0.64	1.04
50	0.56	0.69	1.12	0.54	0.66	1.08	0.72	0.88	1.44	0.54	0.66	1.08
55	0.66	0.81	1.32	0.56	0.69	1.12	0.84	1.03	1.68	0.78	0.96	1.56
60	0.84	1.03	1.68	0.86	0.81	1.32	1.00	1.22	2.00	0.82	1.00	1.64

Table 15.22. Mean Monthly Latitudinal Density Gradients (Percent Change per 180 km) in the Tropics

Altitude (km)	January Gradient (%)	April Gradient (%)	July Gradient (%)	October Gradient (%)
10	0.01	0.02	0.03	0.04
15	0.15	0.17	0.08	0.05
20	0.12	0.23	0.08	0.06
25	0.04	0.14	0.10	0.14
30	0.26	0.13	0.14	0.21
35	0.13	0.22	0.16	0.23
40	0.03	0.16	0.16	0.20
45	0.14	0.01	0.17	0.21
50	0.11	0.09	0.12	0.20
55	0.08	0.12	0.04	0.27
60	0.09	0.04	0.10	0.25

atmosphere density profiles at altitudes below 60 km. Arrays of means and standard deviations of density at 2-km intervals of altitude from the surface to 60 km, together with interlevel correlation coefficients between levels have been developed for tropical, temperate, and arctic regions.⁸ Tables 15.23a to 15.23f contain statistical arrays of density for the months of January and July at Kwajalein (9°N), Wallops Island (38°N), and Ft. Churchill (59°N).

Variations in the range or deceleration of free falling objects or ballistic missiles that arise from day-to-day changes in atmospheric density can be estimated from Tables 15.23a to 15.23f. The integrated effect, E, of mean monthly density on the trajectory or impact point of a missile can be determined for a specific location by computer "flights" through mean monthly or seasonal density profiles, if the proper influence coefficients, C_i, for the missile at various levels are given. For example, we can write

$$E = \sum C_i \bar{\rho}_i , \quad (15.26)$$

where $\bar{\rho}_i$ is the mean monthly density at the ith level. The influence coefficients depend upon aerodynamic characteristics, reentry angle, and the speed of the vehicle. The integrated standard deviation in range or deceleration, σ_{int} , due

Table 15.23a. Kwajalein - Correlation of January Density (kg/m^3) From Surface to 60 km

KM	KILOMETERS ABOVE SEA LEVEL																															
	MEAN AVERAGE OF OBSERVED VALUES					STDEV STANDARD DEVIATION OF VALUES																										
STDV	IN PERCENT OF MEAN TIMES 10																															
	N NUMBER OF VALUES AT EACH ALTITUDE																															
0.006	2	4	6	8	10	12	14	16	18	20	22	24	26	28	30	32	34	36	38	40	42	44	46	48	50	52	54	56	58	60		
*MEAN 11.67	963	706	639	516	416	382	261	199	141	934	654	450	342	248	182	133	930	725	533	405	303	239	175	134	105	826	644	544	397	316		
N	4	4	5	4	5	5	10	28	15	13	12	16	15	15	17	16	16	16	16	17	18	21	20	23	28	22	26	33	34	37	37	
2	17	37	22	14	17	37	22	14	17	49	27	49	27	49	27	49	27	49	27	49	27	49	27	49	27	49	27	49	27	49		
4	6	6	-9	-24	-24	-9	-24	-24	-9	-24	-10	-24	-10	-24	-10	-24	-10	-24	-10	-24	-10	-24	-10	-24	-10	-24	-10	-24	-10	-24		
10	9	10	17	9	58	17	21	49	21	49	21	49	21	49	21	49	21	49	21	49	21	49	21	49	21	49	21	49	21	49		
12	7	17	21	21	49	21	49	21	49	21	49	21	49	21	49	21	49	21	49	21	49	21	49	21	49	21	49	21	49			
14	17	21	21	21	49	21	49	21	49	21	49	21	49	21	49	21	49	21	49	21	49	21	49	21	49	21	49	21	49			
16	2	17	21	21	49	21	49	21	49	21	49	21	49	21	49	21	49	21	49	21	49	21	49	21	49	21	49	21	49			
18	-1	-1	-1	-1	-1	-1	-1	-1	-1	-1	-1	-1	-1	-1	-1	-1	-1	-1	-1	-1	-1	-1	-1	-1	-1	-1	-1	-1	-1	-1		
20	-1	9	6	19	7	28	17	7	12	15	-1	9	6	19	7	28	17	7	12	15	-1	9	6	19	7	28	17	7	12	15		
22	-1	-2	-22	-28	-25	-16	-45	-5	-27	-21	-38	-27	-21	-38	-27	-21	-38	-27	-21	-38	-27	-21	-38	-27	-21	-38	-27	-21	-38	-27	-21	
24	-1	-30	-30	-30	-30	-30	-30	-30	-30	-30	-30	-30	-30	-30	-30	-30	-30	-30	-30	-30	-30	-30	-30	-30	-30	-30	-30	-30	-30	-30		
26	-1	-16	-16	-16	-16	-16	-16	-16	-16	-16	-16	-16	-16	-16	-16	-16	-16	-16	-16	-16	-16	-16	-16	-16	-16	-16	-16	-16	-16	-16		
28	-1	-14	-14	-14	-14	-14	-14	-14	-14	-14	-14	-14	-14	-14	-14	-14	-14	-14	-14	-14	-14	-14	-14	-14	-14	-14	-14	-14	-14	-14		
30	4	13	13	14	14	14	14	14	14	14	14	14	14	14	14	14	14	14	14	14	14	14	14	14	14	14	14	14	14	14		
32	15	6	5	17	17	49	49	49	49	49	49	49	49	49	49	49	49	49	49	49	49	49	49	49	49	49	49	49	49	49		
34	6	6	6	17	17	49	49	49	49	49	49	49	49	49	49	49	49	49	49	49	49	49	49	49	49	49	49	49	49	49		
36	6	6	6	17	17	49	49	49	49	49	49	49	49	49	49	49	49	49	49	49	49	49	49	49	49	49	49	49	49	49		
38	10	21	12	12	12	12	12	12	12	12	12	12	12	12	12	12	12	12	12	12	12	12	12	12	12	12	12	12	12	12		
40	-1	-16	-16	-16	-16	-16	-16	-16	-16	-16	-16	-16	-16	-16	-16	-16	-16	-16	-16	-16	-16	-16	-16	-16	-16	-16	-16	-16	-16	-16		
42	-4	-4	-4	-4	-4	-4	-4	-4	-4	-4	-4	-4	-4	-4	-4	-4	-4	-4	-4	-4	-4	-4	-4	-4	-4	-4	-4	-4	-4	-4	-4	
44	-4	-4	-4	-4	-4	-4	-4	-4	-4	-4	-4	-4	-4	-4	-4	-4	-4	-4	-4	-4	-4	-4	-4	-4	-4	-4	-4	-4	-4	-4	-4	
46	-4	-4	-4	-4	-4	-4	-4	-4	-4	-4	-4	-4	-4	-4	-4	-4	-4	-4	-4	-4	-4	-4	-4	-4	-4	-4	-4	-4	-4	-4	-4	
48	-4	-4	-4	-4	-4	-4	-4	-4	-4	-4	-4	-4	-4	-4	-4	-4	-4	-4	-4	-4	-4	-4	-4	-4	-4	-4	-4	-4	-4	-4	-4	
50	3	-1	12	26	-22	-3	-5	-5	-32	-37	-4	-11	14	-1	22	25	3	37	52	44	50	64	63	56	67	60	62	56	67	60	62	56
52	7	15	49	49	49	49	49	49	49	49	49	49	49	49	49	49	49	49	49	49	49	49	49	49	49	49	49	49	49	49	49	
54	-6	6	6	20	20	49	49	49	49	49	49	49	49	49	49	49	49	49	49	49	49	49	49	49	49	49	49	49	49	49	49	
56	-6	6	6	24	24	49	49	49	49	49	49	49	49	49	49	49	49	49	49	49	49	49	49	49	49	49	49	49	49	49	49	
58	-6	6	6	24	24	49	49	49	49	49	49	49	49	49	49	49	49	49	49	49	49	49	49	49	49	49	49	49	49	49	49	
60	-27	5	7	27	-20	6	1	7	-37	-29	4	14	4	-25	-20	-32	-1	6	18	14	51	58	45	64	33	97	86	91	60	62	56	

* MULTIPLY MEAN BY INDICATED NEGATIVE POWER OF 10

Table 15.23b. Kwajalein - Correlation of July Density (kg/m^3) From Surface to 60 km

* MULTIPLY MEAN BY INDICATED NEGATIVE POWER OF 10

MULTIPLY INVERSE VALUES BY 0.8911 TO OBTAIN CORRELATION COEFFICIENTS

Table 15.23c. Wallops Island - Correlation of January Density (kg/m^3) From Surface to 60 km

KH	KILOMETERS ABOVE SEA LEVEL									
	MEAN AVERAGE OF OBSERVED VALUES									
STDV	STANDARD DEVIATION OF MEAN TIMES 10									
	N NUMBER OF VALUES AT EACH ALTITUDE									
0.015	2	4	6	8	10	12	14	16	18	20
*MEAN	10292	921	650	524	411	310	227	160	122	676
-0.3	-3	-3	-3	-3	-3	-3	-3	-3	-3	-3
STDV	23	26	16	10	15	35	51	41	39	29
N	44	44	44	44	44	44	44	43	43	43
2	74	**92	66	56	46	36	26	16	10	2
6	6	56	53	50	25	29	24	22	20	10
8	-29	-62	-50	-25	-29	-29	-24	-22	-20	-10
10	-33	-75	-74	-9	66	92	97	97	92	94
12	-42	-72	-79	-34	61	64	66	66	66	66
14	-43	-78	-84	-34	62	64	66	66	66	66
16	-39	-82	-84	-23	63	65	67	67	67	67
18	-34	-76	-84	-23	63	65	67	67	67	67
20	-37	-76	-72	-9	57	70	67	79	63	92
22	-51	-47	-5	32	46	49	49	52	61	72
24	-51	-49	-5	32	46	49	49	52	61	72
26	-50	-49	-5	32	46	49	49	52	61	72
28	-50	-49	-5	32	46	49	49	52	61	72
30	-45	-37	11	46	46	41	43	55	53	41
32	-12	-28	-25	-3	21	16	28	33	36	36
34	-16	-24	-24	-1	21	16	28	33	36	36
36	-16	-24	-24	-1	21	16	28	33	36	36
38	-16	-24	-24	-1	21	16	28	33	36	36
40	-8	-14	-23	-1	-8	6	3	6	4	-13
42	-32	-7	-7	-6	-16	-3	-5	-8	-18	-13
44	-34	-5	-5	-5	-13	-1	-4	-7	-16	-13
46	-32	-5	-5	-5	-13	-1	-4	-7	-16	-13
48	-6	-1	-4	-1	-10	-2	-7	-9	-13	-1
50	-12	-7	-5	-2	1	0	3	12	13	3
52	-3	9	-3	-5	-5	-5	-2	7	7	-3
54	-2	9	-6	-6	-6	-6	-12	8	8	-16
56	15	15	-3	-12	-12	-12	-12	-12	-12	-12
58	2	15	4	-7	-12	-10	-9	-5	-17	-12
60	-6	26	-8	-47	-46	-32	-29	-23	-41	-52

* MULTIPLY MEAN BY INDICATED NEGATIVE POWER OF 10

** MULTIPLY TABULAR VALUES BY 0.01 TO OBTAIN CORRELATION COEFFICIENTS

Table 15.23d. Wallops Island - Correlation of July Density (kg/m^3) From Surface to 60 km

KM	KILOMETERS ABOVE SEA LEVEL									
	MEAN		AVERAGE OF OBSERVED VALUES		STDEV		STANDARD DEVIATION OF VALUES IN PERCENT OF MEAN TIMES 10		N	
	NUMBER OF VALUES AT EACH ALTITUDE									
.015	2	4	6	8	10	12	14	16	18	20
*MEAN	980	798	647	522	420	333	254	184	131	934
1192	-3	-3	-3	-3	-3	-3	-3	-3	-3	673
12	0	16	16	20	27	74	42	10	10	486
14	-16	-24	-16	-20	-25	-20	-12	-12	-10	360
16	-20	-34	-14	-18	-22	-12	-2	-12	-10	264
18	-7	-15	-14	-18	-22	-12	-2	-12	-10	194
20	-1	13	-6	12	7	-2	-3	24	36	143
22	-12	11	-9	14	3	8	16	12	21	106
24	-14	17	0	24	5	18	23	12	21	94
26	21	34	10	19	8	12	19	5	4	75
28	3	7	-16	-9	-4	5	-4	-3	13	53
30	3	7	-16	-9	-4	5	-4	-3	67	75
32	6	16	-17	-1	-13	-6	0	4	30	59
34	-3	13	-19	-5	-10	-7	0	4	29	59
36	16	-16	-19	-5	-10	-7	0	4	29	51
38	19	-16	-19	-5	-10	-12	11	1	30	46
40	4	8	-15	-4	-17	-20	-9	2	-2	22
42	2	7	-18	-5	-19	-22	-1	14	10	28
44	21	27	-12	-6	-7	-9	-2	12	5	47
46	14	18	-14	-2	-10	-12	-4	13	5	42
48	7	17	-24	-9	-14	-22	-6	20	4	29
50	12	12	-22	-11	-10	-15	-1	14	4	33
52	11	5	-32	-21	-15	-22	-4	16	8	33
54	8	5	-31	-21	-15	-22	-4	15	8	31
56	9	8	-22	-6	-17	-14	-6	12	9	35
58	12	6	-22	-5	-6	-17	-15	9	6	40
60	-3	-16	-43	-13	-35	-2	35	50	24	31

* MULTIPLY MEAN BY INDICATED NEGATIVE POWER OF 10

** MULTIPLY TABULAR VALUES BY 0.01 TO OBTAIN CORRELATION COEFFICIENTS

Table 15.23e. Ft. Churchill - Correlation of January Density (kg/m^3) From Surface to 60 km

KH YEAR	KILMETERS ABOVE SEA LEVEL									
	MEAN AVERAGE OF OBSERVED VALUES					STDEV STANDARD DEVIATION OF VALUES IN PERCENT OF MEAN TIMES 10				
	N NUMBER OF VALUES AT EACH ALTITUDE									
	KH	4	6	8	10	12	14	16	20	22
.035	2	4	6	8	10	12	14	16	20	22
1446	1076	848	665	511	375	273	201	148	109	806
-3	-7	-3	-3	-3	-3	-3	-3	-3	-3	-3
STDV	31	19	15	12	24	26	22	20	26	30
N	50	50	50	50	50	50	50	50	40	30
	24	36	72	**	70	60	55	55	46	30
	6	-6	-36	-6	6	55	55	55	46	30
	10	-25	-49	-22	33	49	49	49	40	30
	12	-34	-59	-32	20	71	94	94	89	70
	14	-45	-69	-49	14	57	63	63	62	55
	16	-59	-79	-59	15	57	62	62	62	55
	20	-45	-22	3	4	-2	9	17	35	60
	22	-10	-19	56	6	-11	-3	2	18	45
	24	-20	-39	56	41	-17	-5	1	11	31
	26	-29	-49	56	41	-17	-5	1	11	31
	28	-35	-53	51	46	-20	-7	10	29	41
	30	-43	-50	-1	17	-3	1	1	20	30
	32	-49	-58	-2	16	-4	-1	1	20	30
	34	-52	-59	-2	16	-4	-1	1	20	30
	36	-52	-59	-2	16	-4	-1	1	20	30
	38	-52	-59	-2	16	-4	-1	1	20	30
	40	-52	-59	-2	16	-4	-1	1	20	30
	42	-52	-59	-2	16	-4	-1	1	20	30
	44	-52	-59	-2	16	-4	-1	1	20	30
	46	-52	-59	-2	16	-4	-1	1	20	30
	48	-52	-59	-2	16	-4	-1	1	20	30
	50	-52	-59	-2	16	-4	-1	1	20	30
	52	-52	-59	-2	16	-4	-1	1	20	30
	54	-52	-59	-2	16	-4	-1	1	20	30
	56	-52	-59	-2	16	-4	-1	1	20	30
	58	-52	-59	-2	16	-4	-1	1	20	30
	60	-49	-42	-31	-6	1	-1	0	-4	-10

* MULTIPLY MEAN BY INDICATED NEGATIVE POWER OF 10

** MULTIPLY TABULAR VALUES BY 0.01 TO OBTAIN CORRELATION COEFFICIENTS

Table 15,23f. Ft. Churchill - Correlation of July Density (kg/m^3) From Surface to 60 km

* MULTIPLY MEAN BY INDICATED NEGATIVE POWER OF 10

to day-to-day variations from the mean seasonal or the mean monthly density profile can be obtained from

$$\sigma_{int}^2 = \sum_{ij} C_i \sigma_i r_{ij} \cdot C_j \sigma_j , \quad (15.27)$$

where σ_{int}^2 is the integrated variance for all layers being considered, C_i and C_j are influence coefficients at the i th and j th levels, σ_i and σ_j are the standard deviations of density at the two levels, and r_{ij} is the correlation coefficient between densities at the two levels. In these computations, the density is assumed to have a Gaussian distribution at all levels. As a result, the error in the CEP (the circle within which 50 percent of the events are expected to occur) will be generally less than 10 percent.

15.2.5 Variability With Time

Studies based on radiosonde observations have shown that there are no significant diurnal variations in density at altitudes up to 30 km. The analysis of meteorological rocket observations, however, indicates the presence of a significant diurnal oscillation in density at altitudes between 35 and 60 km. The phases and amplitudes of the diurnal oscillation at these altitudes are best defined in the tropics. The decrease in the number of available observations above 60 km and the larger random observational errors at the higher altitudes make it difficult to obtain reliable estimates of the magnitude of the diurnal variations at altitudes between 60 and 90 km.

The 50-km densities from a series of soundings taken at Ascension during a 48-h period in April 1966¹⁹ are plotted versus local time in Figure 15.21. Densities are given as per cent departure from the 1976 U.S. Standard Atmosphere. The crosses represent averages of observations taken within 2 h of each other. A harmonic analysis of the eight average values produced the solid curve when the first and second harmonics for the 48-h period were added together. An F-test indicates that the second harmonic, which represents the diurnal oscillation in density, has an amplitude of slightly less than 4 percent (a range of almost 8 percent) and is significant at the 1 percent level; it reduces the observed variance by 91 percent. Maximums occur at 1600 and minimums near 0400 local time. From this analysis it is apparent that the diurnal oscillation is the dominant short-period fluctuation at 50 km.

The rms differences between density observations taken from 1 to 36 h apart also provide a measure of the rate of change in density with time at a given altitude. Computed rms values from the Ascension series mentioned

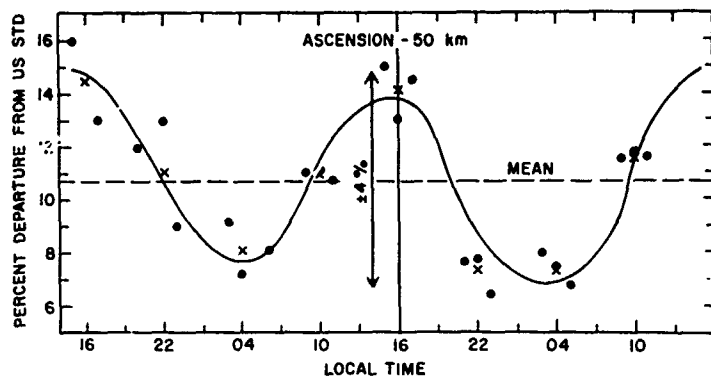


Figure 15.21. Diurnal Density (50 km) Variation at Ascension (Dots Indicate Observed Values, x's Represent 3-h Averages, and the Solid Line Depicts the Computed Diurnal Cycle)

above are shown as a function of time in Figure 15.22 for altitudes from 35 to 60 km. The number of pairs of observations available for each time interval is also shown. Since at time $T = 0$ the rms change in space is zero, an estimate of the random observational error can be obtained from the observations themselves by extrapolating curves in Figure 15.22 back to zero hours. This procedure indicates that the random rms errors are approximately 1 percent at 35 and 40 km, and 1.5 to 2.0 percent at altitudes between 45 and 60 km.

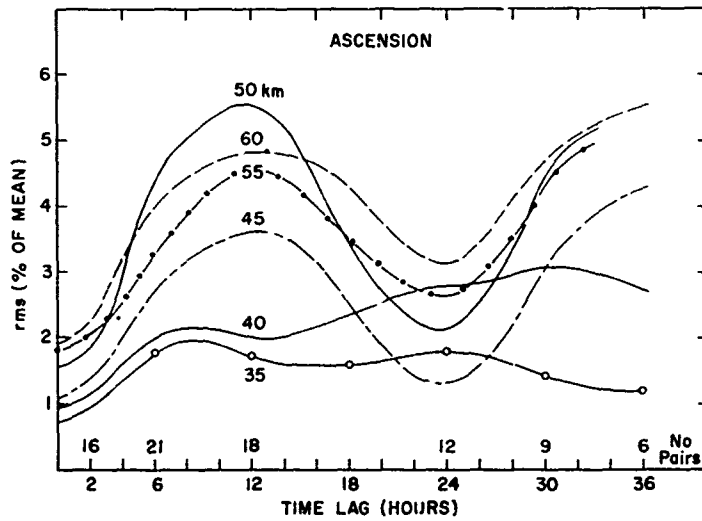


Figure 15.22. Root Mean Square (rms) Lag Variability of Density With Time at Ascension

If there are no well-defined periodic oscillations within a 24-h period, the rms variability would be expected to increase smoothly with time until it reached a value representing the climatic or the day-to-day variability around the monthly mean. However, a well-defined 24-h oscillation can be seen (Figure 15.22) in the rms density variations at all altitudes between 40 and 60 km with maximums at 12 and 36 hours and a minimum at 24 hours. An analysis of meteorological rocket observations taken at Kwajalein (9° N) and Ft. Sherman (9° N) show similar results.²⁰ The diagram in Figure 15.22 and the results of similar studies show that, in the tropics, an observation 24-h old is more representative of actual conditions than one 12-h old.

The observed rms variations of density with time lags of 1, 2, 4, and 6 h are shown in Figure 15.23 for levels between 60 and 90 km at Kwajalein. This information, from Cole et al.,²¹ is based on a July 1978 series of high-altitude ROBIN falling sphere flights at Kwajalein. The first profile represents the estimated rms observational error.

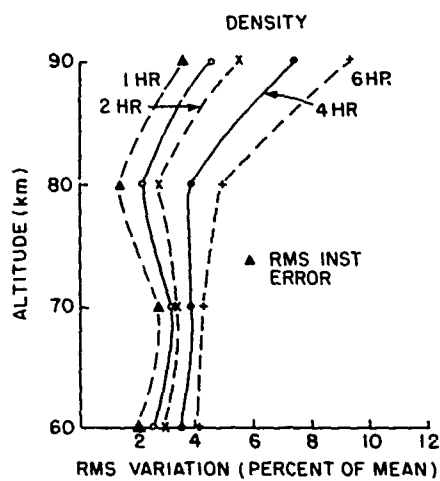


Figure 15.23. The rms Variation in Density for Time Lags of 1 to 6 h at Kwajalein

-
- 20. Kantor, A.J., and Cole, A.E. (1981) Variations of Density and Wind With Time at Altitudes 30 to 60 km, AFGL-TR-81-0281, AD A109804.
 - 21. Cole, A.E., Kantor, A.J., and Philbrick, C.R. (1979) Kwajalein Reference Atmospheres, 1979, AFGL-TR-79-0241, AD A081780.

The rms variations of density with time at the 50-km level in Figure 15.24 are shown for Wallops Island (38°N) and Ft. Churchill (59°N) for the months of January and July. Unlike the tropics, a 24-h oscillation in density is not apparent from this analysis, which is based on 8 years of data at Ft. Churchill and 10 years at Wallops Island. The diurnal oscillation is relatively small and is probably masked by instrumentation errors and changing synoptic patterns. The rms variability at both locations increases with time until the climatic values of day-to-day variations around the monthly means are reached.

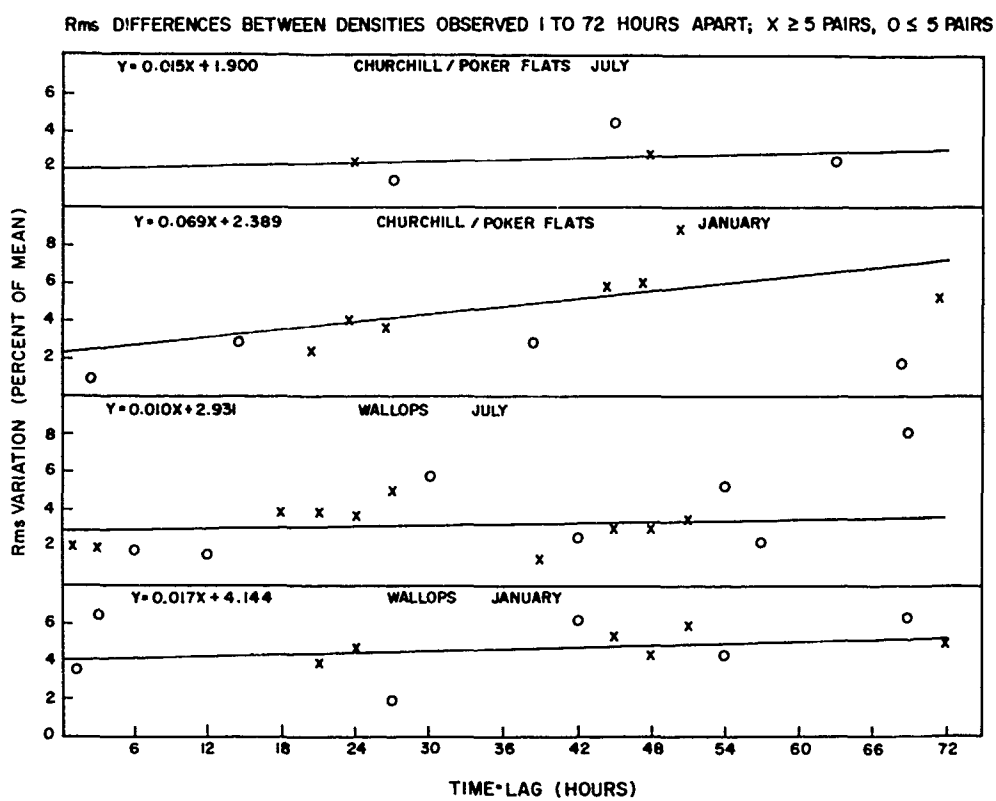


Figure 15.24. The rms Differences Between Densities Observed 1 to 72 h Apart at 50 km ($x \geq 5$ pairs, $o \leq 5$ pairs)

15.3 ATMOSPHERIC PRESSURE UP TO 90 km

Pressure data provided in this section are based on (1) routine radiosonde observations taken by national weather services and extending to approximately 30 km, and (2) measurements from rockets and instruments released from rockets at altitudes between 25 and 90 km. Both data sources are supplemented with pressures derived from measurements made from earth-orbiting satellites. Although atmospheric pressure above radiosonde altitudes is occasionally measured directly, it normally is calculated hydrostatically [as discussed in Standard and Reference Atmospheres (Chapter 14 of the Handbook of Geophysics)] from observed temperatures or densities for altitudes above 30 km. These data are intended for use in design problems involving variations in the heights of constant pressure surfaces and/or changes in pressure at specific altitudes.

15.3.1 Sea-Level Pressure

The variations of sea-level pressure normally have little effect on the operation of surface equipment. However, in the design of sealed containers that could possibly explode or collapse with pressure changes, the range of surface pressures likely to be encountered should be considered. Surface pressures vary with the height of the station above sea level as well as with changing weather patterns. The standard atmospheric pressure at sea level is 1013.25 mb, but there are sizable variations from this value with both time and location.

Table 15.24 indicates extreme sea-level pressures that may be encountered in the Northern Hemisphere. During the month of January, pressures exceeded

Table 15.24. Sea-Level Pressures Exceeded 99 and 1 Percent of the Time in January

Location	Pressure (mb)
	Exceeded 99% of time
Aleutian low	965
Icelandic low	953
	Exceeded 1% of time
Siberian high	1057
Pacific high	1038
Canadian high	1052

Table 15.25. Worldwide Pressure Extremes

		Pressure (mb)	Location	Date
LOW				
World	870*	17°N, 138°E, Typhoon Tip (Wagner ²²)		12 Oct 1979
	876*	13°N, 141°E, Typhoon June (Holliday ²³)		19 Nov 1975
	877*	19°N, 135°E, Typhoon Ida (Riordan ²⁴)		24 Sep 1958
		15°N, 128°E, Typhoon Nora (Holliday ²⁵)		6 Oct 1973
No. America	892. $\bar{3}$	Matcumbe Key, Florida, hurricane (Riordan ²⁴)		2 Sep 1935
HIGH				
World	1083. $\bar{8}$	Agata, Siberia (Riordan ²⁴)		31 Dec 1968
	1075. $\bar{2}$	Irkutsk, Siberia (AFCRL ²⁶)		14 Jan 1893
No. America	1067. $\bar{3}$	Medicine Hat, Alberta (Riordan ²⁴)		24 Jan 1897

*Dropsonde measurements

22. Wagner, A.J. (1980) Weather and circulation of October 1979, Mo. Wea. Rev., 108(No. 1):119.
 23. Holliday, C.R. (1976) Typhoon June - most intense on record, Mo. Wea. Rev., 104(No. 5):1188.
 24. Riordan, P. (1974) Weather Extremes Around the World, Report ETL-TR-74-5, U.S. Army Engineer Topographic Laboratories, Ft. Belvoir, Va.
 25. Holliday, C.R. (1975) An extreme sea-level pressure reported in a tropical cyclone, Mo. Wea. Rev., 103(No. 1):163.
 26. Valley, S.L., Ed. (1965) Handbook of Geophysics, A.F.C.R.L.

99 percent of the time are given for areas under the influence of semipermanent cyclones, and pressures exceeded 1 percent of the time are given for areas under the influence of anticyclones. In the Northern Hemisphere, extreme values, excluding tropical cyclones and tornadoes, are most likely to occur in these regions during January. Table 15.25 lists, for comparison, actual worldwide pressure extremes, including those resulting from storms of tropical origin.

Examples of mean sea-level pressures and typical fluctuations are given in Table 15.26, which contains mean sea-level pressures for the four midseason months and the standard deviations of daily values around these means for 16 specific locations in the Northern Hemisphere.

Table 15.26. Mean Monthly Sea-Level Pressures and Standard Deviations of Daily Values

Location		January		April		July		October	
Latitude	Longitude	Mear. (mb)	S.D. (mb)	Mean (mb)	S.D. (mb)	Mean (mb)	S.D. (mb)	Mean (mb)	S.D. (mb)
10°N	70°W	1013	2	1012	1	1012	1	1011	1
20°N	70°W	1018	2	1017	2	1018	2	1013	2
30°N	70°W	1022	6	1019	5	1021	3	1018	4
40°N	70°W	1018	10	1017	9	1016	5	1018	8
50°N	70°W	1016	12	1014	10	1011	6	1013	11
60°N	70°W	1008	11	1014	10	1008	7	1008	19
70°N	70°W	1004	11	1014	10	1009	6	1006	10
80°N	70°W	1011	11	1020	9	1011	6	1013	8
10°N	20°E	1012	4	1008	3	1009	2	1009	2
20°N	20°E	1017	4	1011	3	1008	2	1012	2
30°N	20°E	1019	5	1014	4	1012	3	1015	3
40°N	20°E	1018	9	1013	3	1013	3	1016	5
50°N	20°E	1020	12	1013	7	1013	5	1017	3
60°N	20°E	1015	16	1012	10	1011	7	1011	11
70°N	20°E	1004	15	1010	10	1012	7	1005	11
80°N	20°E	1008	15	1016	10	1014	7	1010	10

15.3.2 Seasonal and Latitudinal Variations

The Reference Atmospheres²⁷ presented in Chapter 3 of the Handbook of Geophysics provide tables of mean monthly pressure-height profiles, surface to 90 km, for 15° intervals of latitude from the equator to the north pole. These atmospheric models describe both seasonal and latitudinal variation of pressure. Figure 15.25 contains the vertical pressure profiles for the midseason months at each of four latitudes: 15° , 30° , 45° , and 60° N. The profiles are displayed as percent departures from the U.S. Standard Atmosphere, 1976. Pressures

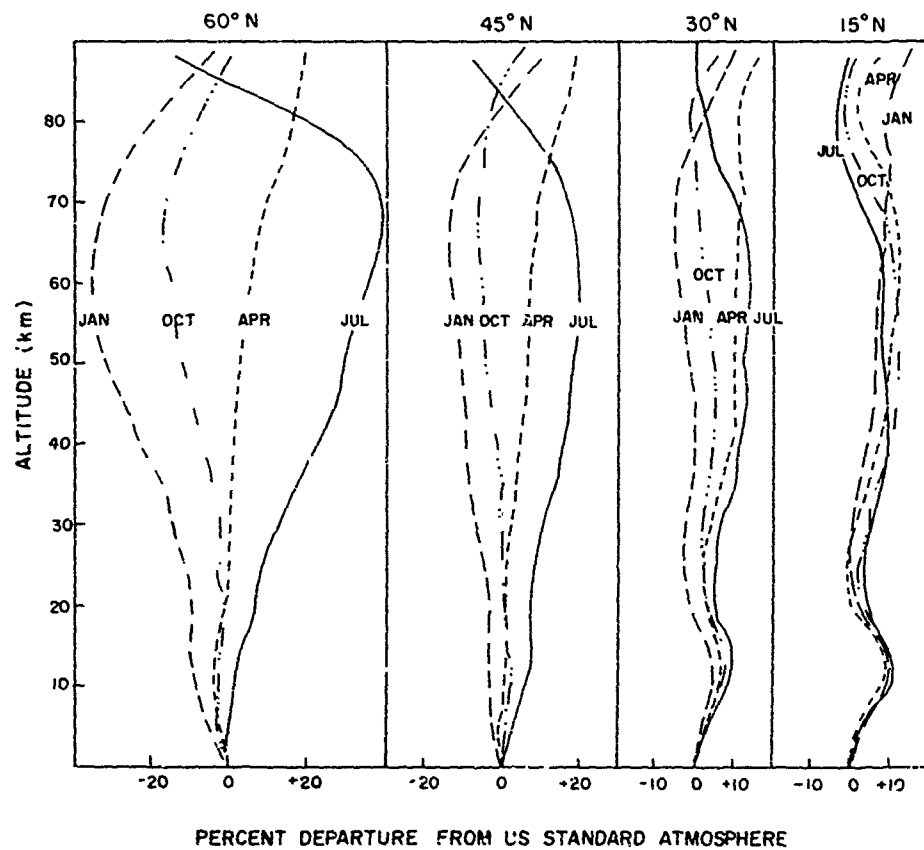


Figure 15.25. Pressure-Altitude Profiles for Midseason Months

27. Cole, A. E., and Kantor, A. J. (1978) Air Force Reference Atmospheres, AFGL-TR-78-0051, AD A058505.

at altitudes between 2 km and 70 or 80 km are highest in summer and lowest in winter over regions poleward of 30°N. In tropical latitudes, seasonal differences are small and do not display a systematic seasonal pattern. Departures from standard generally increase with latitude. Thus, the largest seasonal differences occur at 60°N where mean monthly pressures at 60 to 70 km are nearly 40 percent greater than standard in July and 30 to 36 percent less than standard in January. Consequently, July values are roughly twice those in January between 60 and 70 km. Pressures at these levels at 75°N (not shown) are roughly 10 percent lower than these values in winter and 15 percent higher in summer.

15.3.3 Day-to-Day Variations

Changing synoptic situations, which include movements of high and low pressure centers and their associated ridges and troughs, and variations in the energy absorbed directly by the atmosphere, cause day-to-day changes in the height of constant pressure surfaces. Information on the magnitude of day-to-day variations in the heights of such surfaces are provided in this section. Detailed information for specific levels and locations should be requested from the authors of this report if conditions appear critical.

Table 15.27 lists monthly mean heights of pressure surfaces in January and July and their standard deviations for middle North America. These data indicate the variation in the mean heights of constant pressure surfaces between 700 and 10 mb with latitude and season, and the estimated distributions of day-to-day variability around the monthly means. Estimated departures from mean monthly pressures, which are equalled or exceeded less than 5 percent of the time between 15° and 75°N, are shown in Table 15.28 as percentages of the mean January and July values, surface to 80 km.

As can be seen in Table 15.28, day-to-day variability generally increases with latitude and altitude in both January and July, although to a much smaller extent in July. The estimated 5-percent extremes are largest at 60 to 65 km at all latitudes, reaching ± 35 percent during 60°N winter. Variability appears to decrease above 65 km, to a probable minimum value near 85 km. The estimated departures shown in Table 15.28 include some diurnal and semidiurnal fluctuations due to solar influences, particularly since the basic pressure data were not observed at the same time every day. Envelopes of these estimated 95-percent values should not be used as profiles since such pressures would not necessarily be found at all altitudes at any one given time and/or location. Decreases in atmospheric pressure in one layer, for example, normally are associated with increases in another layer.

Table 15.27. Average Height and Standard Deviation at Standard Pressure Levels Over North America, 90° to 100° W

Pressure (mb)	\bar{N}_{eff} (km)	S_{D} (m)	Average Height and Standard Deviation						80° N Mean (km)	S.D. (m)	
			20°N	30°N	40°N	50°N	60°N	70°N			
JANUARY											
700	3.165	30	3.115	55	3.015	85	2.865	100	2.770	100	2.710
500	5.845	40	5.745	85	5.565	125	5.340	145	5.180	150	5.075
300	9.595	55	9.425	125	9.150	175	8.825	195	8.585	230	8.425
200	12.280	70	12.090	130	11.765	165	11.430	175	11.180	190	10.995
100	16.455	55	16.325	95	16.110	110	15.890	145	15.655	175	15.400
50	20.540	130	20.500	200	20.415	215	20.280	215	20.075	200	19.775
25	24.900	210	24.865	245	24.790	335	24.555	275	24.380	245	23.905
15	28.100	245	28.050	335	28.000	365	27.750	365	27.650	350	27.000
10	30.600	250	30.550	380	30.500	440	30.250	380	30.150	380	29.500
JULY											
700	3.185	15	3.190	20	3.170	35	3.080	55	3.005	60	2.975
500	5.890	20	5.910	25	5.875	50	5.720	85	5.600	90	5.540
300	9.675	30	9.705	35	9.630	80	9.405	130	9.215	125	9.125
200	12.395	40	12.430	50	12.345	100	12.080	135	11.870	135	11.790
100	16.570	45	16.625	50	16.605	65	16.515	80	16.455	85	16.420
50	20.765	75	20.865	90	20.940	105	20.975	105	21.005	105	21.045
25	25.180	150	25.330	150	25.440	175	25.530	175	25.625	165	25.715
15	28.300	170	28.450	170	28.650	175	28.800	175	28.900	175	29.100
10	30.800	190	30.950	190	31.200	190	31.400	190	31.550	190	31.750

Table 15.28. Departures From Mean Monthly Pressures (Percent) Exceeded Less Than 5 Percent of the Time in January and July. Values below 30 km are based on radiosonde observations. Those values above 30 km are based on rocketsonde observations

HEIGHT (km)	JANUARY					JULY				
	75°N	60°N	45°N	30°N	15°N	15°N	30°N	45°N	60°N	75°N
0	±2.5	±3	±2.5	±1	±0.4	±0.4	±0.5	±1	±1	±1.5
10	7	4	3	2	0.8	0.7	0.8	2	3	4
20	10	10	10	7	4	2	2	3	3	3
30	20	16	14	12	7	4	4	4	5	5
40		25	20	15	8	7	8	8	10	
50		30	25	18	10	10	12	13	14	
60		35	30	20	12	12	14	16	18	
70		30	25	18	10	10	12	15	16	
80		20	16	12	8	8	9	10	10	

15.3.4 Diurnal and Semidiurnal Variations

Mean hourly sea-level pressures follow a systematic diurnal and semidiurnal periodicity somewhat variable in amplitude and phase according to location and season. The sea-level pressure cycle is generally characterized by minima near 0400 and 1600 h and maxima near 1000 and 2200 h local time. The amplitude approaches 1 mb, which is small relative to synoptic changes in middle latitudes. In the tropics only minor synoptic changes occur from day to day, so that interdiurnal pressure changes are small compared to the systematic daily variations in these latitudes.

Upper-air pressures appear to follow a systematic diurnal/semidiurnal cycle similar to that at sea-level; however, extremes occur at somewhat different hours. Table 15.29 lists amplitudes and times of occurrence of diurnal and semidiurnal maxima to 10 mb (roughly 30 km) over Terceira, Azores, which provides an estimate of mean annual systematic pressure variations at a maritime location near 40°N. The semidiurnal variations at climatically and geographically different locations such as Washington, D. C. and Terceira, Azores, appear to be similar.²⁶ The diurnal maxima and minima, however, that result from solar insolation and terrestrial radiation, may differ considerably in time of occurrence and amplitude at various locations, particularly at or near surface levels.

Table 15.29. Amplitudes of Systematic Pressure Variations and Time of Maximum at Terceira, Azores (Harris et al²⁸)

Pressure Level (mb)	(m)*	Diurnal		Semidiurnal	
		Ampl. (mb)	Time (h)	Ampl. (mb)	Time (h)
Sfc	0	0.10	2100	0.50	0948
1000	122	0.10	1904	0.53	0950
950	570	0.12	1824	0.46	0956
900	1033	0.16	1612	0.49	1002
850	1454	0.18	1604	0.47	1002
800	2027	0.20	1612	0.44	1002
750	2569	0.20	1616	0.38	1010
700	3127	0.25	1548	0.37	1002
650	3731	0.18	1608	0.40	1030
600	4365	0.25	1608	0.33	1020
550	5051	0.27	1508	0.33	1034
500	5782	0.28	1516	0.29	1032
450	6587	0.27	1424	0.24	1036
400	7449	0.31	1504	0.24	1046
350	8409	0.31	1504	0.20	1046
300	9482	0.32	1444	0.18	1108
250	10708	0.33	1420	0.16	1102
200	12149	0.32	1408	0.14	1110
175	12991	0.32	1352	0.13	1120
150	13948	0.30	1348	0.11	1100
125	15066	0.28	1328	0.11	1124
100	16423	0.26	1304	0.09	1128
80	17776	0.24	1300	0.09	1120
60	19547	0.23	1256	0.07	1124
50	20668	0.21	1256	0.07	1114
40	22077	0.20	1244	0.06	1116
30	24012	0.18	1256	0.05	1110
20	26673	0.16	1256	0.04	1128
15	28005	0.15	1252	0.03	1136
10	30507	0.12	1304	0.01	1204

*Estimated mean annual height

28. Harris, M.F., Finger, F.G., and Teweles, S. (1962) Diurnal variation of wind, pressure and temperature in the troposphere and stratosphere over the Azores, *J. Atmos. Sci.* 19:136.

References

1. Lettau, H. (1954) A study of the mass, momentum and energy budget of the atmosphere, Archiv fur Meteorologie, Geophysik and Bioklimatologie, Serie A, 7:133.
2. Davidson, B., and Lettau, H., Eds. (1957) Great Plains Turbulence Field Program, Pergamon Press, New York.
3. National Weather Service (1979) Surface Observations (Federal Meteorological Handbook 90.1) Superintendent of Documents, Government Printing Office, Washington, D.C. 20402.
4. Gringorten, I. I. (1979) Probability models of weather conditions occupying a line or an area, J. Appl. Met. 18(No. 8):957.
5. Tattelman, P., and Kantor, A.J. (1977) A method for determining probabilities of surface temperature extremes, J. Appl. Meteorol. 16(No. 11):1175.
6. Tattelman, P., Sissenwine, N., and Lenhard, R.W. (1969) World Frequency of High Temperature, AFCRL-69-0348.
7. Tattelman, P. (1968) Duration of Cold Temperature Over North America, AFCRL-68-0232.
8. Cole, A.E., and Kantor, A.J. (1980) Interlevel Correlations of Temperature and Density, Surface to 60 km, AFGL-TR-80-0163, AD A090515.
9. Albrecht, F. (1952) Mikrometeorologische Temperaturmessungen vom Flugzeug aus, Ber. Deutsch. Wetterd. Bad Kissingen 38:332.
10. Draeger, R.H., and Lee, R.H. (1953) Meteorological Data Eniwetok Atoll, Naval Medical Res. Inst. Memo Rept. 53-8, Bethesda, Md.
11. Lettau, H. (1954) Improved models of thermal diffusion in the soil, Trans. Am. Geophys. Union 35:121.
12. Geiger, R. (1957) The Climate Near the Ground, Harvard University Press (translated by M.N. Stewart et al).

13. Kreutz, W. (1943) Der Jahresgang der Temperatur in verschiedenen Boeden unter gleichen Witterungs Verhaeltnisser, Zeitschr. f. angewandte Meteorologie 60:65.
14. Singer, I. A., and Brown, R. M. (1956) Annual variation of sub-soil temperatures about a 600-foot diameter circle, Trans. Am. Geophys. Union 37:743.
15. Sissenwine, N., and Court, A. (1951) Climatic Extremes for Military Equipment, Env. Protection Br., Rpt. No. 146, Dept. of Army, Washington, D.C.
16. Bertoni, E. A., and Lund, I. A. (1964) Winter Space Correlations of Pressure, Temperature and Density to 16 km, AFCRL-64-1020, AD A611002.
17. Cole, A. E. (1979) Review of data and models of the middle atmosphere, Space Research 1979.
18. Kantor, A. J., and Cole, A. E. (1979) Time and Space Variations of Density in the Tropics, AFGL-TR-79-10, AD A074472.
19. Cole, A. E., and Kantor, A. J. (1975) Tropical Atmospheres, 0 to 90 km, AFCRL-TR-75-0527, AD A019940.
20. Kantor, A. J., and Cole, A. E. (1981) Variations of Density and Wind With Time at Altitudes 30 to 60 km, AFGL-TR-81-0281, AD A109804.
21. Cole, A. E., Kantor, A. J., and Philbrick, C. R. (1979) Kwajalein Reference Atmospheres, 1979, AFGL-TR-79-0241, AD A081780.
22. Wagner, A. J. (1980) Weather and circulation of October 1979, Mo. Wea. Rev. 108(No. 1):119.
23. Holliday, C. R. (1976) Typhoon June - most intense on record, Mo. Wea. Rev. 104(No. 5):1188.
24. Riordan, P. (1974) Weather Extremes Around the World, Report ETL-TR-74-5, U.S. Army Engineer Topographic Laboratories, Ft. Belvoir, Va.
25. Holliday, C. R. (1975) An extreme sea-level pressure reported in a tropical cyclone, Mo. Wea. Rev. 103(No. 1):163.
26. Valley, S. L., Ed. (1965) Handbook of Geophysics, A. F. C. R. L.
27. Cole, A. E., and Kantor, A. J. (1978) Air Force Reference Atmospheres, AFGL-TR-78-0051, AD A058505.
28. Harris, M. F., Finger, F. G., and Teweles, S. (1962) Diurnal variation of wind, pressure and temperature in the troposphere and stratosphere over the Azores, J. Atmos. Sci. 19:136.

END